Action in support of the federal authority’s strategic priorities
Contract NR/AP/00/36

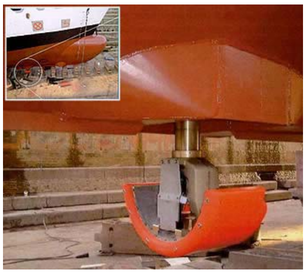

# Relationships between vertical reference planes in the Belgian marine area

*Final Report*

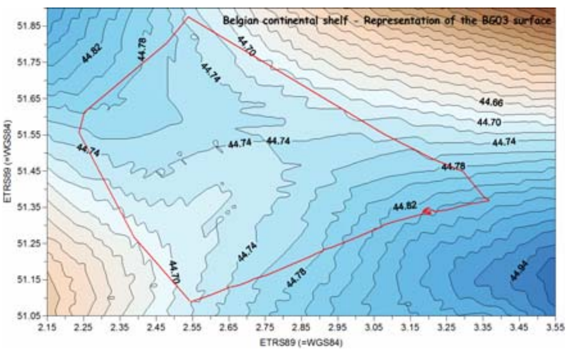


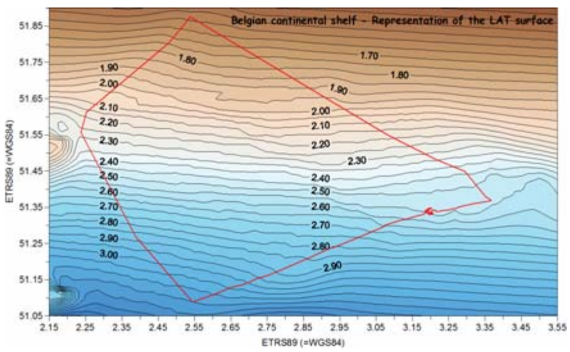



Royal Belgian Institute of Natural Sciences
*Management Unit of the Mathematical Models of the North Sea*

National Geographic Institute
*Department of Geodesy*

University of Ghent
*Department of Geography*

*Agentschap voor Maritiem Dienstverlening en Kust, Afdeling Kust*
Flemish Hydrography


.: May 2010 :.

Avenue Louise 231
Louizalaan 231
B-1050 Brussels
Belgium
Tel: +32 (0)2 238 34 11 – Fax: +32 (0)2 230 59 12
http://www.belspo.be

Contact person: David Cox
+32 (0)2 238 34 03



S. Scory, J. Ozer, M. Devolder, Ph. Lambot, P. Voet, F. De Doncker, A. De Wulf, Ph. De Maeyer, S. De Mûelenaere, H. Poppe, K. Van Parys. ***Relationships between vertical reference planes in the Belgian marine area G2_LAT -*** Final Report. Brussels/ Belgian Science Policy 2009 – 114 p. (Action in support of the federal authority's strategic priorities)

*Relationships between vertical reference planes in the Belgian marine area*
Action in support of the federal authority's strategic priorities
Contract NR/AP/00/36
Final report
May 2010

**Partners:**


- **Royal Belgian Institute of Natural Sciences** (RBINS)
  ***Management Unit of the Mathematical Models of the North Sea*** (MUMM)

  *Coordinator*

  Serge SCORY
  José OZER
  Mia DEVOLDER

  *Gulledelle 100, 1200 Brussels*

- **National Geographic Institute** (NGI)
  ***Department of Geodesy***

  Philippe LAMBOT
  Pierre VOET
  Filip DE DONCKER

  *Abdij ter Kameren/Abbaye de la Cambre 13, 1000 Brussels*

- **University of Ghent** (UGent)
  ***Department of Geography***

  Alain DE WULF
  Philippe DE MAEYER
  Stephanie DE MÛELENAERE

  *Krijgslaan 281 (S8), 9000 Ghent*

- **Flemish Hydrography**
  (MDK – Agentschap voor Maritiem Dienstverlening en Kust, Afdeling Kust)

  Hans POPPE
  Kris VAN PARYS

  *Vrijhavenstraat 3, 8400 Ostend*

# TABLE OF CONTENT

# SUMMARY


The main purpose of the present study was to meet the needs expressed by the Belgian federal public service "Economy" , *i.e.* the definition a "corrective model" which would allow to define in real–time the vertical position of the multi–beam sounders available onboard the R/V BELGICA with respect to various usual reference surfaces (LAT, GLLWS, …).

In nominal circumstances, the use of the signals provided by the GPS, processed by the RTK/LRK technology, allows to reach a precision of the order of magnitude of 1 cm, with respect to the WGS84 ellipsoïd. However, the reference surface for hydrography in the North Sea is from now the LAT (Lowest Astronomical Tide, succeeding to GLLWS). The requested corrective model had to make the link between the ellipsoid, the gravimetric geoid and the practical vertical reference levels (LAT, GLLWS, …).

The question has be tackled in two ways, both from the theoretical side and from the experimental side.

On the theoretical side, existing data on the heights of the practical reference levels (LAT & GLLWS, available at the Flemish Hydrography) have been referred to the WGS84 ellipsoïd by means of an interpolator, on a regular grid.

On the practical side, extensive measurement campaigns at sea and on land have been performed, in order to:

- calibrate the current positioning instrumentation of the R/V BELGICA;
- test the corrective model;
- estimate the accuracy of the measurements.

Where the RTK/LRK can be used, there is no more need to know the specific tidal reduction. However, the current RTK/LRK system along the Belgian coast, does not cover the whole area of interest with centimetric precision. This study also offered the opportunity to compare the method currently used (based on the knowledge of the $M_2$ component of the tide at various places and of the actual tidal signal at coastal stations) with the information delivered by operational 2D storm-surge models.

Besides the results requested by the FPS Economy (the "corrective model" allowing to convert RTK-heights to LAT), the G2LAT consortium also explored in a detailed way the possible sources of errors bound to LRK positioning and expressed recommendations on how to improve the use of this system at sea.


*Keywords:* GPS, RTK/LRK, Vertical positioning at sea

# RÉSUMÉ


Le but premier de la présente étude était de rencontrer les besoins exprimés par le SPF Économie, à savoir la construction d'un « modèle correctif » permettant de définir en temps réel la position verticale des écho–sondeur multi–faisceaux montés sur le BELGICA, par rapport à différentes surfaces de référence usuelles (LAT, GLLWS, …).

Dans des conditions nominales, l'utilisation des signaux GPS traités par la technologie RTK/LRK permet d'espérer une précision de l'ordre du centimètre par rapport à l'ellipsoïde WGS84. Mais la surface de référence en matière d'hydrographie dans la mer du Nord est depuis peu le « LAT » (« Lowest Astronomical Tide », qui succède au GLLWS). Le modèle correctif demandé devait donc faire le lien entre l'ellipsoïde, le géoïde gravimétrique et les niveaux de référence usuels (LAT, GLLWS).

La question a été abordée par ses aspects théoriques comme par ses aspects pratiques.

Pour ce qui est de l'approche théorique, les informations concernant les hauteurs des niveaux de référence usuels (LAT & GLLWS, disponibles auprès de la Vlaamse Hydrografie) ont été rapportés à l'ellipsoïde WGS84 à l'aide d'un interpolateur sur une grille régulière.

Pour l'approche pratique, des campagnes de mesures en mer comme sur terre ont été réalisées pour :

- calibrer l'instrumentation disponible à bord du R/V BELGICA ;
- tester le modèle correctif ;
- évaluer la précision des mesures.

Là où le RTK/LRK peut être utilisé, il n'est pas nécessaire de connaître la réduction de marée. Toutefois, ce système ne couvre pas l'ensemble de la zone d'intérêt avec une précision centimétrique. Cette étude s'est donc également attachée à comparer la méthode actuellement utilisée (basée sur la connaissance de la composante $M_2$ à différentes stations et sur le signal de marée mesuré aux stations côtières) avec les informations fournies par les modèles de marée–tempête opérationnels.

Au–delà du résultat demandé par le SPF Économie (un « modèle correctif » permettant de convertir les hauteurs RTK vers le LAT), le consortium « G2LAT » a également exploré en détail les sources possibles d'erreurs dans le référencement LRK et a émis des recommandations permettant d'accroître la précision de ce positionnement en mer.


*Mots-clefs :* GPS, RTK/LRK, Positionnement vertical en mer

# SAMENVATTING

De doelstelling van de hier gepresenteerde studie was tegemoet te komen aan de noden, zoals geformuleerd door de Belgische Federale Overheidsdienst "Economie", zijnde de definiëring van een "correctiemodel", dat zou toelaten de verticale positie van *Multi-beam sounders* te bepalen aan boord van de R/V BELGICA, rekening houdend met de verschillende gebruikte referentievlakken (LAT, GLLWS, …).

Onder normale omstandigheden staat het gebruik van signalen, verkregen door GPS en verwerkt met behulp van de RTK/LRK technologie, toe om een precisie te bereiken met een grootteorde van 1 cm, gerelateerd aan de WGS84 ellipsoïde. Het referentievlak voor hydrografische toepassingen in de Noordzee is momenteel echter het LAT (*Lowest Astronomical Tide*, als opvolger van GLLWS). Het gevraagde correctiemodel dient een koppeling te maken tussen de ellipsoïde, de gravimetrische geoïde en de gebruikte referentie niveau□s (LAT, GLLWS, ..).

Deze onderzoeksvraag wordt benaderd vanuit een theoretisch en een experimenteel luik.

Het theoretische luik bestaat uit hoogtegegevens van de gebruikte referentieniveau□s (LAT en GLLWS, beschikbaar gesteld door de Vlaamse Hydrografische Dienst), welke gerefereerd zijn naar een equidistant grid op de WGS84 ellipsoïde met behulp van een *interpolator*.

Het praktische luik bestaat uit een uitgebreide meetcampagne op zowel zee als land, met de bedoeling om:

- de gebruikte positioneringapparatuur aan boord van de R/V BELGICA te kalibreren;
- het correctiemodel te testen;
- de nauwkeurigheid van de metingen te schatten.

Op plaatsen waar RTK/LRK kan worden gebruikt, is geen kennis betreffende getijde-reductie meer vereist. Het huidige RTK/LRK systeem langs de Belgische kust dekt niet het volledige gebied met centimeter precisie. Deze studie bood eveneens de mogelijkheid om de momenteel gebruikte methode (gebaseerd op de kennis van de $M_2$-component van het getijde op verschillende locaties en het actuele getijde signaal van verschillende kust stations) te vergelijken met de informatie die bekomen werd uit operationele 2D hydrodynamische modellen.

Naast de resultaten die gevraagd worden door de FOD Economie (nl. het correctiemodel dat toelaat RTK-hoogten te converteren naar LAT) onderzocht het G2LAT consortium op gedetailleerde wijze de mogelijke foutenbronnen van de LRK positionering en formuleerde aanbevelingen voor de verbetering van het gebruik van dit systeem op zee.

*Sleutelwoorden:* GPS, RTK,LRK, verticale positionering op zee, foutenbudget.

# 1. INTRODUCTION

The Belgian federal public service "Economy" is in charge of continuously monitoring the evolution of sand and gravel stocks on the Belgian Continental Plate. In 2008, it acquired a new multibeam echosounder that has been installed onboard of the R/V BELGICA. This device, a Kongsberg-Simrad EM3002 Dual, is suited for detailed seafloor mapping and inspection with water depths between 0.5 and 150 meters. Table 1 shows the main acoustic characteristics of the newly installed system compared to the older one.

**Table 1:** Acoustic parameters of the old and the newer multibeam echosounders onboard the R/V BELGICA.

| | EM1002 | EM3002 Dual |
|---|---|---|
| Number of beams | 111 | 508 |
| Nominal frequency | 100 kHz | 300 kHz |
| Sampling frequency | 10 Hz | 40 Hz |

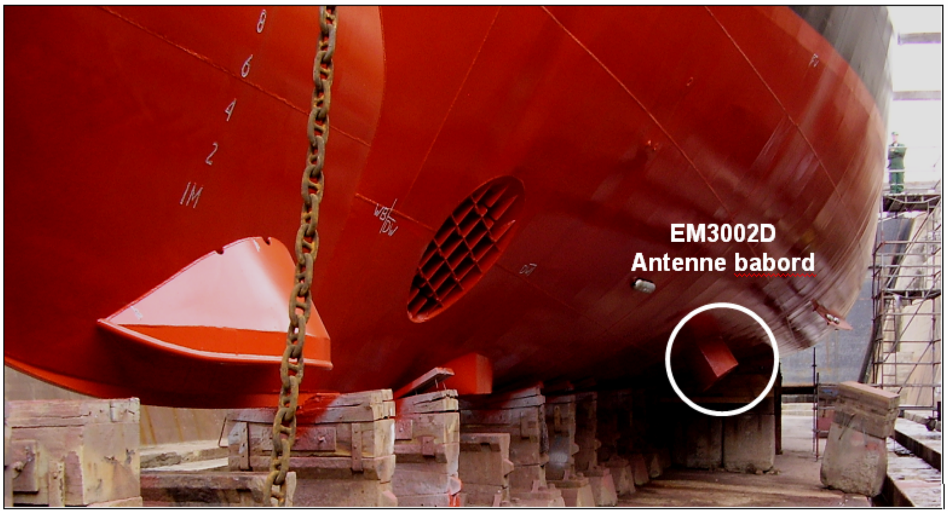


**Picture 1:** View of the port side antenna of the EM3002 Dual mounted on the hull of the R/V BELGICA.

This highly sophisticated system required a lot of sea trials and tuning before being formally accepted for the intended purpose of monitoring the sand banks. It is fully operational since spring 2009 and has already allowed the mapping a large part of the zones of interest.

Figure 1 shows the zones where the sand and gravel extraction activity is allowed by law. The most Northern (and biggest) zone is an "exploration zone" not yet open to the extraction activity.

When processing the signal of the echo-sounder to transform it into depths and slopes of the sea bottom it is necessary to take a lot of parameters into account. Besides the acoustical properties of the water and the bottom itself, the most important are the position of the sensors with respect to the centroïd of the vessel and the position of that centroïd in a relative or an absolute reference system.

In order to be able to get the most accurate depth measurements, with respect to a reference system that would allow to follow their evolution over the years, the FPS "Economy" opened a call to ask scientists to build a "corrective model" which would allow to define in real–time the "vertical" position of the multi–beam sounder available onboard the R/V BELGICA with respect to various usual reference surfaces (LAT, GLLWS, …). More specifically, the signals provided by the GPS, processed by the RTK/LRK technology, needed to be combined

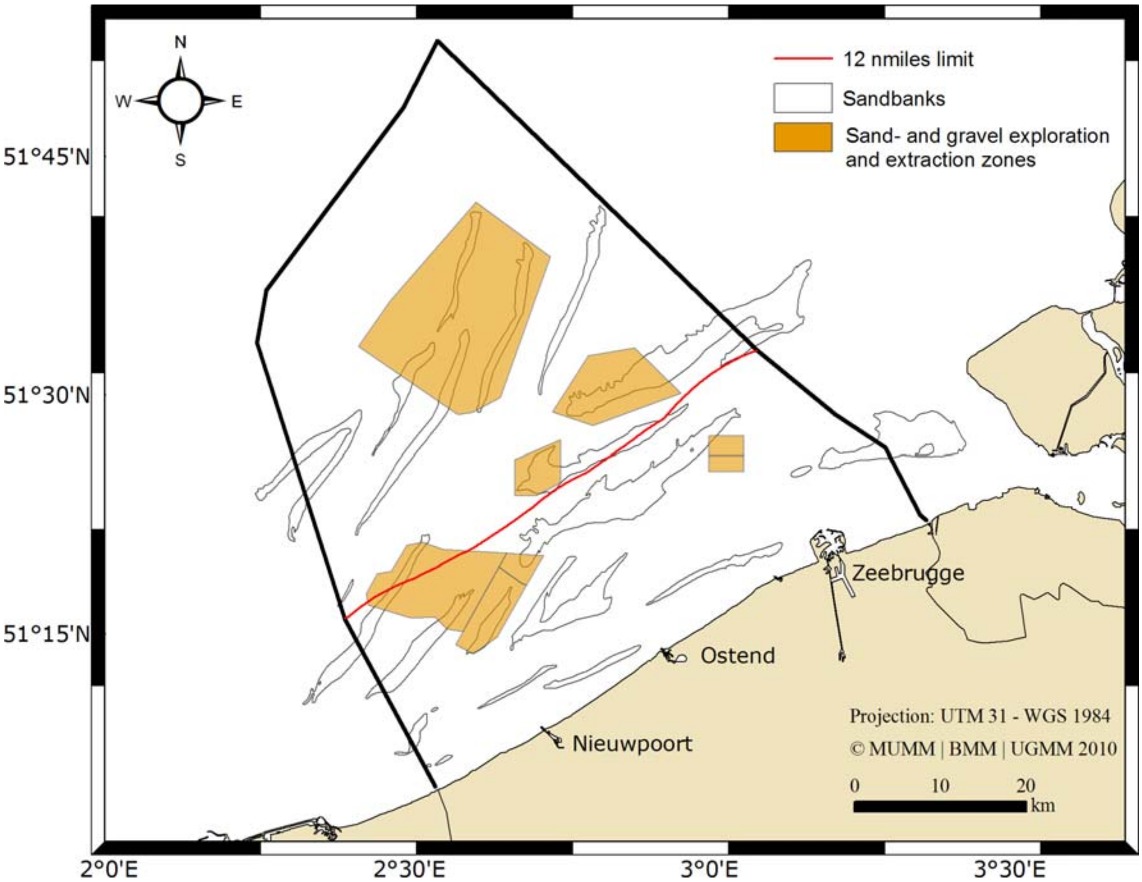


**Figure 1:** Map of the sand and gravel extraction zones on the Belgian Continental Plate.

A consortium made of four Institutions was set up to give the most detailed answer to the problem:

- The Management Unit of the Mathematical Models of the North Sea (Royal Belgian Institute of Natural Sciences), which operates the R/V BELGICA;
- The Department of Geodesy of National Geographic Institute;
- The Department of Geography of the University of Ghent;
- The Hydrography department of the Flemish Region, operating the hydrographic vessel TER STREEP.

The project was split into five workpackages:

- WP 0 Co–ordination and internal auditing (all partners)
- WP 1 Theoretical aspects (NGI, Flemish Hydrography)
- WP 2 Practical approach (NGI, UGent)
- WP 3 Sea campaigns (all partners)
- WP 4 Tidal reduction (RBINS–MUMM, Flemish Hydrography)
- WP 5 Synthesis and dissemination (all partners)

The present report is a synthesis of the outcomes of the project. It first gives a description of the tidal reduction method currently in use and compares it with the possibilities offered by the operational storm surge models (Chapter 2). Chapter 3 clearly states the problem, develops the conversion model based on the RTK/LRK system and evaluates how it competes with the traditional method.

The various extensive measurements campaigns performed at sea and on land are described in Chapter 4 and interesting practical figures on the accuracy of LRK and DGPS are given.

Chapters 5 to 8 give a detailed analysis of the possible errors when using LRK positioning.

Finally, Chapter 9 summarizes the lessons learned and formulates some recommendations.

# 2. Comparison between the results of the $M_2$ tidal reduction method and of some operational hydrodynamic models

## 2.1 Introduction

In this chapter, a summary of the work done on the comparison between the results of the $M_2$ tidal reduction method (Van Cauwenberghe *et al.*, 1993) and those of some operational storm surge models is presented.

Main objectives were to provide elements to answer the two following questions:

- could results of operational storm surge models be an option for a correction in real time of depth soundings made on board of research vessels (e.g., the BELGICA)?
- could the information on the M2 tide provided by these models help to extend the area actually covered be the M2 method?

These questions were raised for the following reasons:

- the $M_2$ tidal reduction method can only be applied in a delay mode. Quality controlled data (including a visual control) are transferred to end users with a delay of approximately one month;
- at the beginning of the study, the area covered by the RTK/LRK method was not precisely known. Moreover, at the same time, it was not precisely known how the accuracy of the method would evolve with the distance with respect to the LRK reference stations;
- the forecast horizon of the operational models is 5 days ahead. Results of these models can thus either be installed on the computers of the research vessel at the time start of a campaign or, better, sent every time a new forecast is available (as quality of the forecast decreases with time). The technical aspects of such a transfer were outside the scope of the project. More important was the quality of the real time model results compared to that of the results of the M2 tide obtained in delay mode;
- so far, the $M_2$ tidal reduction method covers only a limited part of the Belgian Continental Shelf (BCS in short). The Flemish Hydrographic service proceeds to new measuring campaigns as well to update the input data of the method as to extend the area it covered;
- amplitude and phase of the M2 tide can be obtained (over a wider area) by an harmonic analysis of long term model tidal runs (one year for instance). A comparison between model amplitudes and phases with those of the $M_2$ method will indicate if the model can help in extending the method to the whole BCS.

This chapter is organized in two main parts.

In the first part, a quite detailed description of the different methods ($M_2$ tidal reduction method and operational storm surge models) is given. The second part deals with the comparative study of the results obtained with the different methods. It is divided in two main subsections. First, a comparison is made with time series of observations at nine stations in the Belgian Coastal waters over a period of three months (September-November 2009). Afterwards, the focus is rather on the characteristics (amplitude and phase) of the $M_2$ tide at the same stations but also on a significant part of the BCS.

## 2.2 DESCRIPTION OF THE $M_2$ TIDAL REDUCTION METHOD AND OF THE OPERATIONAL MODELS

### 2.2.1 The $M_2$ tidal reduction method

#### 2.2.1.1 Introduction

The description of the $M_2$ tidal reduction method presented hereafter is largely based on that proposed in Van Cauwenberghe *et al.* (1993).

The method was first developed[1] by the former Advisory Department of the Rijkswaterstaat at Flushing (Adviesdienst Vlissingen). It has been accepted as the standard method for tidal reduction as well for the mouths of the Eastern and Western Scheldt as for the Belgian Coast by a series of governmental services in the Netherlands and in Belgium. During the discussions and studies dealing with the choice of the most appropriate method, a special attention has been paid to accuracy and ease of use. For the former, it has been stipulated that generated water levels could not be affected by errors larger than 0.1 m as well for the bias as for the standard deviation.

A complete list of past and today applications of the method would be too long. Let us simply mention a few of them: production of hydrographic charts for Belgian coastal waters, bathymetric surveys of the navigation channels towards sea harbours (dredging activities), morphodynamic studies in Belgian coastal waters (*e.g.*, De Moor, 2002), investigations dealing with the impact of sand and gravel extractions in our area of interest (*e.g.*, Norro *et al.*, 2006).

In what follows, the method is described in 3 steps: theoretical aspects, information on how the method was developed and its accuracy controlled, present status of the input data required by the method.

#### 2.2.1.2 Theory

In the $M_2$ tidal reduction method, the water level (with respect to MSL, Mean Sea level) at one location at sea is computed from the measured water level (with respect to MSL) at a reference station[2], the latter being corrected by means of 3 factors:

- a difference in MSL;
- an amplitude factor which is equal to the ratio between the amplitude of the $M_2$ at the sea point and at that the reference station;
- a time shift factor which is equal to the difference between the phase of the $M_2$ at the point at sea and that at the reference stations.

In Belgian coastal waters, the reference level for the water levels is TAW (Tweede Algemene Waterpassing) which lies (in the description given in Van Cauwenberghe *et al.*, 1993) 2.303 m below NAP (the Normaal Amsterdams Peil). Still according to Van Cauwenberghe *et al.* (1993), variations in mean sea levels with respect to NAP along the coast are marginal and the factor pertaining to mean sea level can be neglected. All elevations with respect to TAW are computed with respect to NAP according to:

$$\eta_{\text{NAP}} = \eta_{\text{TAW}} - 2.303$$

where $\eta$ denotes the elevation of the sea surface.

[1] Worth to mention that 'developed' means, here, for areas of interest to Dutch and Belgian hydrographic services. Similar methods are used worldwide in coastal zones where the lunar semi-diurnal constituent, $M_2$, is the major tidal constituent.

[2] In Belgian coastal waters, the reference stations are the three sea ports: Nieuwpoort, Ostend and Zeebrugge.

In the latest publication of the Flemish Hydrographic service dealing with reference levels along the Belgian Coast[3], NAP is now 2.333 m above TAW. According to more recent measurements made by the IGN, a mean value of 2.311 m should be used in our area of interest.

Now, in a recent analysis of the trend in yearly averaged values of water levels along the Belgian Coast (more precisely at Ostend), Ozer *et al.* (2008) shows that at Ostend these values have been rising by 1.7 mm/yr over the period 1927-2007. This rising seems to have recently increased up to approximately 2.7 mm/yr since 1967 but more data are required to confirm such an increase. Yearly averaged water levels at Ostend are well above 2.30 m with respect to TAW since 1998 (Figure 2).

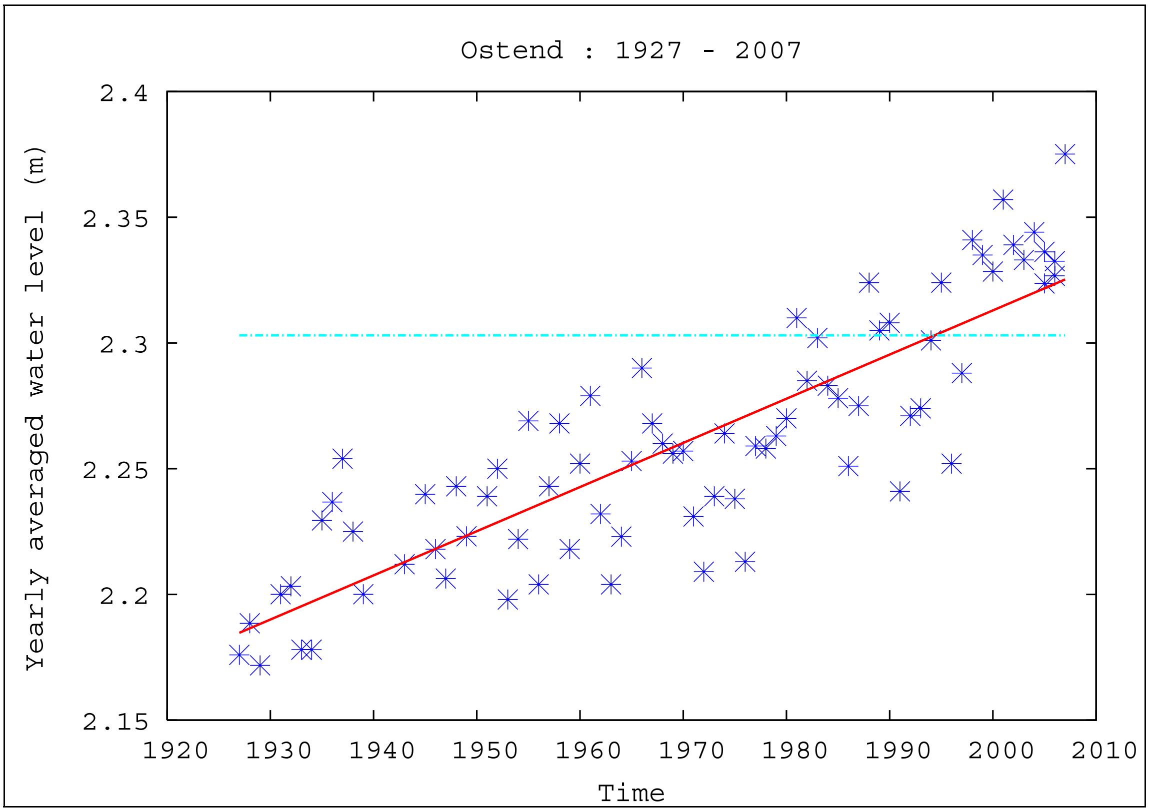


**Figure 2:** Yearly averaged water levels (m) with respect to TAW at Ostend during the period 1927-2007.

Once the factor pertaining to mean sea level is neglected, the equation of the $M_2$ tidal reduction method reads:

$$\eta_{\mathrm{NAP}}(\vec{s},t) = \frac{a_{M_2}(\vec{s})}{a_{M_2}(\vec{s}_r)} \eta_{\mathrm{NAP}}(\vec{s}_r, t - (f_{M_2}(\vec{s}) - f_{M_2}(\vec{s}_r))$$

where, $t$ denotes time, $\vec{s}$ the position at sea, $\vec{s}_r$ the position of the reference station (for the position at sea considered), $a_{M_2}$ the amplitude of the $M_2$ and $f_{M_2}$ its phase. For each position at sea, the reference station must be chosen with some care.

According to Van Cauwenberghe *et al.* (1993), a reasonable level of accuracy can be achieved only if the (time) variations in tidal levels are similar at the sea location and at its reference station. The extent of the area that can be "attached" to each reference station is mainly limited by the presence of banks and shoals.

[3] Onderlinge ligging van enkele vergelijkingsvlakken. Toestand 27-04-2007. Vlaamse Hydrographie.

#### 2.2.1.3 Development and validation of the method

Measurements at sea were made to determine the amplitude and the phase of the lunar semi-diurnal component of the tide ($M_2$). A measuring period of at least one month was necessary and preferably measurements had to be done in relatively calm weather conditions (spring and summer).

At that time, the objective was to cover the Belgian coast from the French border to the mouth of the Eastern Scheldt and up to 30 km offshore. In the choice of the number and position of measuring points, practical experience, budgetary considerations and usefulness of the data for other applications were determining.

First measurements were made to the East of Ostend between 1982 and 1986 using pressure sensors (DAG6000) deployed on the sea bed in the Dutch area and Aanderaa equipments in the Belgian area. The Belgian area to the west of Ostend (up to the French border) has been covered later. No specific measuring campaigns were required to be made at the three sea ports since water levels are there continuously registered.

Analysis of the data involved the following steps:

- identification of a reference site for each location at sea;
- determination of the $M_2$ characteristics (amplitude and phase) at each reference site for each measuring period at sea;
- determination of the $M_2$ characteristics (amplitude and phase) at each reference site for the water levels measured in 1983;
- translation of pressure measurements at sea into water levels taking into account specific weight of sea water, barometric pressure and mean sea levels;
- water levels were visually controlled and corrected when appropriate;
- determination of the $M_2$ characteristics (amplitude and phase) at each measuring point at sea;
- as the $M_2$ characteristics vary slowly in time[4], it was necessary to normalize them for the year 1983 (the $M_2$ nodal correction for that year is close to one).

Once the characteristics of $M_2$ were determined at each measuring point at sea, the reduction method has been applied as described previously and results compared to the *in*

*situ* data. The largest standard deviation value was equal to 0.07 m and more than 95% of bias values were well in the range -0.1 m to 0.1 m. The conclusion was then that the method met the stipulated accuracy requirements.

#### 2.2.1.4 Overview of the input data of the $M_2$ tidal reduction method

One of the primary applications of the M2 tidal reduction method is to convert depth soundings at sea in heights of the water column above the sea bed that is useful for navigation purposes. Clearly these heights should correspond to some kind of minimum so that captains know the areas they must avoid according to the characteristics of their ship. So, in addition to the removal of the time variations in sea levels due to tide and atmospheric conditions, there is also a need to provide the distance between NAP and the chart datum relevant for navigation. Up to 2007 this level was MLLWS (Mean Low Low Water Spring). However, different definitions in MLLWS were used in different countries and navigation sea charts were not always compatible (near the borders, the depths on navigational charts sometimes differed quite significantly). To solve this problem it has been decided to implement a seemly uniform surface namely the LAT. The definition of LAT states that it stands

[4] Nodal corrections must be applied to the amplitude of the harmonic constituents to take into account their slow variations over a 18.61 Julian years period (corresponding to the regression of Moon's nodes to complete a circuit of 360° (see http://tidesanddocuments.noaa.gov/publications/glossary2.pdf)

for the lowest astronomical tide. In order to determine it, tidal predictions have to be made for a period that is a least equal to the nodal cycle, *i.e.*18.6 years. At the Flemish Hydrographic service, it was chosen to extend this period to 19 years (Poppe, 2007).

The depth soundings correction finally reads:

$$h_{\mathrm{LAT}}(\vec{s}) = h_{mes}(\vec{s},t) + \eta_{\mathrm{NAP}}(\vec{s},t) - Z_{\mathrm{LAT}}(\vec{s})$$

where $h_{\mathrm{LAT}}(\vec{s})$ is the height of the water column between the bottom and the LAT reference level at the sea location $\vec{s}$, $h_{mes}(\vec{s},t)$ the depth sounding taken at this location at time $t$, $\eta_{\mathrm{NAP}}(\vec{s},t)$ the surface elevation with respect to NAP computed the M2 method and $Z_{\mathrm{LAT}}(\vec{s})$ is the local distance between NAP and LAT. In this equation, all terms are positive except $\eta_{\mathrm{NAP}}(\vec{s},t)$ which can be either positive or negative depending on the position of the free surface with respect to NAP (positive above; negative below).

$M_2$ characteristics (amplitude and phase) and distance between NAP and LAT ($Z_{\mathrm{LAT}}$) are today provided on a grid which has a horizontal resolution of 1 by 1 km. These gridded data are presented on the three following figures.

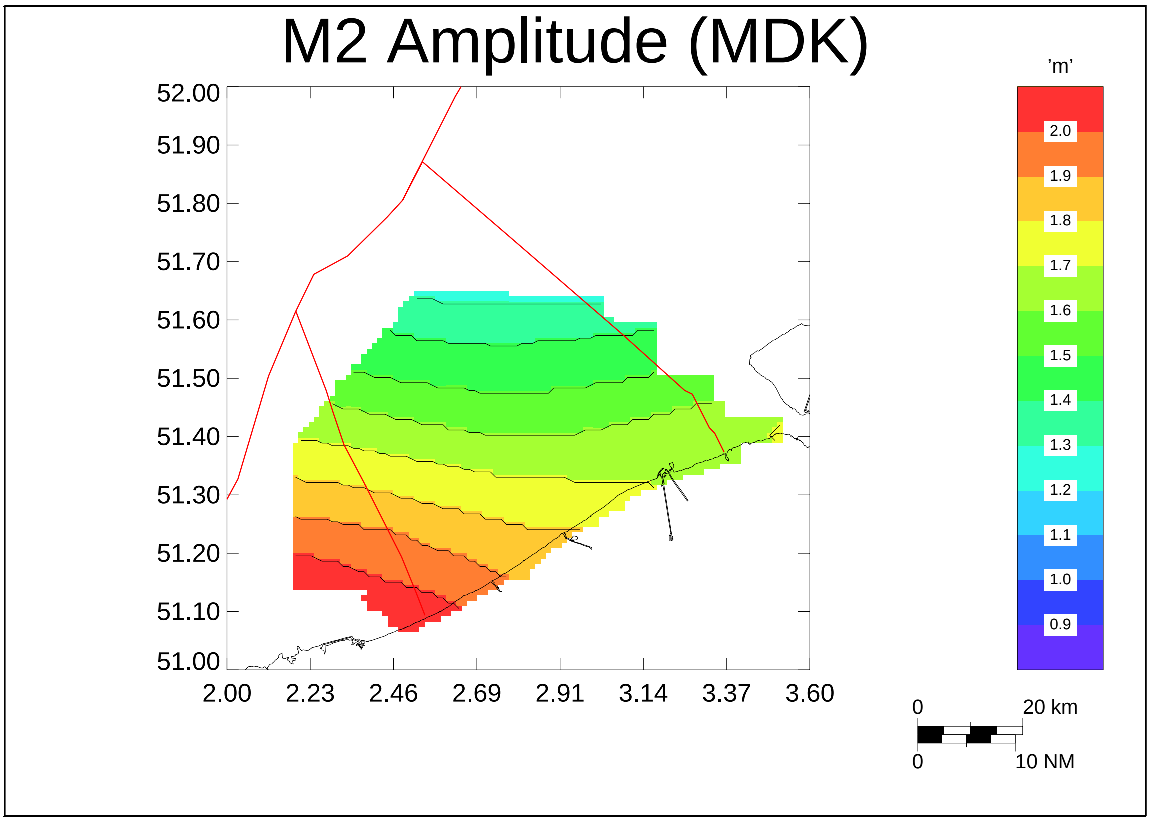


**Figure 3:** Amplitude (m) of the $M_2$ tide on the 1 by 1 km grid (data provided by the Maritieme Dienstverlening and Kust, MDK in short).

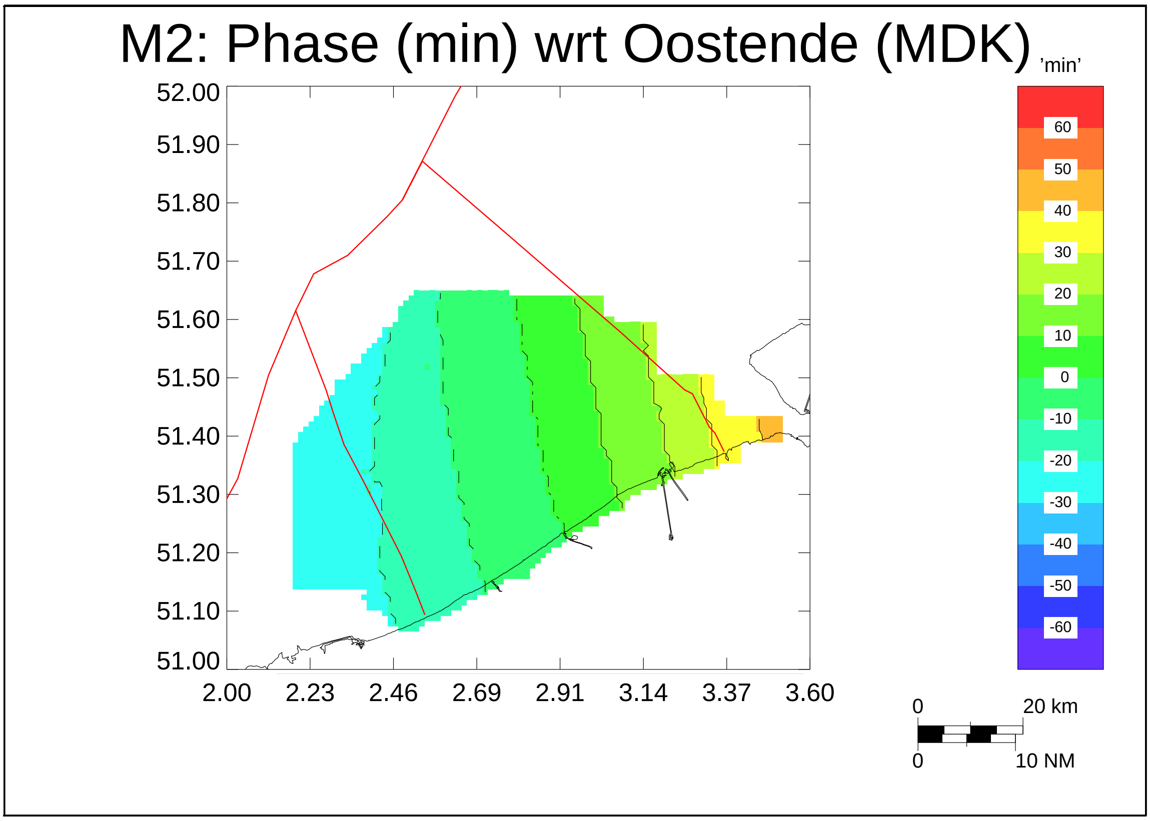


**Figure 4: Phase** (min) of the $M_2$ tide on the 1 by 1 km grid. For comparison with other methods, the phase shown here is, at each point, the difference between the phase in the input file and the phase at Ostend.

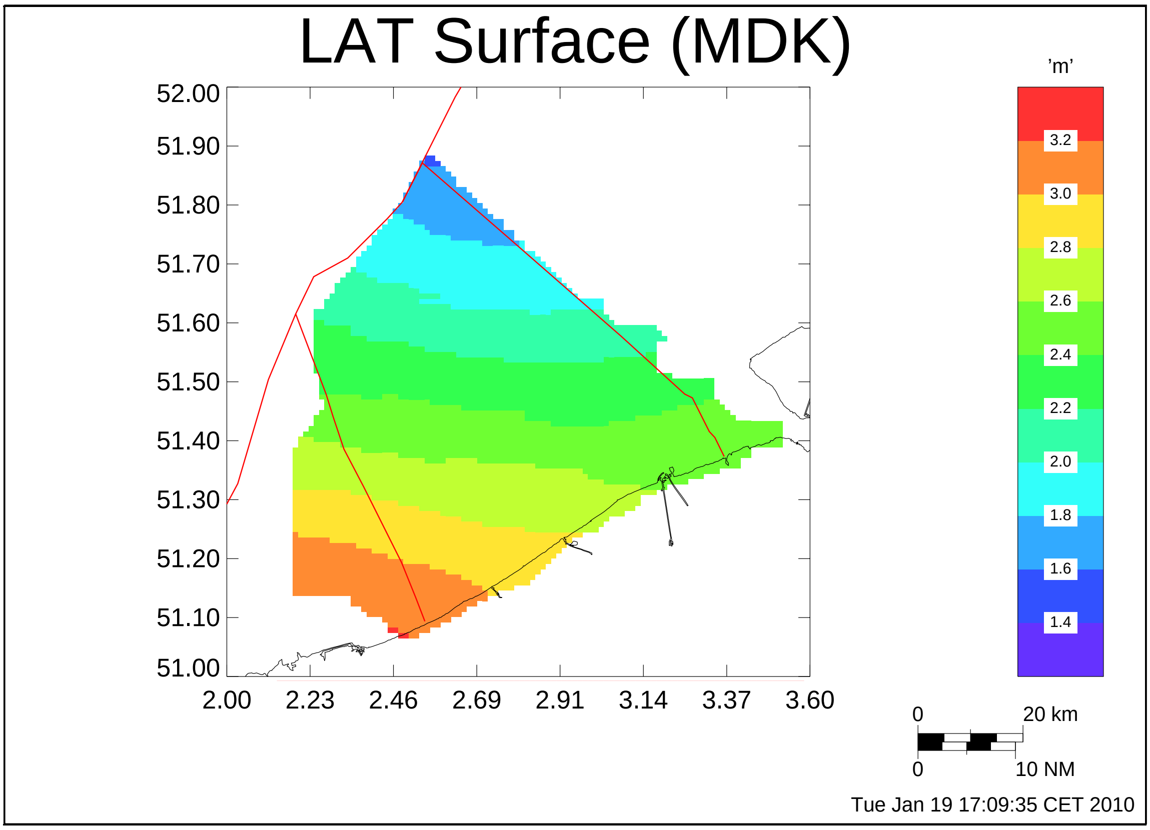


**Figure 5:** Distance (m) between NAP and LAT ( $Z_{\mathrm{LAT}}$ ) on the 1 by 1 km grid (latest data provided by MDK).

Concerning the LAT grid, $Z_{\text{LAT}}$ has been determined as follows:

- for the three reference stations, hourly observations made over a period of 19 years have been analyzed to determine the amplitude and phase of as much as possible constituents of the tide;
- harmonic tidal time series (over the same time period) of water level at those stations were reconstructed using the obtained amplitude and phase of the constituents;
- from those time series, the minimum water level ($Z_{\text{LAT}}$) has been extracted;
- offshore values of $Z_{\text{LAT}}$ were determined by application of the M2 tidal reduction method: $Z_{\text{LAT}}(\vec{s}) = \dfrac{a_{M_2}(\vec{s})}{a_{M_2}(\vec{s}_r)} Z_{\text{LAT}}(\vec{s}_r)$ ;
- in that part of the BCS were $a_{M_2}(\vec{s})$ is not known yet (see Figure 3), the Flemish Hydrographic service decided to use results from another model.

### 2.2.2 Operational storm surges models

#### 2.2.2.1 Introduction

A brief overview of some of the operational hydrodynamic models available for the area of interest is given in the two following sub-sections. The first one deals with the MUMM OPTOS suite of models (Pison and Ozer, 2003). The second concerns the 2D storm surge model run by the Flemish Hydrographic service.

#### 2.2.2.2 Theory

Results of two types of hydrodynamic models will be used in this study. A first class of models is referred to as 3D baroclinic hydrodynamic model and the second class is referred to as 2D barotropic storm surge models.

The 3D baroclinic models solve the three-dimensional, time-dependent, governing equations of the Geophysical Fluid Dynamics that express conservation of mass, momentum, heat and salt. To get these equations, several assumptions and approximations have to be made. In the COHERENS model (Luyten *et al.*, 1999), the following assumptions are introduced:

- along the vertical, the hydrostatic equilibrium is assumed (*i.e.*, vertical pressure gradient is balance by gravity);
- density variations are neglected everywhere except in the buoyancy term (Boussinesq approximation);
- vertical turbulent fluxes of momentum, heat and salt, can be parameterized by means of eddy coefficients. Various turbulence closure schemes are available for the computation of these coefficients;
- various formulations are proposed for the computation of the density of the sea water.

Governing equations express thus the conservation of mass, momentum, heat and salt. Open boundary conditions and surface forcing are varying from one application to another. Those used in the operational models run by MUMM will be shortly described below.

In 2D storm surge models, the density is taken as constant and the vertical variations of both components of the horizontal velocity are removed by integrating the 3D momentum equations over the height of the water column. State variables of these models are then the elevation of the sea surface with respect to a reference level (set equal to zero when the sea is at rest) and both components of the horizontal transport. The bottom stress is a function of the components of the transport.

#### 2.2.2.3 The MUMM OPTOS suite of hydrodynamic operational models

Twice a day, MUMM operates a suite of three nested hydrodynamic models that forecast, up to five days ahead, sea surface elevation, currents, temperature and salinity. The models are driven by tide (4 diurnal and 4 semi-diurnal components of the tide are used)[5], atmospheric forcing (wind, atmospheric pressure, and, when appropriate, air temperature, cloud coverage, specific humidity, rainfall) as well as (climatological) fresh water discharges from the main rivers. These models are part of the so-called MUMM suite of OPerational TOols end Services referred to as OPTOS.

The core of this suite of hydrodynamic models is the public domain COHERENS code (A Coupled Hydrodynamical and Ecological model for REgioNal Shelf seas; Luyten *et al.*, 1999). A new version of the model code has been recently released in the public domain (Luyten *et al.*, 2005) and will be soon used for the new generation of MUMM's operational hydrodynamic tools.

OPTOS is based on three different implementations of COHERENS. They are referred to as: Optos_CSM, Optos_NOS and Optos_BCZ. In what follows, we will often simply refer to these models as CSM, NOS and BCZ.

The areas covered by these three implementations are shown on Figure 6. Further characteristics of these implementations are given hereafter.

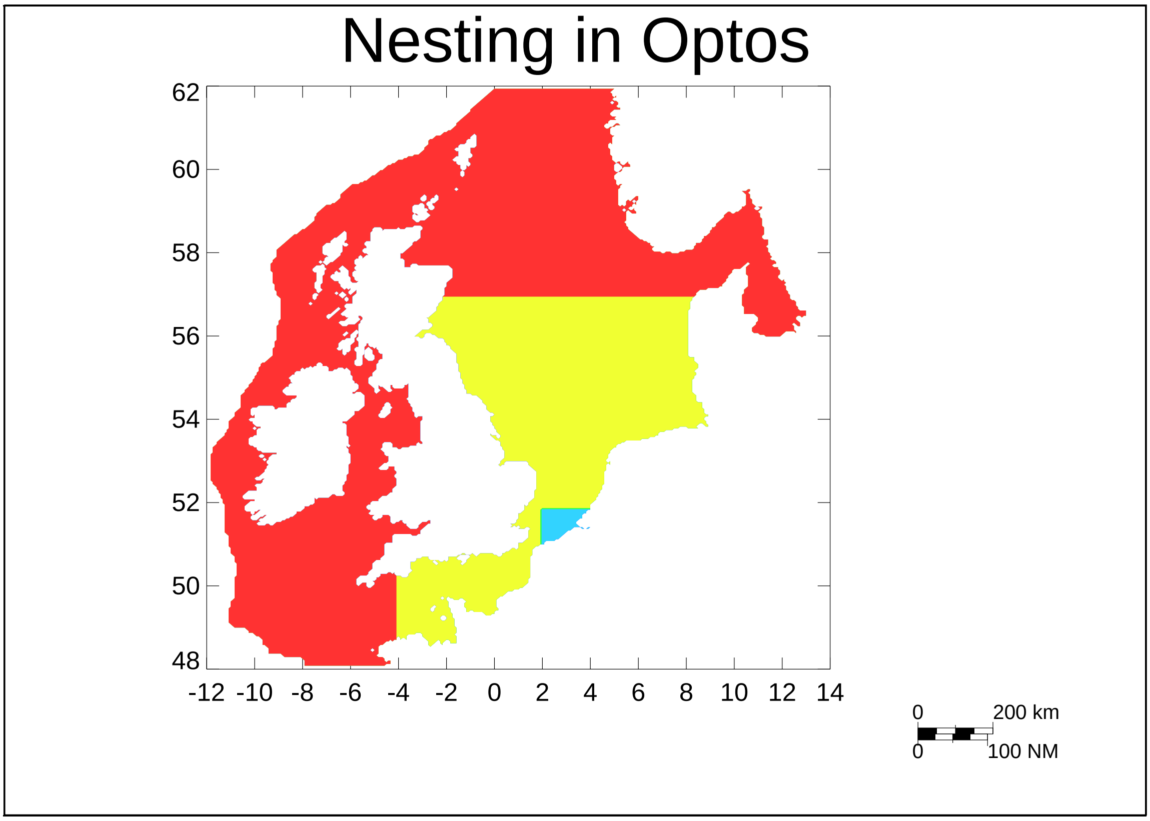


**Figure 6:** Areas covered by the three nested MUMM operational hydrodynamic models. In red, the CSM area; in yellow, the NOS area and finally in blue, the BCZ area. Please note that the nesting is a one way nesting. In other words, CSM provide (parts of) the open boundary conditions needed by NOS which, in turn, provide open boundary conditions to BCZ.

[5] The nodal corrections previously mentioned are taking into account in the model tidal forcing.

***CSM***

The area covered by CSM is the Northwest European Continental shelf. In this implementation of COHERENS, only the 2D barotropic mode is turned on. CSM belongs to the class of the so-called conventional vertically integrated models. The state variables are the elevation of the free surface with respect to a zero mean sea level (when the sea is at rest) and both components of the transport integrated over the total height of the water column. Spherical coordinates are used. The horizontal resolution is equal to 5′ in latitude and 2.5′ in longitude. The model is driven by tides along its open boundary (which closely follows the 200 m isobath), fields of surface wind ($\vec{W}_{10}$) and atmospheric pressure ($P_a$) (from Met Office, previously UKMO). Concerning the time stepping procedure, an explicit scheme is implemented. The time step for the integration of the model equations is limited by the so-called CFL (Courant–Friedrichs–Lewy) criterion and is set equal to 20″.

***NOS***

NOS covers the North Sea between 4° West and 57° North. It is a full 3D baroclinic model. Model forcing include: sea surface elevation and transports (from CSM) along the open boundaries; fields of surface wind, atmospheric pressure, air temperature, cloud coverage, rainfall and specific humidity (from Met Office); fresh water discharges from main rivers (monthly values from climatology). Some information on open boundary conditions for temperature and salinity are given later in this section. Horizontal resolution is as in CSM and, along the vertical, 20 $\sigma$ layers are used. The time step for the barotropic mode is as in the CSM. That for the 3D baroclinic mode is equal to 5 min.

***BCZ***

The latest model of the suite, BCZ, covers the Belgian Continental Shelf. As NOS, it is a full 3D baroclinic model. Horizontal resolution is of the order of 750 m in both directions. Vertically, 10 $\sigma$ layers are used. Lateral open boundary conditions come from NOS. Surface forcing are as in NOS. Time steps are equal to 10 sec (barotrobic mode) and 10 min (baroclinic mode), respectively.

***The Maritieme Dienstverlening and Kust (MDK) storm surge model***

For its own evaluation of the risk of flood along the Belgian coast, MDK also operates twice a day a conventional vertically integrated model. That model, referred to as OMNECS (often simply referred to as OMN in what follows), was jointly developed by MUMM and K.U.Leuven in the nineties (Van den Eynde, 1998).

The area, horizontal resolution and bottom topography are as in CSM. The bottom topography used by both models is presented on Figure 7.

Like CSM, the model is driven by tide along its open boundary (8 tidal constituents). The tide is introduced in a slightly different way in both models. In CSM, radiation boundary conditions are used (*i.e.*, a combination of incoming and outgoing Riemann invariants) while in OMN the time evolution of the elevation of the free surface of the sea is directly specified. Moreover, in OMN, the impact of incoming external surges is mimic by the so-called inversed barometric effect (*i.e.*, in addition to the tide, the elevation of the sea surface along the open boundary is instantaneously adapted to any difference between the local atmospheric pressure and a long term mean value set equal to 1012 hPa). From a numerical perspective, the main difference between CSM and OMN comes from the fact that in the latter, governing equations are solved by an Alternate Direction Implicit method (ADI, see, *e.g.*, Yang and Ozer, 1997). Note that OMN boundary conditions for tide and barometric effect are already included in the new code of COHERENS and that an implicit (or semi-implicit) time stepping scheme for COHERENS is being developed within the framework of the VLABEL project (supervised by Dr. P. Luyten from MUMM).

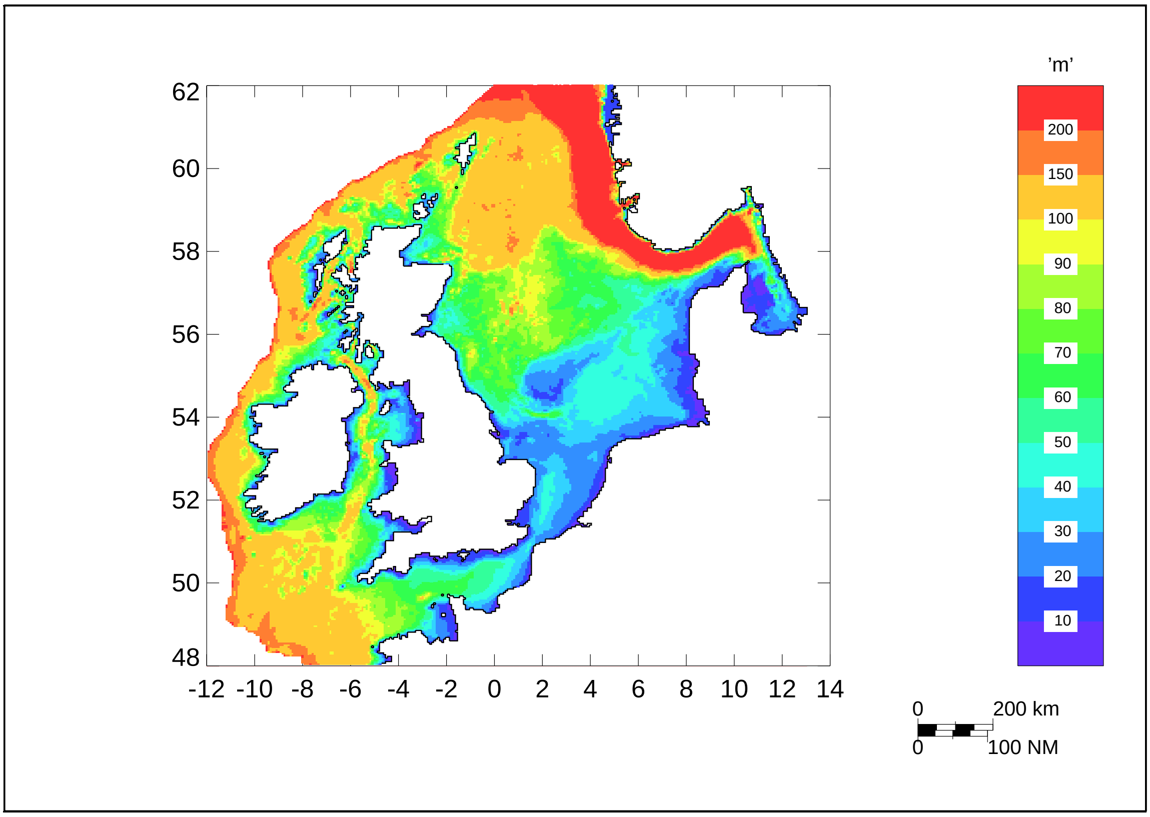


**Figure 7:** Bottom topography of the North West European continental shelf used by CSM and OMN.

We would like to mention that according to an agreement between MUMM and MDK, the OMNECS model is run on MUMM computers as well and that a lot of the results of the MUMM operational models are made available to MDK by ftp.

Before entering the comparison of the results of the M2 tidal reduction method and those of the operational models, we would like to point out some specificities of these models that should help the reader to better understand the results of the comparison:

- in a relatively small area like the BCS, the efficiency of the M2 tidal method does not come only from the fact that the semi-diurnal lunar tidal constituent, $M_2$, is dominant but also from the fact that other important semi-diurnal constituents have similar patterns (amplitude ratio and phase difference with respect to $M_2$ almost constant).
- The main objective of 3D hydrodynamic models is to provide three dimensional fields of currents, salinity and temperature needed by, *e.g.*, ecosystem models, oil spill models search and rescue models, ... It is well known that their ability to forecast the water levels is still less than that of 2D storm surge models which are in place since decades and have a long history of "tuning". Just to give an example: BSH as a long experience in 3D modeling in the North Sea, however, their storm surge forecast are still based on a 2D model.
- Nesting different models is never an easy task. In OPTOS, the open boundary conditions for NOS are a mixture of information coming from a 2D model (CSM) while for temperature and salinity, either constant values or a zero gradient condition in the direction perpendicular to the boundary are used. Such a "mixture" is probably not the best solution. Within the framework of the European FP7 MyOcean[6] project, nesting between models covering different areas (from global ocean to coastal areas) is one of the research topics. At

[6] See http://www.myocean.eu.org

MUMM, NOS open boundary conditions coming from Met Office 3D baroclinc shelf wide model will be tested. We hope this will have a positive impact on NOS performances. Regarding the nesting between NOS and BCZ, it is certainly affected by a too large difference in the horizontal resolutions used by both models (~6km in NOS and ~750 m in BCZ). All these nesting procedures are being reviewed within the framework of the implementation of the new version of OPTOS.

- 2D storm surge models like CSM and OMN aim at providing reliable information on the set up induced by wind and atmospheric pressure in bad weather conditions. To reach this objective, a detailed description of the tide is not always necessary. For the evaluation of the risk of flood, it is not uncommon to take the elevation due to tide from tidal predictions and the surge elevation forecasted by the model to get the total water level.
- In the tidal forcing used in CSM and OMN, 8 tidal constituents are introduced (4 diurnal and 4 semi-diurnal). Due to nonlinearities in the model equations, other tidal constituents (referred to as shallow water constituents) are generated inside the model area. However, this remains insufficient to get an accurate representation of the tide and we know, from experience, that both models tend to underestimate the tidal range at spring and to overestimate it at neap. Now, thanks to satellite altimetry data and coastal data, global ocean tidal models are able to provide quite accurate characteristics (amplitude and phase) for a relatively large number of tidal constituents. As well for CSM as for OMN, a tidal forcing based on a larger number of tidal constituents determined by the finite element model FES2004 (Lyard *et al.*, 2006) will soon be implemented and tested.
- CSM and OMN do not have a wetting and drying scheme. A minimum depth (10 m) is imposed everywhere. As a consequence, tide is not well represented in very shallow areas like the German Bight. Such a wetting and drying scheme is now available in the new version of COHERENS and others will be implemented and tested within the framework of the VLABEL project.
- There is no data assimilation scheme in the hydrodynamic operational models used in this study. An Ensemble Kalman Filter data assimilation algorithm has been recently implemented in COHERENS-V2 and preliminary tests in the North Sea have been performed (Ponsar and Luyten, 2009). In the MYOcean project, the study of the most appropriate data assimilation schemes, as well for the physical variables as for those of ecosystem models, for the Northwest European Continental Shelf is also an important research activity to which MUMM is associated.

The operational models used in the present study have not been developed for the same purpose as the M2 tidal reduction method and it can be expected, *a priori*, that they will not perform as well as the M2 method. The objective of the comparative study is to provide as much as possible information on the quality of each of the different approaches. Such information is of primary importance for the end users. In some circumstances, it is better to get an information with a relatively large uncertainty than no information at all.

## 2.3 COMPARISON BETWEEN THE RESULTS OF THE $M_2$ TIDAL REDUCTION METHOD AND THOSE OF THE HYDRODYNAMIC OPERATIONAL MODEL.

### 2.3.1 Introduction

The section deals with a comparative study of the results obtained with the different methods. It is divided in two main subsections. First, a comparison is made with the observations at nine stations in the Belgian Coastal waters over a period of three months (September-November 2009). Afterwards, the focus is on the characteristics (amplitude and phase) of the $M_2$ at the stations and in a significant part of the BCS.

### 2.3.2 Comparison of time series

#### 2.3.2.1 Introduction

In Belgian Coastal waters, the Meetnet Vlaamse Banken (MNVB in short) is made of a series of fixed stations where sea parameters (water level, SST, significant wave height, wave spectra, …) and atmospheric parameters (air temperature, atmospheric pressure, wind speed and direction …) are recorded continuously. A complete list of stations and parameters can be found on the web site of the Flemish Hydrographic service[7]. The information delivered by the network is of major importance to those who have to manage a series of activities at sea (*e.g.*, ship traffic, dredging activities, search and rescue…) as well as to those who have to give advices in case of the risk of flood (storm surge warnings).

Water levels are recorded at nine fixed stations (3 onshore and 6 offshore). The position of these stations is presented on Figure 8.

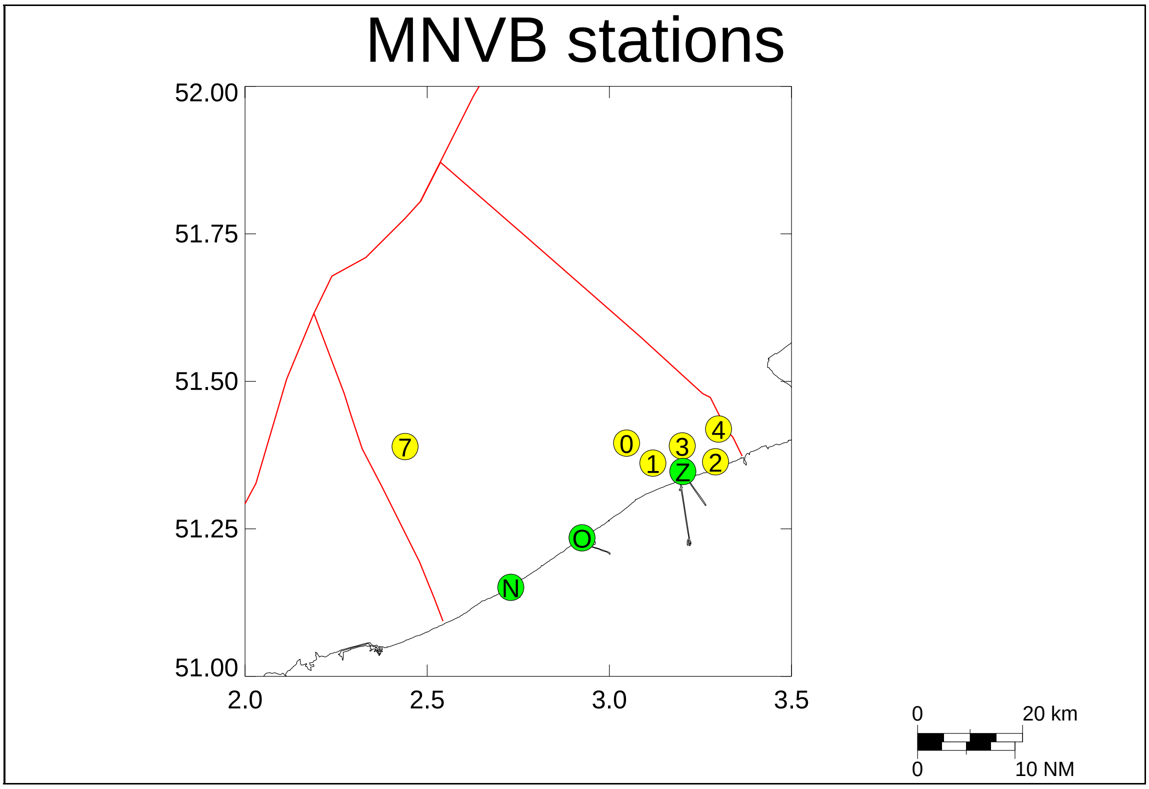


**Figure 8:** Locations where water levels are continuously recorded in the MNVB. The three reference coastal stations are shown in green (N: Nieuwpoort [Npt]; O: Ostend [Ost]; Z: Zeebrugge [Zee]). The six offshore stations are shown in yellow and the numbers refer to the stations as follows: 0, Wandelaar [Wan]; 1, A2 [A2]; 2, Appelzak [App]; 3, Bol van Heist [BvH]; 4, Bol van Knokke [BvK]); 7, Weshinder [Wsh]. For each station, the abbreviation given in brackets will be used in the various tables and figures presented hereafter.

The three coastal stations (Nieuwpoort, Ostend and Zeebrugge) play the role of reference stations in the applications of the M2 tidal reduction method. In this case, the quality controlled data (including a visual control) from these stations are made available with a delay of approximately one month.

[7] http://www.vlaamsehydrografie.be/level1.asp?TAAL_ID=1&ITEM_L1_ID=11

Data from the nine stations are downloaded in near real time at MUMM[8] mainly for model validation purposes. The quality control applied to these data at MUMM is very basic. Data obviously out of range and spikes are removed.

For the comparison of the results of the different methods, a period of three months (September – November 2009) has been selected mostly on the basis of the data availability (*in situ* and from hydrodynamic model archives). A common time sampling rate equal to 10 minutes has been chosen for all time series. For the operational models, let us recall than these are normally run twice a day[9]. There is always an overlap of twelve hours between two successive runs. As a consequence, each model produces in fact eight values of the water level for each time *t*. In the model archives, it is always the latest computed value that is stored.

For the M2 tidal reduction method, time series have been generated at all stations following closely the guidelines given in Van Cauwenberghe *et al.* (1993). A constant value equal to 2.303 m was first subtracted from data measured at all stations. The amplitude and phase correction were applied afterwards.

Our assessment of the various methods will be slightly biased as 4 offshore stations around Zeebrugge (Wan, A2, App, BvH and BvK, see Figure 8) are close to their reference station. Only, the station Westhinder (7) will allow to partly estimate the impact of the distance between the point at sea and the reference station.

The (arithmetic) mean value of all the time series are listed in Table 2.

**Table 2:** Time averaged values, in m, over the period September – November 2009 at all stations in all time series. The stations (first column) are referred to as on Figure 8. The mean value in the different time series at those stations are given in the other columns (OBS: Observations; M2: M2 tidal reduction method; CSM: Optos_CSM model; NOS: Optos_NOS model; BCZ: Optos_bcz model; OMN: OMNECS model).

| Station | OBS m | M2 m | CSM m | NOS m | BCZ m | OMN m |
|---|---|---|---|---|---|---|
| Wsh | 2.47 | 0.08 | 0.02 | 0.06 | 0.06 | 0.05 |
| Npt | 2.39 | 0.09 | 0.04 | 0.09 | 0.08 | 0.06 |
| Ost | 2.39 | 0.09 | 0.03 | 0.09 | 0.08 | 0.06 |
| Zee | 2.43 | 0.13 | 0.04 | 0.09 | 0.09 | 0.06 |
| Wan | 2.38 | 0.13 | 0.03 | 0.09 | 0.08 | 0.05 |
| A2 | 2.40 | 0.13 | 0.03 | 0.09 | 0.09 | 0.06 |
| App | 2.36 | 0.13 | 0.03 | 0.09 | 0.09 | 0.05 |
| BvH | 2.38 | 0.13 | 0.03 | 0.09 | 0.08 | 0.05 |
| BvK | 2.37 | 0.13 | 0.03 | 0.09 | 0.09 | 0.06 |

Averaged values of the observations with respect to TAW over a relatively short time period (3 months in this study) are influenced by meteorological effects and long term (semi-annual or annual) tidal constituents. Over the period September – November 2009, the time averaged value (in the observations) is varying between 2.36 m (Appelzak) and 2.47 m (Westhinder). It is surprising to observe that the largest time averaged value is found at the most offshore station and that, along the coast, the time averaged value at Zeebrugge is greater than that at Nieuwpoort. The fact that we have been working with data downloaded in near real time might have play a role.

[8] http://www.mumm.ac.be/EN/Models/Operational/forecasts.php
[9] if a meteorological forecast is not available for a reason or another, there is no run.

For the M2 reduction method, the time averaged values (with respect to NAP) should approximately be equal to:

$$\overline{\eta}_{M2}(\vec{s}) \approx \frac{a_{M_2}(\vec{s})}{a_{M_2}(\vec{s}_r)}(\overline{\eta}_{obs}(\vec{s}_r) - 2.303)$$

where the over bar indicates a time averaged value and where other symbols have already been defined. It is only at the reference stations that the equation is correct (there is no phase shift). Moreover, the ratio between the amplitudes of the $M_2$ being equal to one, the difference between the M2 time averaged values and the observed time averaged value is exactly equal to 2.303 m. At the other stations, a slightly different equation is used because, due to the phase shift, observations are numerically interpolated between values sampled every ten minutes. Moreover, the ratio between the amplitudes of the $M_2$ is no more equal to one. As a consequence, the difference with respect to the mean observed value is no more equal to 2.303 m. In the area around Zeebrugge, we note that, for the time period considered, the bias is above 0.10 m (using the old correction 2.303 m between NAP and TAW).

Hydrodynamic models compute the time evolution of the elevation of the free surface due to different forcing (tides, wind, atmospheric pressure, density gradients…). This elevation is set equal to zero when the sea is at rest. Due to nonlinearities in model equations, there is always a (small) mean residual elevation even when the models are driven by tide only. Over shorter time periods, atmospheric forcing can also have some influence. In OMNECS and the Optos suite of models, there is, so far, no long term (semi-annual or annual) tidal constituent in the model tidal forcing. According to the results presented in **Error! Reference source not found.**, we note that there is less spatial variability in the model time averaged values than in the observations and that the smallest values are provided by CSM and the largest ones by NOS and BCZ. In these two models, baroclinic effects can have an influence on the long term mean value of the sea surface elevation. For BCZ, the horizontal resolution (~750 m) should play a role as well.

#### 2.3.2.2 Description of the estimators

The following estimators are considered:

- percentage of the differences within the range [-0.1,+0.1] m; this was also one of the estimators used during the development of the M2 method.
- two times the standard deviation of the differences:

$$2\sigma = 2\sqrt{\left(\frac{1}{T}\int_0^T (\eta_{obs}(t) - \eta_{\mathrm{mod}}(t))^2\, dt\right)}$$

  where $t$ denotes time, $T$ the three months period considered; $\eta$ the elevation of the free surface at time $t$ with respect to the averaged value over the period $T$; the subscript *obs* refers to the observations and the subscript mod refers to one of the models (M2, CSM, NOS, BCZ, OMN). Recall that one of the requirements of the Dutch and Belgian Hydrographic Services was that $\sigma$ must be less than 0.1 m. $2\sigma$ is used for coherence with other sections dealing with the error budget of the methods.
- the cumulative distribution, at each station, of the differences for the various methods in the range of $[-0.5,+0.5]$ m.

#### 2.3.2.3 Presentation and discussion of the results

The value of the different estimators at the various stations are presented on Figure 9 (percentage of differences in the range [-0.1,+0.1] m), Figure 10 ($2\sigma$) and Figure 11 (cumulative distribution of the differences at the various stations). When considering these results, one should not forget that the three months averaged value has been removed from all time series.

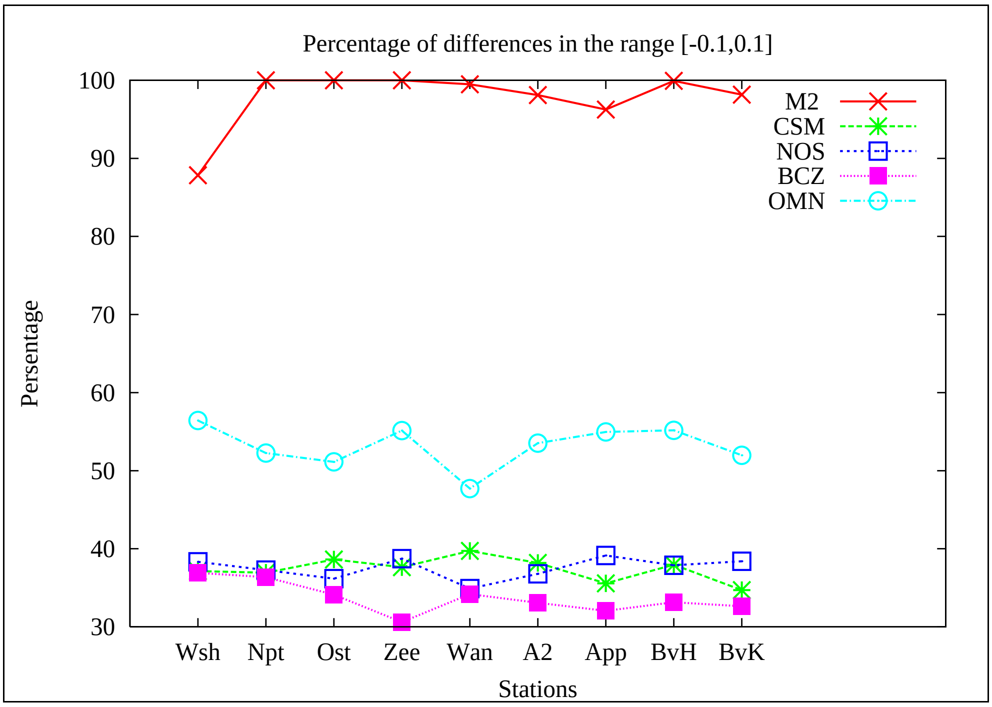


**Figure 9:** Percentage of the differences, at each station, within the range [-0.1:+0.1] m computed over the three months period considered in this study at the various stations and for the different modeling techniques.

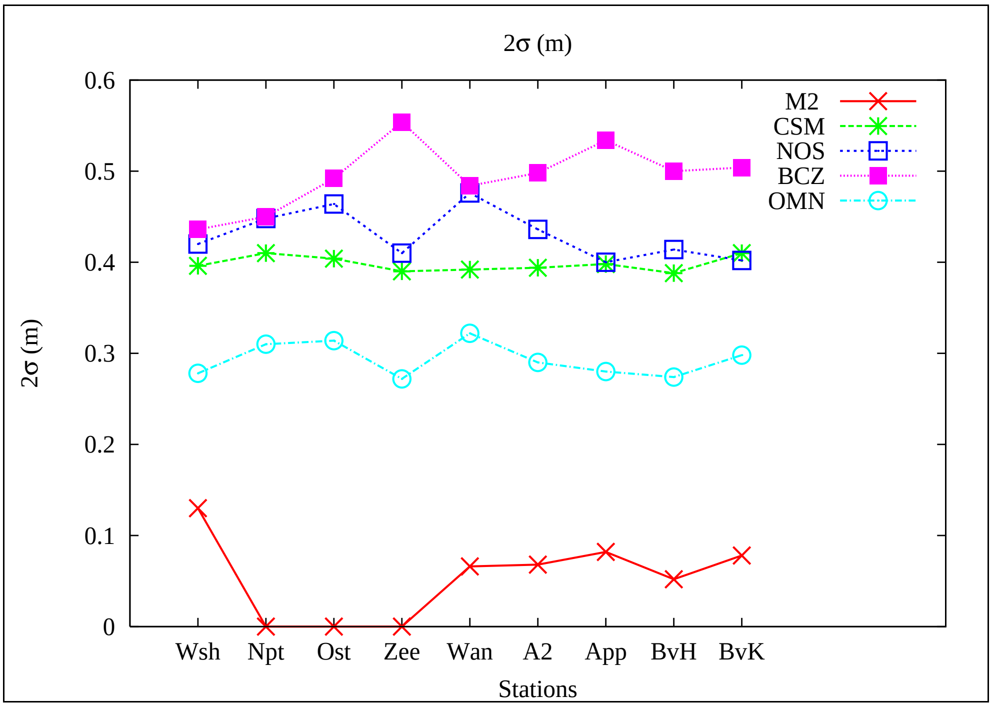


**Figure 10:** Two times the standard deviation ($2\sigma$ in m), at each station, of the differences computed over the three months period considered in this study. Lines and symbols are the same as on Figure 9.

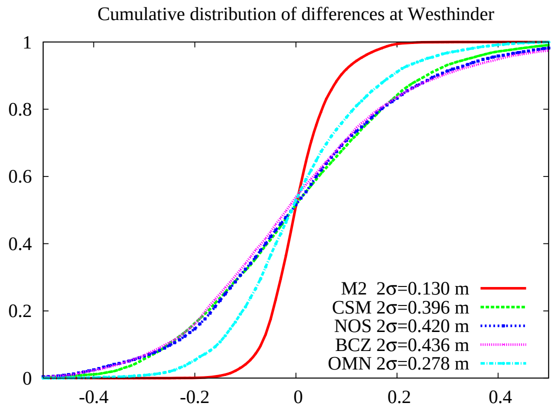
Cumulative distribution of differences at Westhinder
M2 2σ=0.130 m
CSM 2σ=0.396 m
NOS 2σ=0.420 m
BCZ 2σ=0.436 m
OMN 2σ=0.278 m
0
0.2
0.4
0.6
0.8
1
-0.4
-0.2
0
0.2
0.4

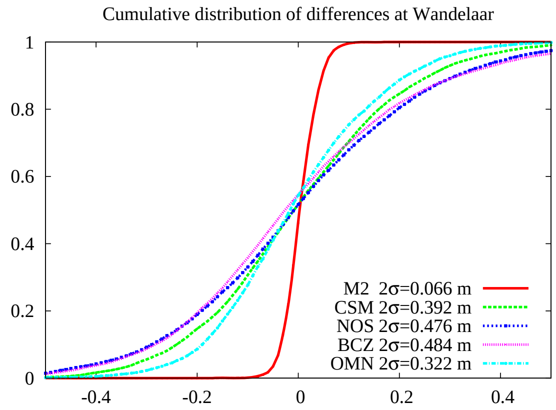
Cumulative distribution of differences at Wandelaar
M2 2σ=0.066 m
CSM 2σ=0.392 m
NOS 2σ=0.476 m
BCZ 2σ=0.484 m
OMN 2σ=0.322 m
0
0.2
0.4
0.6
0.8
1
-0.4
-0.2
0
0.2
0.4

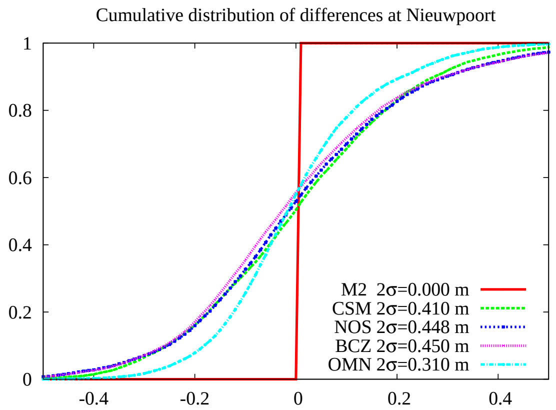
Cumulative distribution of differences at Nieuwpoort
M2 2σ=0.000 m
CSM 2σ=0.410 m
NOS 2σ=0.448 m
BCZ 2σ=0.450 m
OMN 2σ=0.310 m
0
0.2
0.4
0.6
0.8
1
-0.4
-0.2
0
0.2
0.4

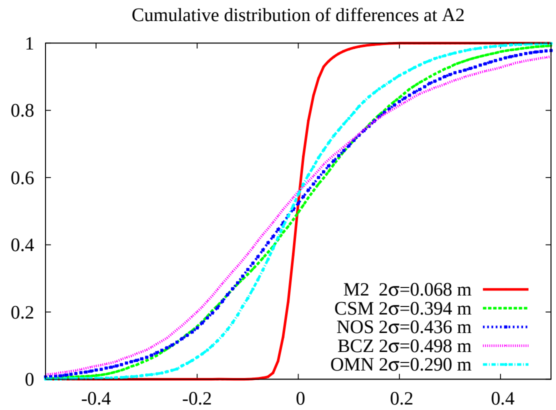
Cumulative distribution of differences at A2
M2 2σ=0.068 m
CSM 2σ=0.394 m
NOS 2σ=0.436 m
BCZ 2σ=0.498 m
OMN 2σ=0.290 m
0
0.2
0.4
0.6
0.8
1
-0.4
-0.2
0
0.2
0.4

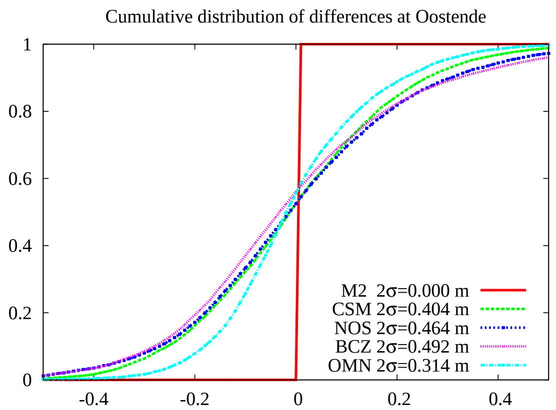
Cumulative distribution of differences at Oostende
M2 2σ=0.000 m
CSM 2σ=0.404 m
NOS 2σ=0.464 m
BCZ 2σ=0.492 m
OMN 2σ=0.314 m
0
0.2
0.4
0.6
0.8
1
-0.4
-0.2
0
0.2
0.4

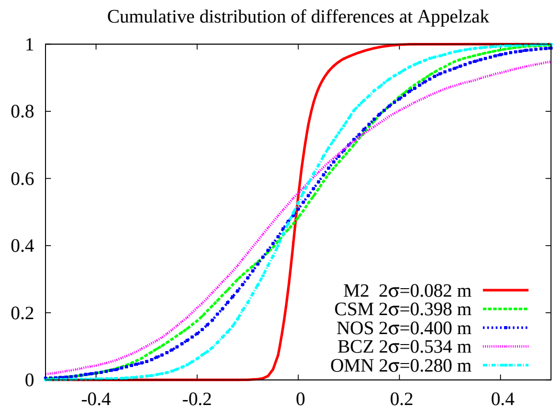
Cumulative distribution of differences at Appelzak
M2 2σ=0.082 m
CSM 2σ=0.398 m
NOS 2σ=0.400 m
BCZ 2σ=0.534 m
OMN 2σ=0.280 m
0
0.2
0.4
0.6
0.8
1
-0.4
-0.2
0
0.2
0.4

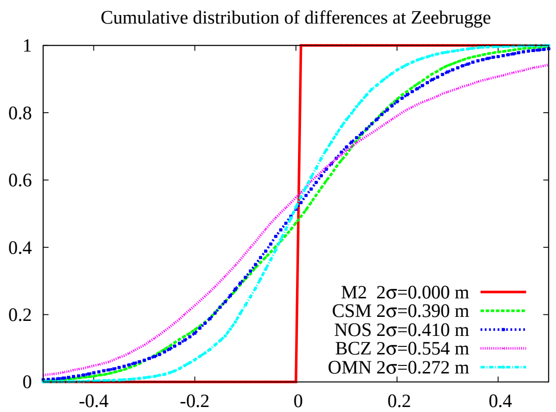
Cumulative distribution of differences at Zeebrugge
M2 2σ=0.000 m
CSM 2σ=0.390 m
NOS 2σ=0.410 m
BCZ 2σ=0.554 m
OMN 2σ=0.272 m
0
0.2
0.4
0.6
0.8
1
-0.4
-0.2
0
0.2
0.4

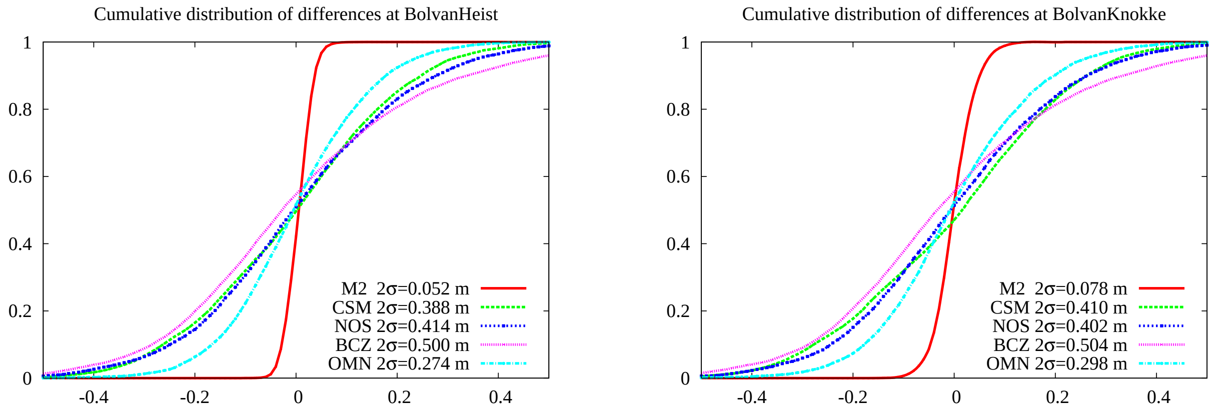


**Figure 11:** Cumulative distribution of the differences between the results of the various models (M2, CSM, NOS, BCZ, OMN) and the observations at the nine stations of the Meetnet Vlaamse Banken. Differences, along the x axis, are in meter and the range is equal to $[-0.5,+0.5]$ m.

Results of the M2 tidal reduction at the reference stations do not need to be discussed (errors are equal to 0 all the time).

At all offshore stations and for all estimators, the method is clearly more efficient than all the operational models. Errors slightly increase with the distance between the point at sea and the reference station. At Westhinder, $2\sigma$ is equal to 0.13 m. Thus $\sigma$ is well below 0.1 m as requested by the Dutch and Belgian Hydrographic Services.

In calm weather conditions (when the signal is clearly dominated by the tide), the success of the M2 tidal reduction method does not come only from the fact that the semi-diurnal lunar $M_2$ tide dominates in the area of interest. It also comes from the fact that over a relatively small area and far away from amphidromic points, all other important constituents in the semi-diurnal frequency band are spatially distributed nearly as the $M_2$ (the ratio between their amplitude and that of the $M_2$ and the difference between their phase and that of the $M_2$ remain almost constant in the area). Results obtained in this study seem to indicate that the method is also quite efficient even when the weather is not particularly calm.

Amongst the various hydrodynamic models we have considered, the most efficient seems to be the OMNECS 2D storm surge model while the less one seems to be Optos_BCZ. In OMN results, the percentage of differences in the range [-0.1,+0.1] m is above 50% almost at all stations except at Wandelaar (47%). In all other models, that percentage is les than 50% at all stations.

For OM and CSM, the estimator $2\sigma$ turns around 0.3 m and 0.4 m, respectively. More variability is observed in the results of NOS and BCZ with, for this latter, some values of $2\sigma$ above 0.5 m.

Regarding the cumulative distribution of the differences between model results and observations at the stations (Figure 11), we also note that the 2D models (OMN and CSM) perform better than the 3D models (NOS and BCZ). For OMN, more than 99% of the differences are in the range $[-0.5,0.5]$ m at all stations. For CSM, this percentage is also around 99% (the smallest value, 98.4% is observed at Ostend).

The reasons why the operational models are today less efficient than the M2 method as well as all the model improvements foreseen to reduce the discrepancies between the different methods have already been presented and discussed.

### 2.3.3 Comparison of $M_2$ characteristics in Belgian Coastal waters

#### 2.3.3.1 Introduction

In this section, we analyze amplitude and phase of the $M_2$ first at the nine stations of the Meetnet Vlaamse Banken and afterwards over the area already covered by the $M_2$ method. The objective of this investigation is to see whether or not amplitude and phase of the $M_2$ extracted from the results of the operational models can help to extend the area actually covered by the M2 method.

The section is divided in two parts.

In a first part, amplitudes and phases are compared at the stations. Moreover, new time series are generated as should be done with the M2 method but now using $M_2$ parameters (amplitude and phase) determined by the analysis of OMN and CSM models. These time series are compared to the observations as done in the previous section.

In the second part, the amplitude and phase of the $M_2$ determined at each node of the OMNECS grid are compared to those used in the M2 method.

#### 2.3.3.2 Comparison at the stations

A harmonic analysis of all time series used within the framework of this study has been performed using the software package developed by Mouchet at the end of the eighties (Mouchet, 1990).

Results for the $M_2$ amplitude are presented on Figure 12 and those for its phase on Figure 13.

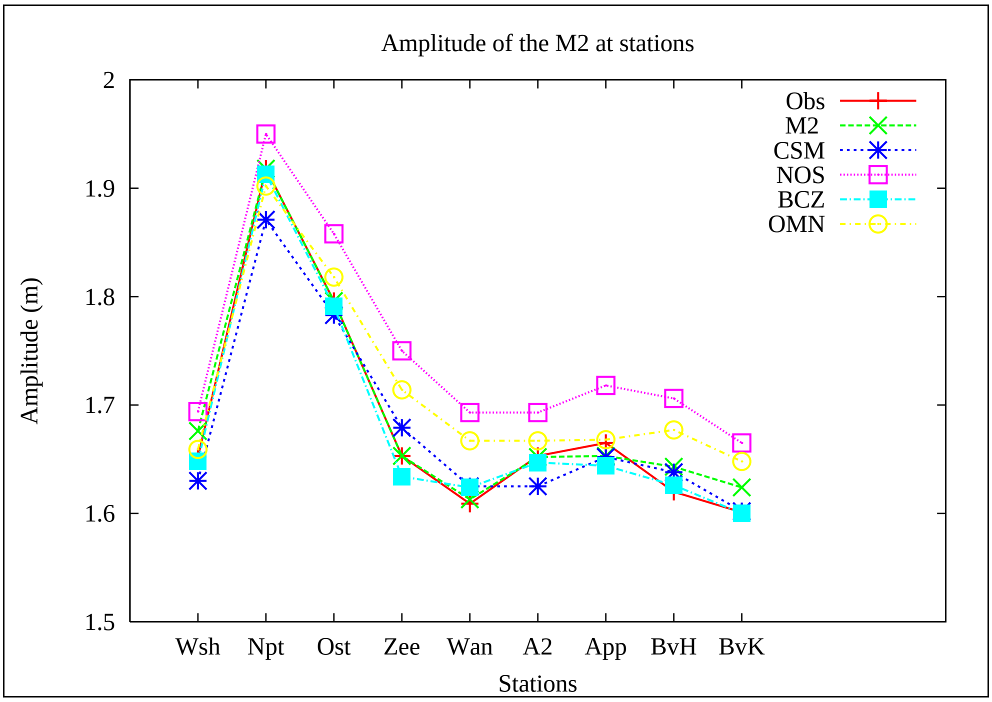


**Figure 12:** Amplitude (m) of the $M_2$ at the various stations extracted by harmonic analysis of the different time series used in this study.

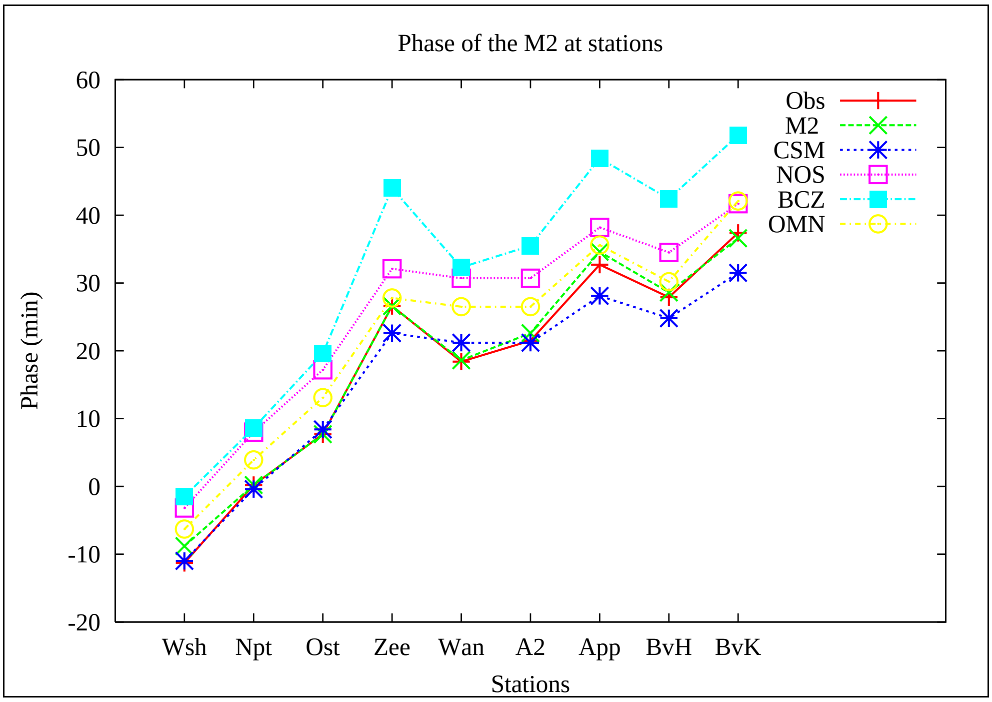


**Figure 13:** Phase (min) of the $M_2$ at the various stations extracted by harmonic analysis of the different time series used in this study. The phase here is the so-called Greenwhich phase lag (expressed in minutes instead of degrees). Lines and symbols are as in Figure 12.

As expected, as well for the amplitude as for the phase, the M2 method is the closest to the observations at all stations. Concerning the models, NOS is the one which is the most away from the observations for the amplitude while for the phase it is BCZ. Phases of CSM are quite close to the observations.

To quantify the agreement between the various models and the observations at the $M_2$ frequency, we consider the amplitude of the differences. For each model, this amplitude reads (see Jamart and Ozer, 1989):

$$\Delta_{\text{mod}} = \sqrt{\left(a_{obs}^2 + a_{\text{mod}}^2 - 2a_{\text{mod}} a_{obs} \cos(\varphi_{obs} - \varphi_{\text{mod}})\right)}$$

where, as usually, the subscript mod refers to one model (M2, CSM, NOS, BCZ, OMN) and the subscript *obs* refers to the observations. $\Delta_{\text{mod}}$ is the amplitude of the differences at the frequency of the $M_2$ for a given model, *a* and $\varphi$ being the amplitude and phase at this frequency.

The amplitudes of the differences are presented on Figure 14.

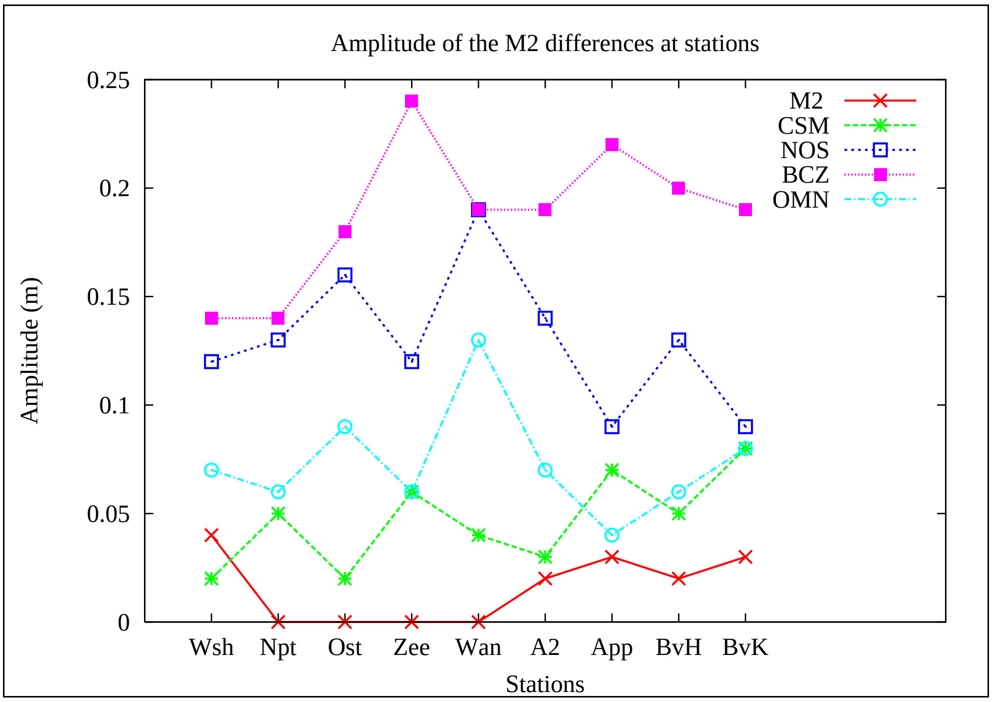


**Figure 14:** Amplitude (m) of the differences at the $M_2$ frequency at the different stations and for the various modeling approaches.

Averaged over the nine stations, the amplitude reads:

**Table 3:** Mean amplitude of the differences at the $M_2$ frequency at the stations for the different reduction methods.

| | |
|---|---|
| $M_2$ | 0.016 m |
| CSM | 0.046 m |
| NOS | 0.130 m |
| BCZ | 0.190 m |
| OMN | 0.074 m |

For the $M_2$ method, the amplitude is rather small at the offshore stations (less than 0.02 m in average). The largest value (0.04 m) is observed at the Westhinder station.

Regarding the hydrodynamic models, the best results at the $M_2$ frequency are those provided by CSM while the worst are those coming from BCZ (more than likely due to the phase shift observed on Figure 13).

Knowing amplitude and phase of the $M_2$ in the models, we can use this information to generate time series at the stations as done with the M2 method and to compare these time series with the observations as done with the time series provided by the operational models. This exercise has been performed only for the two 2D storm surge models (CSM and OMN) as these two models have the smallest error at the $M_2$ frequency. In what follows, we will refer to these "new models" as CSMM2 and OMNM2, respectively.

For one model, the time series at one station is generated using the following equation:

$$\eta_{\mathrm{NAP}}^{\mathrm{mod}}(\vec{s},t) = \frac{a_{M_2}^{\mathrm{mod}}(\vec{s})}{a_{M_2}^{obs}(\vec{s}_r)} \eta_{\mathrm{NAP}}^{obs}(\vec{s}_r, t - (f_{M_2}^{\mathrm{mod}}(\vec{s}) - f_{M_2}^{obs}(\vec{s}_r)))$$

where the superscript mod will identify CSMM2 or OMNM2. The variables and symbols used in this equation have the same meaning than in the equation used in the M2 tidal reduction method (see the description of that method). Results for the percentage of differences in the range [-0.1,+0.1] m are presented on Figure 15, those for two times the standard deviation ($2\sigma$ in m) on Figure 16 and the cumulative distribution of the differences on Figure 17.

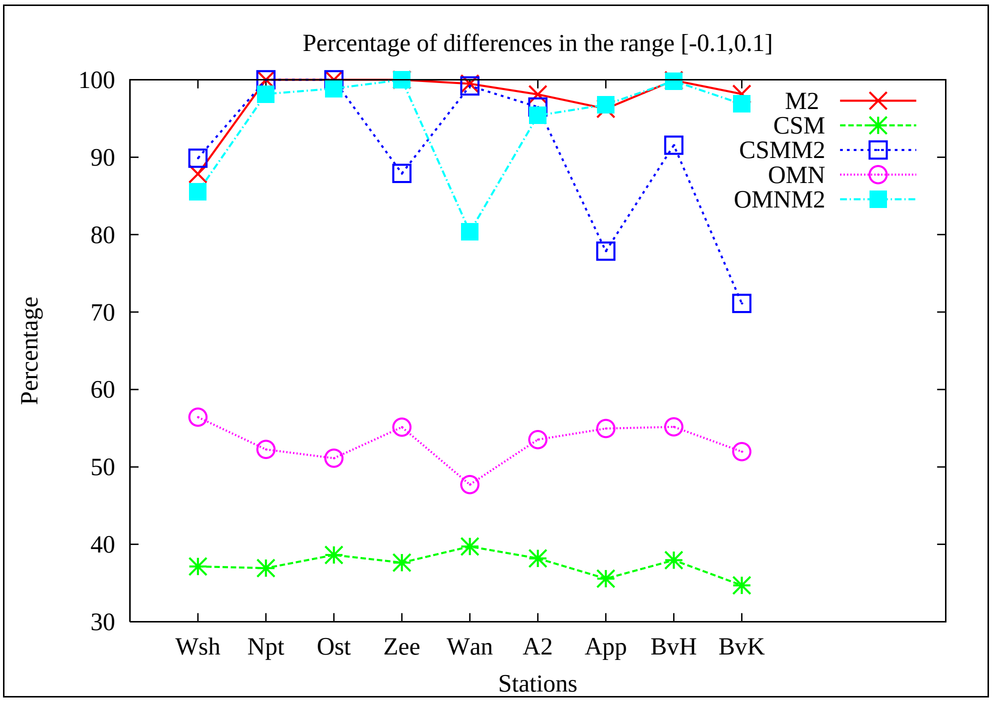


**Figure 15:** Percentage of differences in the range [-0.1,+0.1] m. Results are presented for the M2 method (M2), the CSM model, the time series generated using amplitude and phase of the $M_2$ of the CSM model (CSMM2), the OM model and the time series generated using amplitude and phase of the $M_2$ of this latter model (OMNM2).

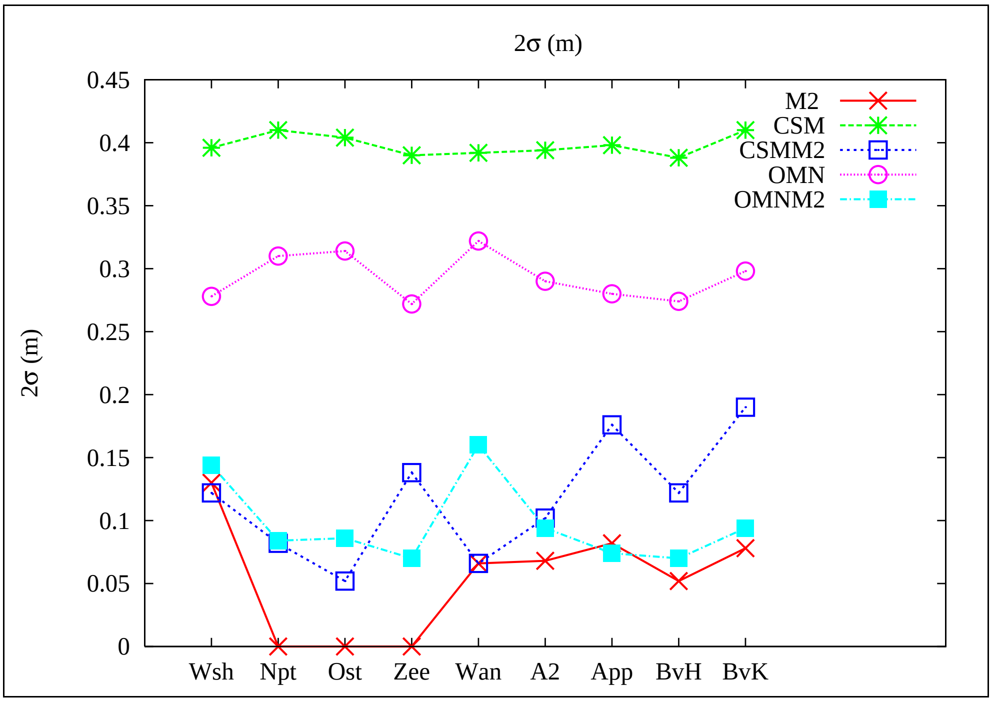


**Figure 16:** Two times the standard deviation of the differences ($2\sigma$ in m) computed over the three months period. Lines and symbol are as for Figure 15.

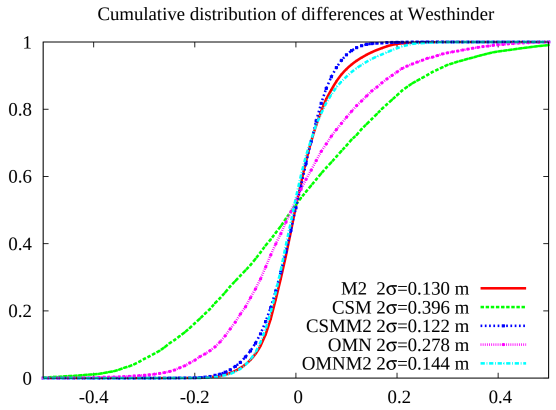
Cumulative distribution of differences at Westhinder
M2 2σ=0.130 m
CSM 2σ=0.396 m
CSMM2 2σ=0.122 m
OMN 2σ=0.278 m
OMNM2 2σ=0.144 m

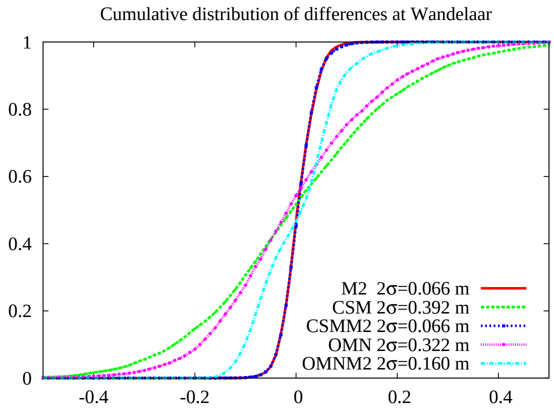
Cumulative distribution of differences at Wandelaar
M2 2σ=0.066 m
CSM 2σ=0.392 m
CSMM2 2σ=0.066 m
OMN 2σ=0.322 m
OMNM2 2σ=0.160 m

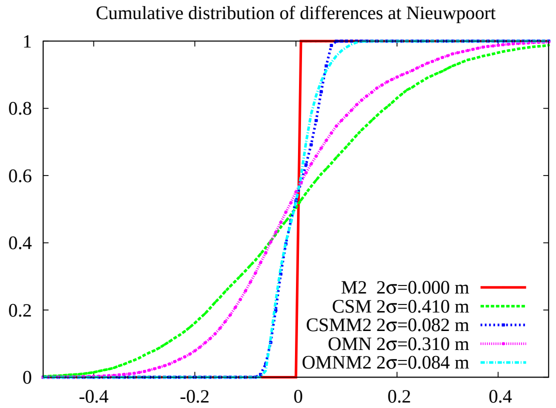
Cumulative distribution of differences at Nieuwpoort
M2 2σ=0.000 m
CSM 2σ=0.410 m
CSMM2 2σ=0.082 m
OMN 2σ=0.310 m
OMNM2 2σ=0.084 m

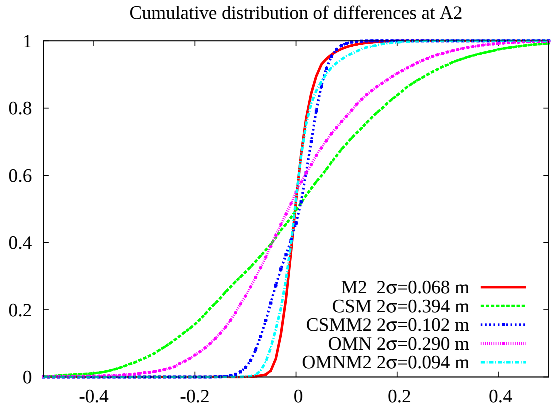
Cumulative distribution of differences at A2
M2 2σ=0.068 m
CSM 2σ=0.394 m
CSMM2 2σ=0.102 m
OMN 2σ=0.290 m
OMNM2 2σ=0.094 m

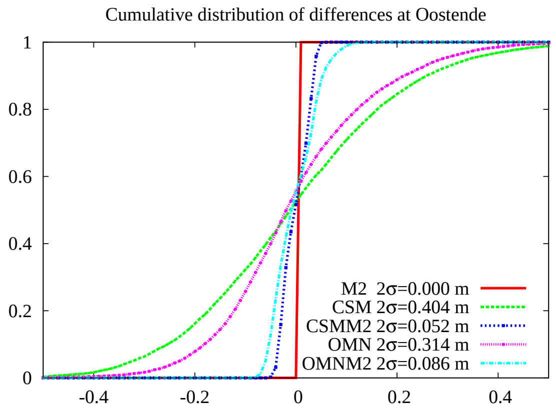
Cumulative distribution of differences at Oostende
M2 2σ=0.000 m
CSM 2σ=0.404 m
CSMM2 2σ=0.052 m
OMN 2σ=0.314 m
OMNM2 2σ=0.086 m

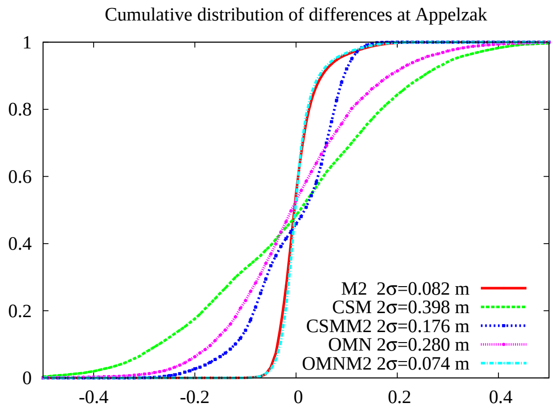
Cumulative distribution of differences at Appelzak
M2 2σ=0.082 m
CSM 2σ=0.398 m
CSMM2 2σ=0.176 m
OMN 2σ=0.280 m
OMNM2 2σ=0.074 m

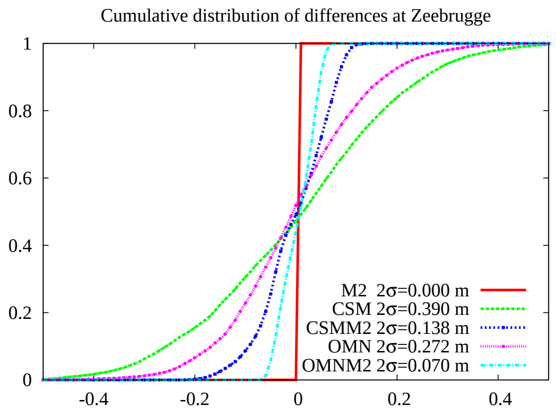
Cumulative distribution of differences at Zeebrugge
M2 2σ=0.000 m
CSM 2σ=0.390 m
CSMM2 2σ=0.138 m
OMN 2σ=0.272 m
OMNM2 2σ=0.070 m

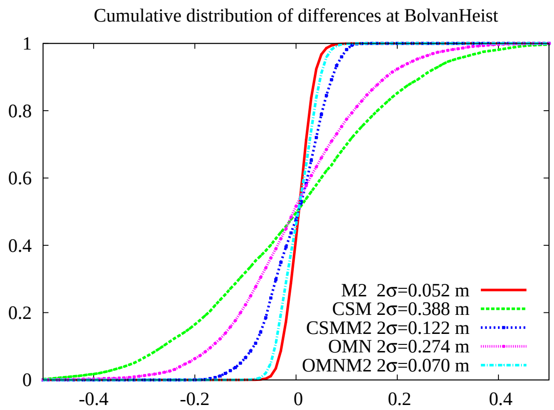
Cumulative distribution of differences at BolvanHeist
M2 2σ=0.052 m
CSM 2σ=0.388 m
CSMM2 2σ=0.122 m
OMN 2σ=0.274 m
OMNM2 2σ=0.070 m

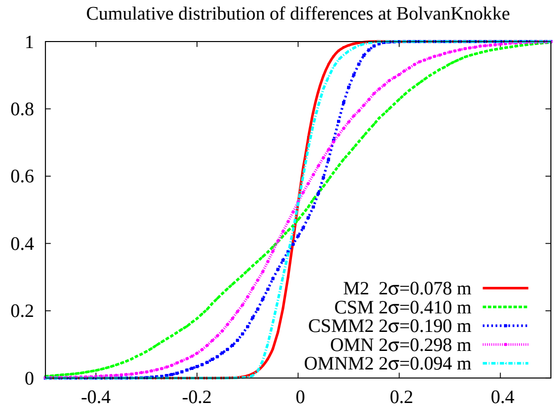


**Figure 17:** Cumulative distribution of the differences between the results of various models (M2, CSM, CSMM2, OMN, OMNM2) and the observations at the nine stations of the Meetnet Vlaamse Banken. Differences, along the x axis, are in meter and the range is equal to $[-0.5,+0.5]$ m.

For all estimators and all stations we do observe a significant improvement in the results obtained with the so-called M2 model reduction method with respect to the results of the operational models. There is more variability in the performances of the CSMM2 than in those of OMNM2 (especially in the area around Zeebrugge). This is partly surprising because the amplitude of the errors at the $M_2$ frequency were smaller at all stations with CSM than with OMN (see Figure 13). However there seems to be a significant correlation with the phase of the $M_2$ (see Figure 13). For instance, it is at the station Wandelaar that the largest discrepancies are observed in the results of OMNM2 (this was already the case with OMN) and it is also at this station that the $M_2$ phase in the OMN results was the most apart with respect to the phase in the observations.

If we consider the percentage of differences in the range $[-0.1,+0.1]$ m, results of OMNM2 are almost undistinguishable with respect to those of M2 at all stations except Wandelaar. CSMM2 performs nearly as well as M2 at 5 stations (Wsh, Npt, Ost, Wan and A2). It is less efficient at the others.

For $2\sigma$, there are various stations at which the value, as well in OMNM2 as in CSMM2, is less than 0.15 m. The exceptions are: Wandelaar for OMNM2, Appelzak and Bol van Heist for CSMM2. At several stations, $\sigma$ less than 0.1 m for both models as required by the developers of the M2 method.

Cumulative distributions of the differences between OMNM2 and CSMM2 provide a similar information. Now, 100% of the differences are in a range that is, at all stations, smaller than $[-0.5,0.5]$ m.

### 2.3.3.3 On the Belgian Continental Shelf

One of the operational models, OMN, has been run driven by tide only for a one year period and results analyzed using the software package developed by Mouchet (Mouchet, 1990). Results covering a one year period, amplitude and phase of a lot of tidal constituents have been determined. In this section, the focus is only on the amplitude and phase of the $M_2$ tide and on the comparison with the values used in the M2 tidal reduction method.

A similar approach is foreseen for the CSM model. Recall that at the stations, the smallest amplitudes of the $M_2$ differences were obtained with this model.

Amplitude and phase (in fact, at each point, the difference between the OMN $M_2$ phase and the observed $M_2$ phase at Ostend) are presented on Figure 18 and on

Figure 19, respectively. Similarities with the input data used in the M2 tidal reduction method are obvious (see Figure 3 and Figure 4).

The amplitude decreases from West to East as well as in the offshore direction. Over the whole BCS it is varying between slightly more than 2 meters in the southwest corner and slightly less than 1 meter at the northern limit.

The tide propagates from West to East. Along the coast, the time require to go from the French border to the Dutch border is approximately equal to 50 minutes.

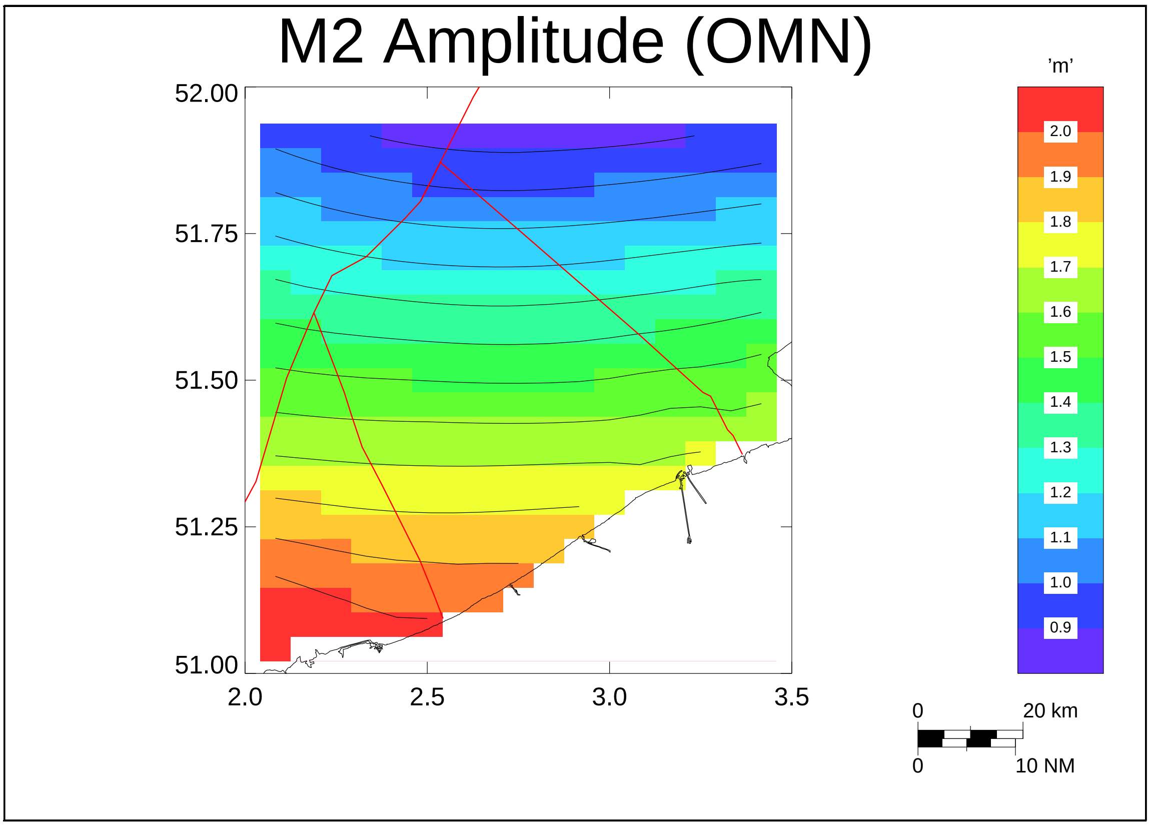


**Figure 18:** Amplitude (m) of the $M_2$ obtained by the analysis of the results of a one year long run of OMN. In this run, the only forcing was the tide along the open boundary.

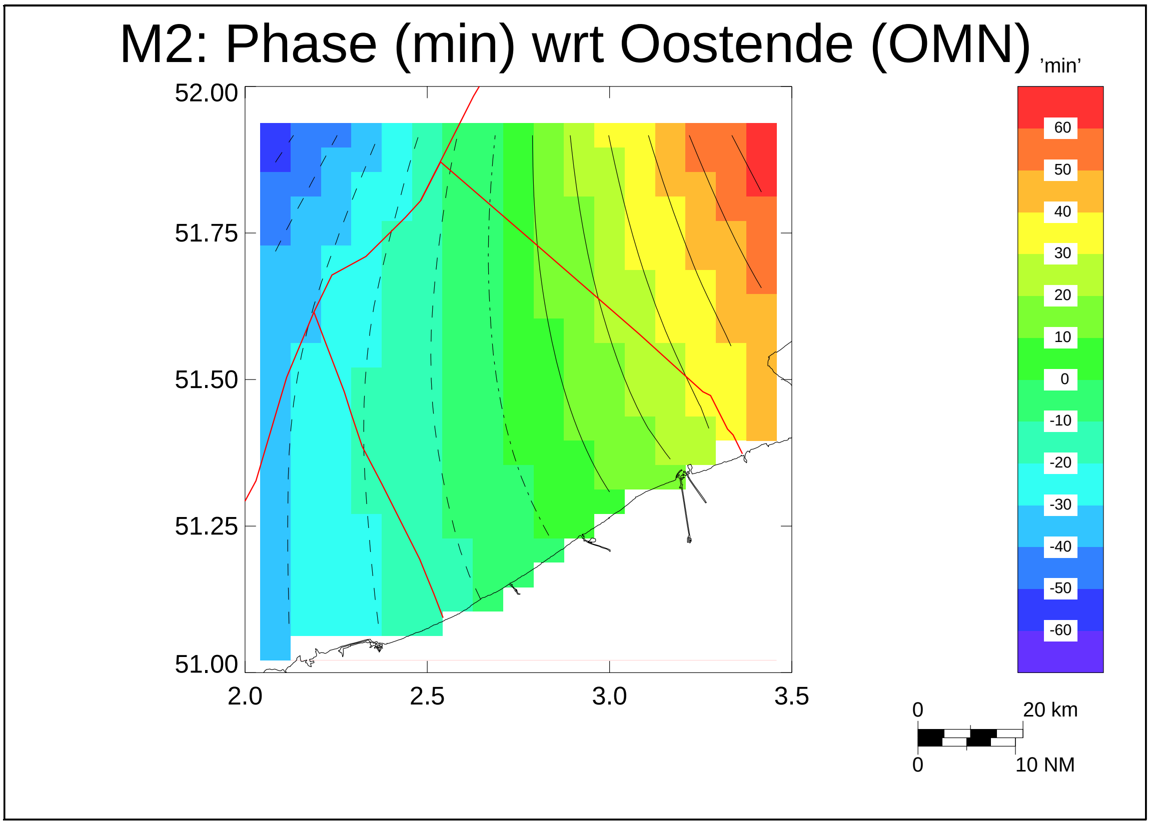


**Figure 19:** Difference (in min) between the phase of the $M_2$ obtained by the analysis of the results of a one year long run of OMN and the phase of the $M_2$ at Ostend. In the model run, the only forcing was the tide along the open boundary.

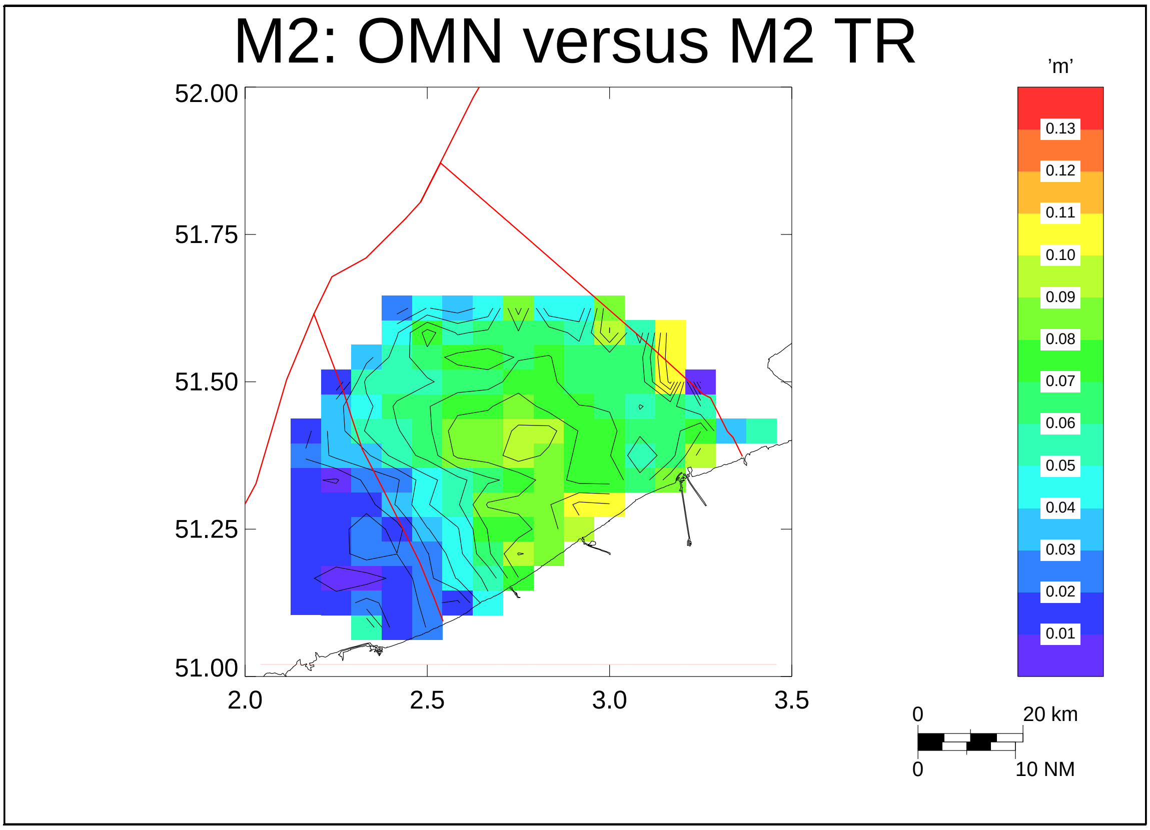


**Figure 20:** Amplitude of the differences between OMN and the M2 tidal reduction at the frequency of the $M_2$ tide.

As done at the stations, the amplitude of the differences at the frequency of the $M_2$ between OMN and the M2 tidal reduction method has been computed at each node of the OMN grid in the area both method have in common. For the sake of completeness, the equation used for this computation is given below:

$$\Delta_{\mathrm{OMN}} = \sqrt{\left(a_{\mathrm{M2}}^2 + a_{\mathrm{OMN}}^2 - 2a_{\mathrm{OMN}}a_{\mathrm{M2}}\cos(\varphi_{\mathrm{M2}} - \varphi_{\mathrm{OMN}})\right)}$$

where the subscript OMN refers to the OMNECS model and the subscript M2 to the M2 tidal reduction method. Results are presented on Figure 20.

Over the area, the amplitude of the differences is varying between 0.001 m and 0.130 m with an average value equal to 0.055 m. The largest values are observed in the central part of the area (along a line perpendicular to the coast and starting at the east of Ostend) while the smallest values are observed along the borders of the BCS (in particular the western border).

## 2.4 SUMMARY AND CONCLUSIONS

In this chapter, a summary of the work done on the comparison between the results of the M2 tidal reduction method (Van Cauwenberghe *et al.*, 1993) and those of some operational storm surge models (Pison and Ozer, 2003; Van den Eynde *et al.*, 1998) has been presented.

Main objectives of the study were to provide elements to answer the two following questions:

- could results of operational storm surge models be an option for a correction in real time of depth soundings made on board of research vessels (*e.g.*, the BELGICA)?
- could the information on the $M_2$ tide provided by these models help to extend the area actually covered be the M2 method?

A relatively detailed description of the different methods has been presented. Strengths and weaknesses of all the methods have been discussed.

Simply recall that, in the M2 method, one assumes that the sea surface elevation with respect to Mean Sea Level (in fact NAP) at any point at sea can be computed from the observed sea surface elevation at one of the coastal stations (Nieuwpoort, Ostend and Zeebrugge) using only the characteristic (amplitude and phase) of the $M_2$ tide. One reference station is attached to each point at sea. Input data to the method are given on a grid with a horizontal resolution equal to 1 km in both directions (eastward and northward). A matrix with the distance between NAP and LAT at each node of the grid is provided as well.

Up to four operational models have been considered in this study. Three of them come from MUMM suite of operational hydrodynamic models referred to as OPTOS. One is the 2D storm surge model used by MDK for its own evaluation of the risk of flood.

OPTOS include a 2D barotropic storm surge model (CSM) covering the whole Northwest European Continental Shelf with a resolution of the order of 6 km and two 3D baroclinic models, one covering the North Sea from 4° West to 57° North (NOS) with the same horizontal resolution as CSM and one (BCZ) covering an area slightly greater than the BCS with a horizontal resolution of the order of 750 m. A one way nesting is used to couple these three models. The tidal forcing is introduced along the open boundary of Optos_CSM. The three models are forced by numerical weather forecast coming from Met Office. The forecast model horizon is equal to 5 days.

The area covered and the horizontal resolution of the MDK storm surge model (OMN) are as in CSM. Main differences are: i) some differences in the introduction of the tidal forcing along the open boundary, ii) introduction of the inverse barometric effect in the forcing along the open boundary, iii) an implicit alternate direction time integration scheme instead of an explicit one. The forecast horizon for OMNECS is 4 days.

The comparative study of the results provided by the different models (including the M2 tidal reduction method) is divided in two parts.

In the first part, the time series generated by the different models are compared to the observations at nine stations (3 coastal and 6 offshore) of the Meetnet Vlaamse Banken. Time series cover a three months period (September – November 2009). Time averaged values over that period are first removed from all time series. Three global estimators are used: the percentage of differences in the range [-0.1,+0.1] m, two times the value of the standard deviation of the differences ($2\sigma$) and, at each station, the cumulative distribution of the differences between the results of the different methods and the observations in the range $\left[-0.5,0.5\right]$ m.

In the second part, the focus is on the characteristics of the $M_2$ tide as well at the stations as in the area covered by the M2 method. At stations, amplitude and phase of the $M_2$ in the observations and in the results of the models have been obtained by a harmonic analysis of the time series. On the Belgian Continental Shelf, amplitude and phase for one model (OMNECS) are coming from the harmonic analysis of the results of a one year run of the model driven by tide only. At the stations, the amplitude of the differences between the models and the observations at the frequency of the $M_2$ is computed. Moreover, new time series are generated for the two 2D storm surge models (Optos_CSM and OMNECS) using only the amplitude and phase of the $M_2$ and proceeding like in the M2 method. These time series have been compared to the observations as done with those of the operational models. In the area covered by the M2 method, the amplitude of the differences between OMNECS and the M2 method is also computed.

The main conclusions of this comparative study can be summarized as follows:

- regarding the time series at the stations:
  - in the M2 method , the errors increase slightly with the distance between the point at sea and the reference station. The largest errors are observed at the station Westhinder where $2\sigma$ is equal to 0.13 m. At this station, the smallest $2\sigma$ value (0.28 m) in the results of the operational models is obtained with OMN;
  - the 2D storm surge models performed better than the 3D baroclinic models. The largest $2\sigma$ values (above 0.5 m at stations around Zeebrugge) are observed in the results of BCZ (more than likely due to the phase shift in the results of this model);
  - in the cumulative distribution of the differences between model results and observations at the stations, we also note that the 2D models (OMN and CSM) perform better than the 3D models (NOS and BCZ). For OMN, more than 99% of the differences are in the range $\left[-0.5,0.5\right]$ m at all stations. For CSM, this percentage is also around 99% (the smallest value, 98.4% is observed at Ostend).
- regarding the amplitude and phase of the $M_2$ at the stations:
  - amplitude an phase at stations used in the M2 method are very close to those obtained by harmonic analysis of the observations;
  - amongst the models, the amplitudes in BCZ are the closest to the observations while these in NOS have the largest distance apart with respect to the observations. The two 2D models are in between;
  - for the phase, CSM is relatively close to the observations and the M2 method. OMN is better than the two 3D baroclinic models. For these two

models, the phases are almost the same up to Ostend but at the east of that station, BCZ phases become quite bad.

- regarding the amplitude of the differences at the M2 frequency, averaged values over the stations read: 0.016 m (M2), 0.046 m (CSM), 0.13 m (NOS), 0.19 m (BCZ) and 0.074 m (OMN).

- regarding the time series generated as done in the M2 method but now with the amplitude and phase of CSM and OMN, the so-called model M2 reduction method (CSMM2 and OMNM2, respectively):
  - a significant improvement with respect to the results obtained with the operational model is observed for all estimators and all stations;
  - there is more variability in the accuracy of the results of CSMM2 than in those of OMNM2;
  - concerning the percentage of differences in the range $[-0.1,+0.1]$ m, results of OMNM2 are almost undistinguishable from those of M2 at all stations except Wandelaar. CSMM2 performs as well as M2 at 5 stations (Wsh, Npt, Ost, Wan and A2). It is less efficient at the others;
  - apart at station Wandelaar for OMNM2 and at stations Appelzak and Bol van Heist for CSMM2, all other values of $2\sigma$ are smaller than 0.15 m.
  - for both models and all stations, all differences are in a range which is clearly smaller than the range $[-0.5,+0.5]$ m.

- concerning the comparison of the amplitude and phase of the $M_2$ between OMN and the M2 method in the area covered by the latter:
  - there are clear similarities in the spatial distribution of these two quantities even if there is a shift as well for the phase as for the amplitude;
  - the amplitude of the differences is the largest along a line perpendicular to the coast starting just to the east of Ostend. That amplitude decreases towards the borders of the area (more towards the western border than towards the eastern border).

The comparative study has provided a lot of information regarding the accuracy of the different approaches. Such an information is of primary importance for the end users.

In a near future, it will be possible to extend the study of the accuracy of the different methods using the water levels measured by the RTK/LRK method installed on board the BELGICA and stored in the ODAS data base.

## 2.5 REFERENCES

De Moor, 2002. Evaluation de la morphodynamique sous-marine en Mer du NORD méridonnale au cours de la période 1985-1995. Géomorphologie : relief, processus , environnement, 2 : 135-150.

Jamart, B.M., and J. Ozer, 1989. Some results and comments on the Tidal Flow Forum exercise. Advances in Water Ressources, Vol. 12, No.4, 211-220.

Luyten P.J., Jones J.E., Proctor R., Tabor A., Tett P., Wild-Allen K., 1999. COHERENS documentation: A coupled hydrodynamical-ecological model for regional and shelf seas: user documentation, MUMM, Brussels.

Luyten, P., Andreu-Burillo I., Norro A., Ponsar S. and Proctor R., 2005. A New Version of the European public Domain Code COHERENS, in Proceedings of the Fourth International Conference on EuroGOOS, 6-9 June 2005, Brest, France.

Lyard, F., F. Lefèvre, T. Letellier and O. Francis, 2006. Modelling the global ocean tides: a modern insight from FES2004. Ocean Dynamics, Vol. 56, No. 5-6: 394-415.

Mouchet, A., 1990. Analysis of Tidal Elevations and Currents along the Belgian Coasts. Final Report, December 1990. Study supported by MUMM (Unité de Gestion du Modèle Mathématique de la Mer du Nord et de l'Estuaire de l'Escaut), Ministère de la Santé Publique, Réf. BH/88/29.

Norro, A., G. Pichot, V. Pison and J. Ozer, 2006. A bi-dimensional approach to assessing the volumetric evolution of an exploited sandbank. ICES Journal of Marine Sciences, 63: 176-186.

Ozer, J., D. Van den Eynde and S. Ponsar, 2008. Trend analysis of the relative mean sea level at Oostende (Southern North Sea – Belgian coast). Technical Report CLIMAR/X/JO/200807/EN/TR3, Report prepared in the framework of the CLIMAR project for the Belgian Science Policy, Contract SD/NS/01A, Management Unit of the North Sea Mathematical Models, Brussels, 13 pp.

Pison, V., and J. Ozer, 2003. Operational products and services for Belgian coastal waters. In: H. Dahlin, N.C. Flemming, K. Nittis and S.E. Peterson (editors), Building the European Capacity in Operational Oceanography. Proceedings of the Third International Conference on EuroGOOS. Elsevier Oceanography Series, 69, pp 503-509.

Ponsar, S. and P. Luyten, 2009. Data assimilation with the EnKF in a 1-D numerical model of a North Sea station, Ocean Dynamics, DOI 10.1007/s10236-009-0224-3.

Poppe, H., 2007. Waar ligt het Nul niveau op Zee. De Grote Rede, Nr. 20, November 2007.

Van Cauwenberghe, C., Dekker L. and Schuurman A., 1993. M2 tidal reduction method for coastal zones. Rapport nr. 33 van de Hydrografische Dienst der Kust.

Van den Eynde, D., J.P. Malisse, J. Ozer and S. Scory, 1998. Operational Modelling of the Northwest European Continental Shelf (OMNECS): Gebruikershandleiding. Voorbereid voor Administratie Waterwegen en Zeewezen, Rapport OMNECS/0/XX/ 199809/NL/TR/3.1, 83 pp.

Yang Lianwu, and J. Ozer, 1997. An ADI technique for solving three-dimensional coastal circulation. Acta Oceanologica Sinica. Vol. 16, No. 3, 281-302.

# 3. Analysis of the coherence between RTK / LRK and the $M_2$ method

## 3.1 Introduction

This project aims at determining the relation between the LAT (Lowest Astronomical Tide) surface used as reference surface for bathymetric depths on the Belgian continental shelf and the heights related to the WGS84 ellipsoid. (The WGS84 ellipsoid can be considered as being equal to the GRS80 ellipsoid and all the calculations are done on the GRS80 ellipsoid. So in the following report we only talk about the GRS80 ellipsoid.) The principal motivation is to directly apply GPS positioning methods to bathymetric measurements in order to obtain sea floor topography in real time.

## 3.2 Principle

Hydro-oceanographic ships sounding the depths with echo sounders use the positioning method based on the processing of GPS signals in LRK (Long Range Kinematic) mode. The GPS technique is associated with the WGS84 terrestrial reference system (World Geodetic System 1984). In this three-dimensional system, coordinates are expressed in longitudes, latitudes and ellipsoidal heights.

LAT is defined as the lowest astronomical tidal prediction in a time span of at least 18.6 years. In the current study this level is with reference to the NAP (Normaal Amsterdams peil) plane. We will call this the NAPtoLAT model. Based on the height conversion model hBG03 , the GRStoNAP model was created. This model provides the height differences between the NAP and the ellipsoid (GRS80) of a terrestrial reference system. Using the "LAT" model which we will call NAPtoLAT, you can then go from the NAP to the lowest astronomic tides.

Figure 21 illustrates in a schematic way the relations existing between the various vertical reference systems

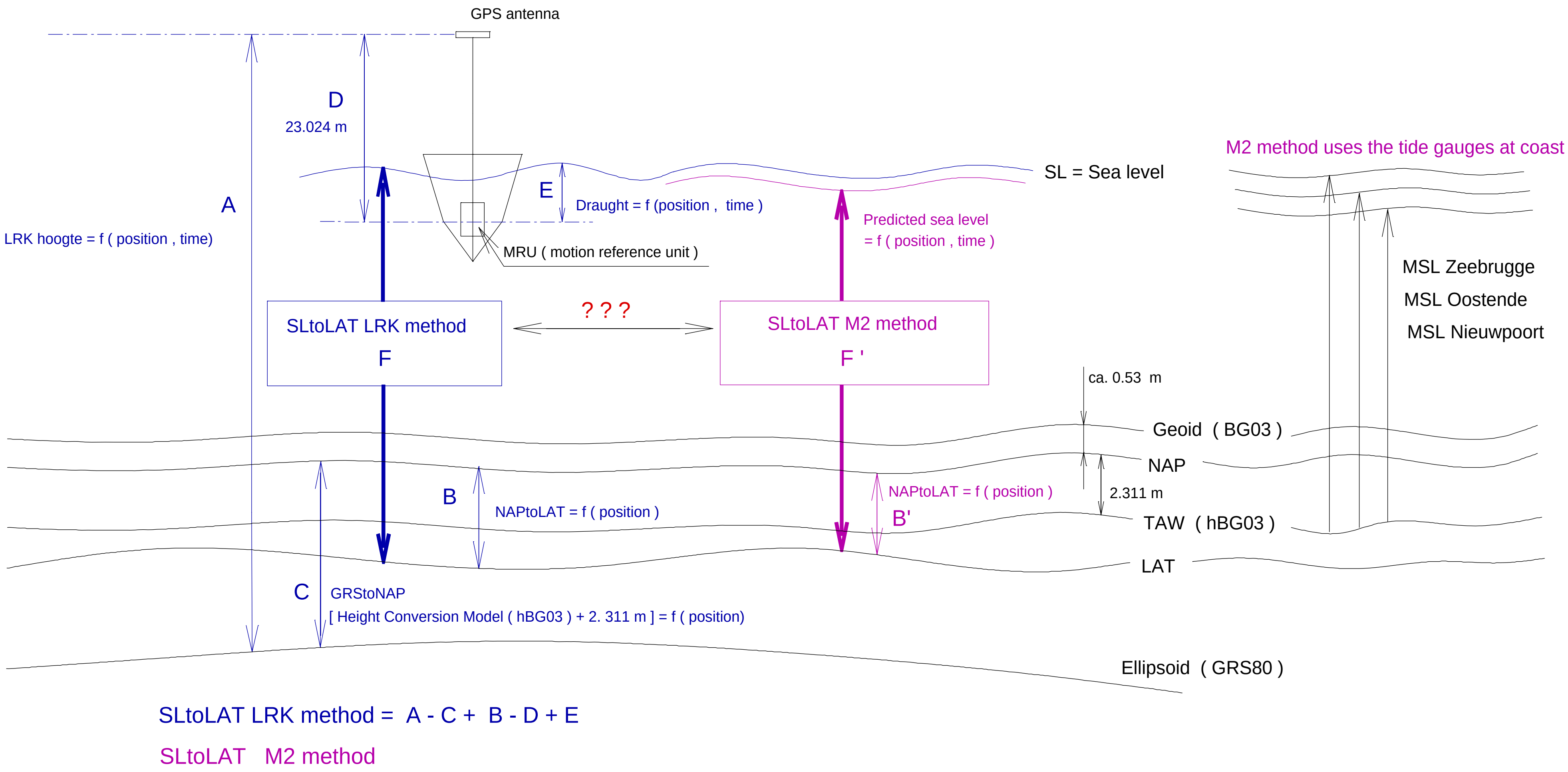


**Figure 21:** Overview of the vertical reference levels in the Belgian Continental Zone area and the two sea level calculation methods (M2 and LRK)

## 3.3 THE CONVERSION MODELS

There are two conversion models :

The GRStoNAP model (value C, Figure 21) is based on the height conversion model hBG03. This height conversion model hBG03 is based on the geoidal model BG03. The BG03 geoidal model (Belgian Geoid 2003) was achieved by the Royal Observatory of Belgium in partnership with the Polytechnical University of Milan. You will find herewith the article « Quasi-geoid BG03 computation in Belgium », by R. Barzaghi, A. Borghi, B. Ducarme, M. Everaerts

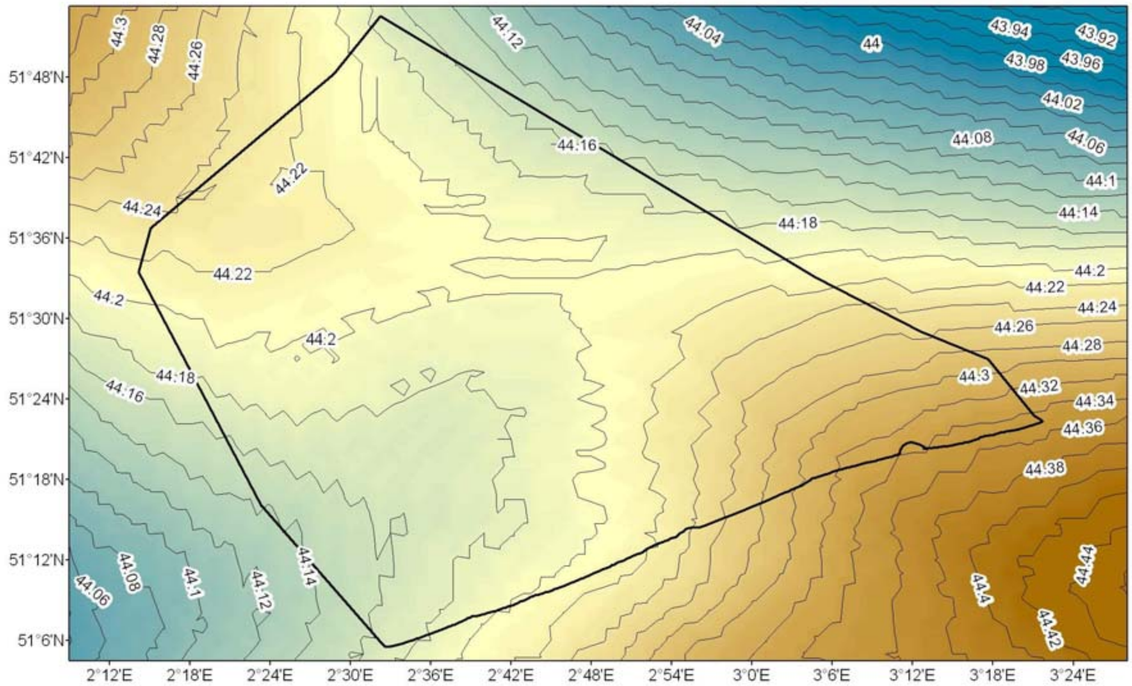


**Figure 22:** GRStoNAP model.

The NAPtoLAT (Lowest Astronomical Tide) model (value B, Figure 21) was achieved by the "*Waterwegen Kust – Hydrographie*" section of the Flemish "*Waterwegen en Zeewezen*" administration.

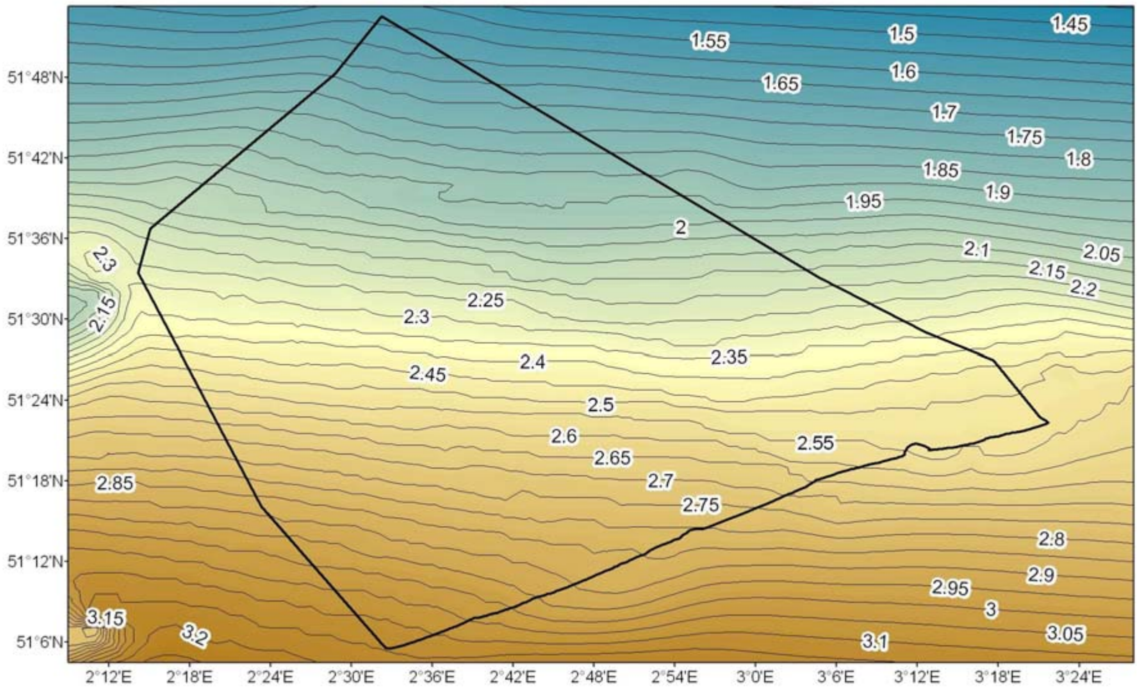


**Figure 23 :** NAPtoLAT model.

For practical reasons, both surfaces above have been readjusted to the Belgian continental shelf in order to represent two regular rectangular grids with the same grid densities in longitude and in latitude (0.01666667° degree square) and whose nodes are expressed in geographic coordinates in the WGS84 system; both grids can be exploited by a bilinear interpolator.

During the application on board of the BELGICA both models will be combined in the "SIS" software (Seafloor Information System)..

The resulting model is GRStoLAT:

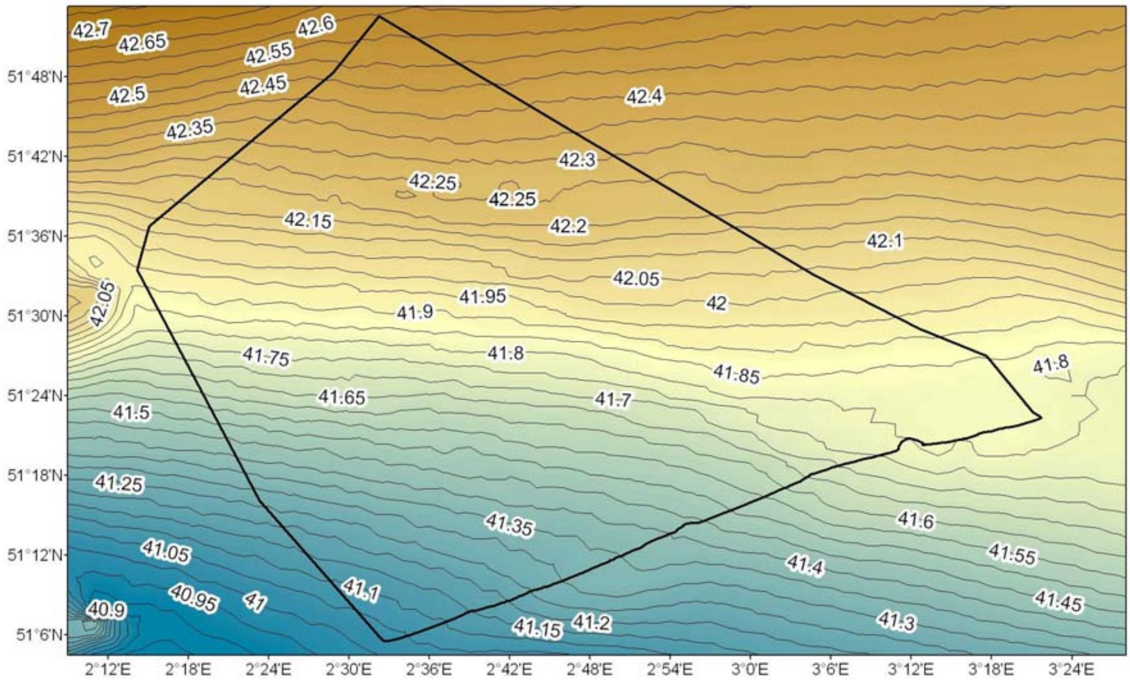


**Figure 24 :** GRStoLAT model.

## 3.4 TEST AND ANALYSIS

When bathymetric observations are performed, the initial result is the distance between the water level and the seafloor. On the BELGICA processing is necessary to obtain a depth relative to a certain vertical reference level (e.g. LAT). Currently this is done using the M2 tidal reduction method, which allows calculating the sea level for a specific moment in time and place.

The purpose of this analysis is to test whether RTK/LRK GPS positioning can be used to calculate the **real-time** depth relative to LAT, and thus eliminate the post-processing step that is necessary when $M_2$ tidal reduction method is used.

We will do this by comparing the real-time sea level via the RTK/LRK method and the $M_2$ method (Figure 25). The value of the real-time sea level depends mainly on the GRStoLAT grid which will be introduced in the "SIS" software (Seafloor Information System). This software is treating the raw data which are coming from the multibeam echo sounder type "EM3002D".

**Table 4:** Extract of GRStoLAT grid.

| ID10 | Latitude | Longitude | GRStoNAP value C (see Figure 21) (m) | NAPtoLAT value B (see Figure 21) (m) | GRStoLAT (m) |
|---|---|---|---|---|---|
| 1 | 51.900000000 | 2.150000000 | 44.336 | -1.533 | 42.803 |
| 3 | 51.900000000 | 2.166666667 | 44.325 | -1.531 | 42.794 |
| 1 | 51.883333333 | 2.150000000 | 44.332 | -1.568 | 42.764 |
| 3 | 51.883333333 | 2.166666667 | 44.321 | -1.565 | 42.756 |
| 1 | 51.866666667 | 2.150000000 | 44.330 | -1.602 | 42.728 |
| 3 | 51.866666667 | 2.166666667 | 44.319 | -1.600 | 42.719 |
| 1 | 51.850000000 | 2.150000000 | 44.327 | -1.637 | 42.690 |
| 3 | 51.850000000 | 2.166666667 | 44.316 | -1.634 | 42.682 |
| 1 | 51.833333333 | 2.150000000 | 44.325 | -1.671 | 42.654 |
| 3 | 51.833333333 | 2.166666667 | 44.314 | -1.668 | 42.646 |

In order to test the validity of the implemented GRStoLAT grid, two aspects will be investigated in this Section:

1. **First aspect:** The NAPtoLAT value B of the GRStoLAT grid (Table 4 and Figure 21), will be compared to the value B' as implemented in the M2 tidal reduction model calculated by the software of the FOD Economic Affairs.
2. **Second aspect:** The GRStoNAP value C, vertical distance between NAP and the GRS80 ellipsoid, of the GRStoLAT grid (Table 4 and Figure 21), will be tested by calculating the sea level using two different methods, i.e. the M2 method and the RTK/LRK method, and these results will be compared. By doing so, the result of the RTK/LRK method, which depends mainly on the GRStoLAT grid (value B and C of the GRStoLAT grid together) will give us information of the validity of value C, because the validity of value B of the GRStoLAT grid has been tested in de first aspect.

### 3.4.1 First aspect

The value B is the vertical distance between NAP and LAT. This value was given by the Flemish Hydrography but with a different interpolation method between the nodes. The coherency between the value B as implemented in the GRStoLAT grid, and the B' value calculated by the software of the FOD Economic Affairs, will be tested.

[10] In the SIS software.

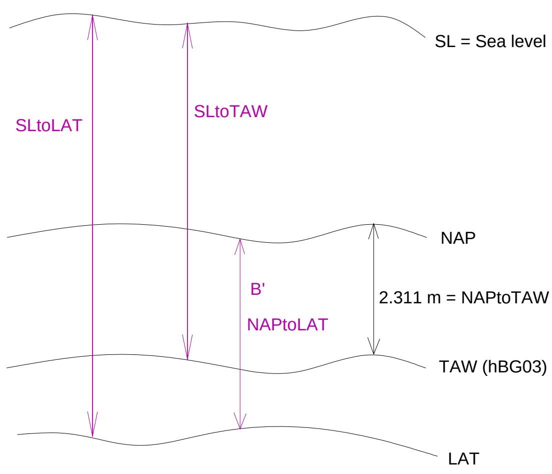


**Figure 25 :** Visualization of the calculated NAPtoLAT value B'.

The sea level values at the position of the R/V BELGICA during campaigns 28 and 33 were calculated by the FOD Economic Affairs using the M2 method. Specifically, two sea level values (frequency: every minute) were produced for each position of the ship: on one hand the sea level SLtoTAW value relative to the TAW vertical reference (Figure 25), and on the other hand the sea level SLtoLAT value relative to the LAT vertical reference (Figure 25). Based on these two values, and the known offset between NAP and TAW (2.311m, see "Coordinate Reference Systems in Europe[11]), the vertical distance between NAP and LAT can be calculated:

**SLtoLAT - SLtoTAW + NAPtoTAW = NAPtoLAT (B')**

These NAPtoLAT value B' were compared to the NAPtoLAT value B in the implemented GRStoLAT model (Table 5).

**Table 5:** Extract of the calculation table.

| Longitude | Latitude | Date and time | SL to TAW | SL to LAT | NAP to LAT B' | NAP to LAT B | B' - B |
|---|---|---|---|---|---|---|---|
| Position of the BELGICA | | | (m) | (m) | (m) | (m) | (m) |
| 3.11846168 | 51.40736658 | 20091019135600 | -4.280 | -4.440 | 2.471 | 2.462 | 0.009 |
| 3.11420600 | 51.40824178 | 20091019135700 | -4.270 | -4.430 | 2.471 | 2.461 | 0.010 |
| 3.10993958 | 51.40911885 | 20091019135800 | -4.250 | -4.410 | 2.471 | 2.459 | 0.012 |
| 3.10564650 | 51.41000545 | 20091019135900 | -4.240 | -4.400 | 2.471 | 2.458 | 0.013 |
| 3.10134935 | 51.41090633 | 20091019140000 | -4.230 | -4.380 | 2.461 | 2.457 | 0.004 |
| 3.09707200 | 51.41177825 | 20091019140100 | -4.210 | -4.370 | 2.471 | 2.454 | 0.017 |
| 3.09282137 | 51.41264188 | 20091019140200 | -4.200 | -4.360 | 2.471 | 2.451 | 0.020 |
| 3.08855845 | 51.41351020 | 20091019140300 | -4.180 | -4.320 | 2.451 | 2.447 | 0.004 |
| 3.08429813 | 51.41439095 | 20091019140400 | -4.170 | -4.310 | 2.451 | 2.444 | 0.007 |
| 3.08005440 | 51.41525492 | 20091019140500 | -4.150 | -4.290 | 2.451 | 2.440 | 0.011 |
| 3.07582682 | 51.41613467 | 20091019140600 | -4.140 | -4.270 | 2.441 | 2.437 | 0.004 |
| 3.07160240 | 51.41702542 | 20091019140700 | -4.130 | -4.260 | 2.441 | 2.434 | 0.007 |

[11] http://www.crs-geo.eu/nn_124226/crseu/EN/CRS__Description/crs-national__node.html?__nnn=true

| | | | | | | | |
|---|---|---|---|---|---|---|---|
| 3.06738263 | 51.41791570 | 20091019140800 | -4.110 | -4.240 | 2.441 | 2.431 | 0.010 |
| 3.06316287 | 51.41879987 | 20091019140900 | -4.100 | -4.230 | 2.441 | 2.429 | 0.012 |
| 3.05893983 | 51.41971352 | 20091019141000 | -4.090 | -4.220 | 2.441 | 2.427 | 0.014 |
| 3.05472083 | 51.42063152 | 20091019141100 | -4.070 | -4.200 | 2.441 | 2.426 | 0.015 |

- The mean difference of B'-B is 0.009 m.
- The standard deviation is 0.007 m.
- (n = 4931 positions)

Since this difference is millimetric, the implementation of the NAPtoLAT value B in the GRStoLAT model of the BELGICA and the NAPtoLAT value B' used by FOD Economic Affairs is considered to be coherent.

### 3.4.2 Second aspect: Comparison of RTK/LRK GPS and M2 sea level values

#### 3.4.2.1 Analyses of the original data.

The M2 tidal reduction method allows to calculate the sea level in function of time and position. Necessary input data include tide gauge measurements at Zeebrugge, Oostende and Nieuwpoort (see 2.2.1).

The sea level can be calculated based on the LRK (GPS) positioning as follows (Figure 21):

**SLtoLAT = A – C + B – D + E**

where

- A = GRS80 ellipsoidal height of the GPS antenna onboard the R/V BELGICA, measured by the Aquarius® using LRK. This height is mainly determined by (1) the sea level and (2) the heave. These two components determine the measured ellipsoidal height.
- B = Vertical distance between NAP and LAT

  Value B (NAPtoLAT) of the implemented GRStoLAT grid (Figure 21 and Table 4). This value is a function of the position.
- C = Vertical distance between NAP and the ellipsoid GRS80.

  Value C (GRStoNAP) of the implemented GRStoLAT grid (Figure 21 and Table 4) It consist of the value of the height conversion model (hBG03), *i.e.* the vertical distance between the ellipsoid (GRS80, used in the GPS reference system) and TAW (*Tweede Algemene Waterpassing*, vertical reference level in Belgium). The height conversion model hBG03 was determined based on the combination of

  - The geoid model BG03, based on gravity measurements
  - 3735 points that were measured using GPS and topographical leveling on land

  This value was increased with a constant offset of 2.311 m (i.e. the difference between TAW and NAP). The value of the hBG03 model is a function of the position.
- D = Vertical distance between the GPS antenna and the MRU (Motion Reference Unit)

  When the ship lies perfectly still and horizontal , this value is 23.024 m. When the ship moves (e.g. roll, pitch), the distance between the antenna and the MRU, measured along the vertical offset, will change. The following analyses in this chapter however, do not consider the influence of these movements as it is of second order. In the "Error budget" it will be discussed.

- E = Draught value

  This is the vertical distance between the water level and the MRU. This value is measured at the beginning and at the end of every sea campaign. The values used during the trajectory, are traditionally calculated by linearly interpolating these values in function of the time, between the beginning and end of the campaign.

Figure 26 and Figure 27 visualize both sea level values (determined using M2 method and LRK method) for the R/V BELGICA campaigns in October and December, in function of the time.

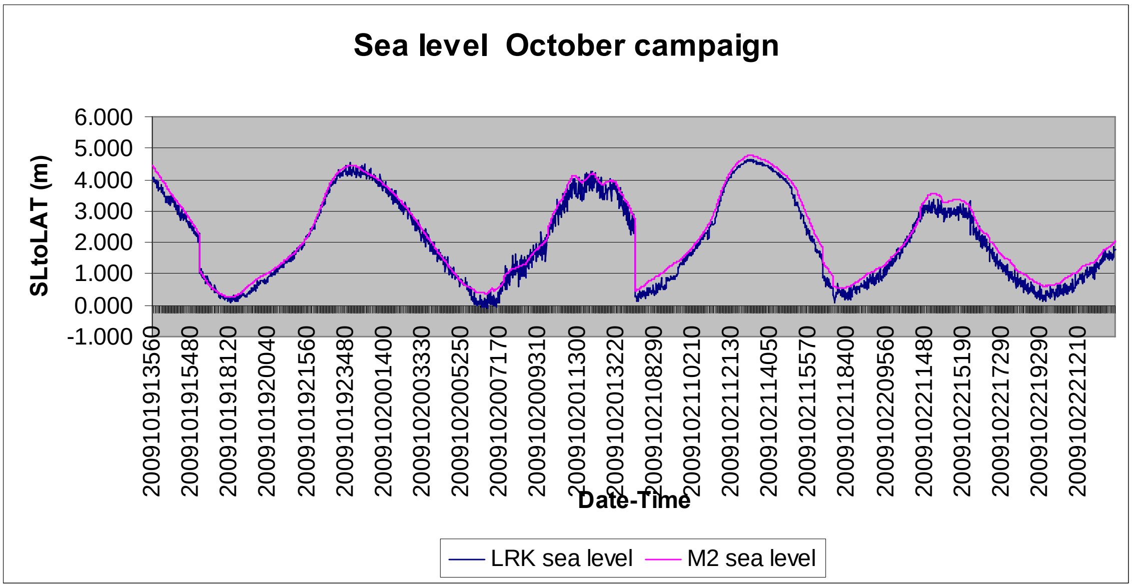


**Figure 26 :** *$M_2$* sea level values (pink line) and LRK sea level values (blue line) for the October campaign.

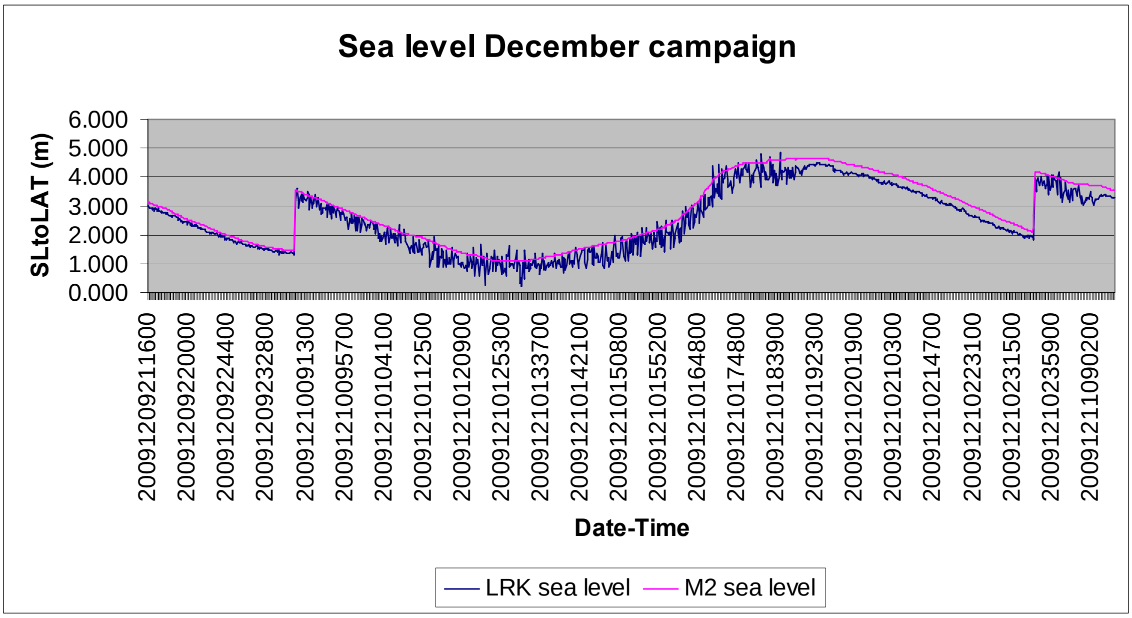


**Figure 27 :** *$M_2$* sea level values (pink line) and LRK sea level values (blue line) for the December campaign.

The M2 sea level values are determined using a model, which generates a smooth line of sea level values in function of the time. The sea level values obtained using the LRK positions however fluctuate significantly more through time, which is caused by the heave movement of the ship. Although both lines are almost parallel to each other, there is a certain offset between the M2 and LRK sea level values.

The average difference between the sea level values of the M2 and LRK method are:

| **Campaign 28 (October)** | |
|---|---|
| $\bar{x}$ | 0.2073 m |
| s | 0.1683 m |
| n | 2795 |
| **Campaign 33 (December)** | |
| $\bar{x}$ | 0.2768 m |
| s | 0.2151 m |
| n | 1084 |

The average difference is thus 21 cm for October and 28 cm for the December campaign.

#### 3.4.2.2 Analyses of the reason of the offset in the data.

On 22 October 2009, during campaign 28, a comparison was made between the EM3002D multibeam echosounders onboard the R/V BELGICA and R/V Ter Streep. The report made by the FOD Economic Affairs mentions the following about the difference between the sea bottom floor measurements performed by the multibeam onboard the BELGICA and Ter Streep vessels: "The mean difference is very close to the value measured with the BELGICA in the Vandamme lock in Zeebrugge: average difference between BELGICA depth measurement and theoretic floor of lock = 0.18 m. This seems to indicate that the BELGICA has a systematic draught error of app. 18 cm and that the Ter Streep depths are correct."

When this systematic error of the draught of the R/V BELGICA is taken into account, the previous analyses regarding the difference between the M2 and LRK sea level values has to be corrected for this offset. In order to implement this systematic error, the E value is increased with 18 cm. The results of both sea level values for both campaigns after adjusting the draught values are visualized in Figure 28 and Figure 29.

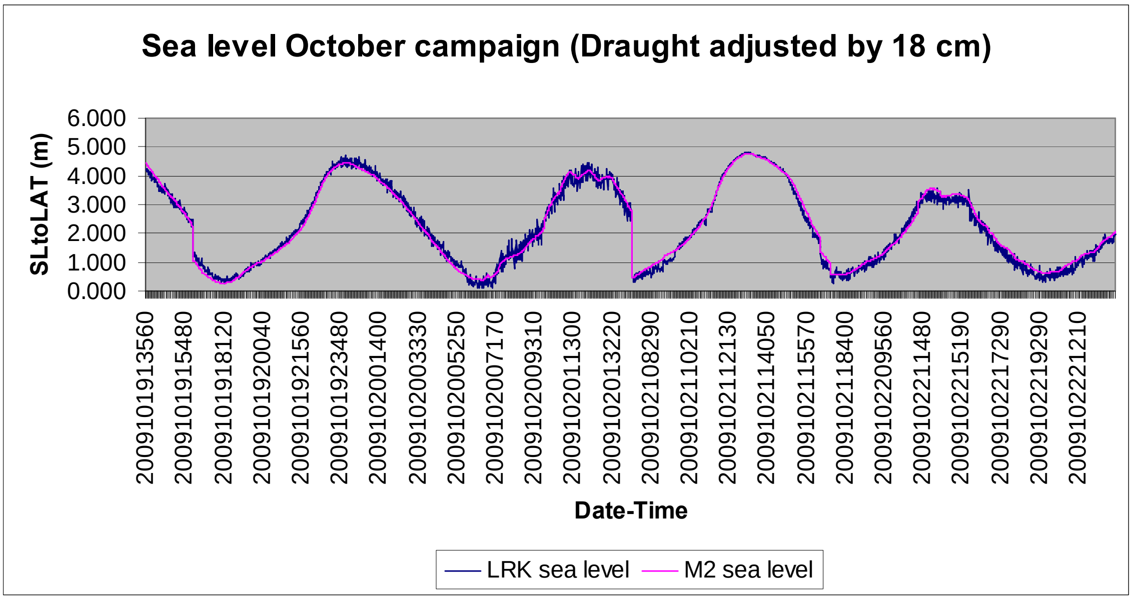


**Figure 28 :** $M_2$ sea level values (pink line) and LRK sea level values (blue line) for the October campaign – after draught correction.

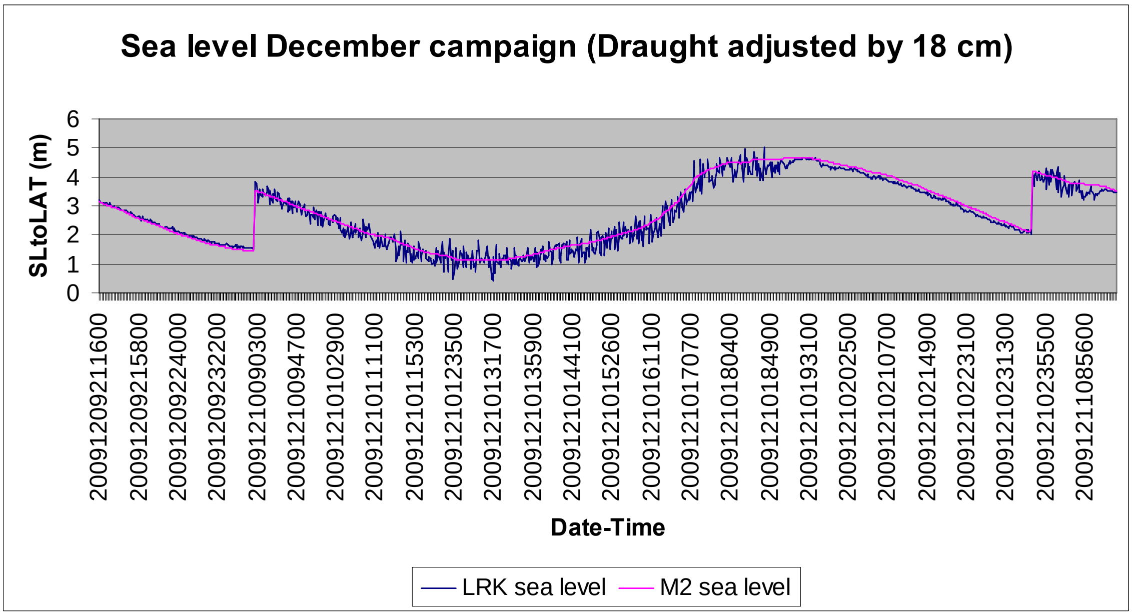


**Figure 29 :** $M_2$ sea level values (pink line) and LRK sea level values (blue line) for the December campaign – after draught correction.

The average difference between the sea level values of the M2 and LRK method after adjusting the draught values are:

| **Campaign 28 (October) – draught correction** | |
|---|---|
| $\bar{x}$ | 0.0273 m |
| s | 0.1683 m |
| n | 2795 |

| Campaign 33 (December) – draught correction | |
|---|---|
| $\bar{x}$ | 0.0970 m |
| s | 0.2151 m |
| n | 1084 |

The difference between both sea level values is now reduced to an average of

- 2.7 cm (Campaign 28) and
- 9.7 cm (Campaign 33).

Figure 8 and 9 visualize this reduced difference between both sea level values, since both lines now almost coincide.

#### 3.4.2.3 Low-pass filtering of the LRK measurements.

An ideal low-pass filter was applied through Fourier transform to smooth the LRK measurements; the cutoff frequencies (*i.e.*, the highest still passed) were, in the October campaign, of a period of 29 minutes and in the December campaign of 27 minutes, we get the following results :

| Campaign 28 (October) – draught correction | |
|---|---|
| $\bar{x}$ | 0.0273 m |
| s | 0.1489 m |
| n | 2795 |
| **Campaign 33 (December) – draught correction** | |
| $\bar{x}$ | 0.0970 m |
| s | 0.1469 m |
| n | 1084 |

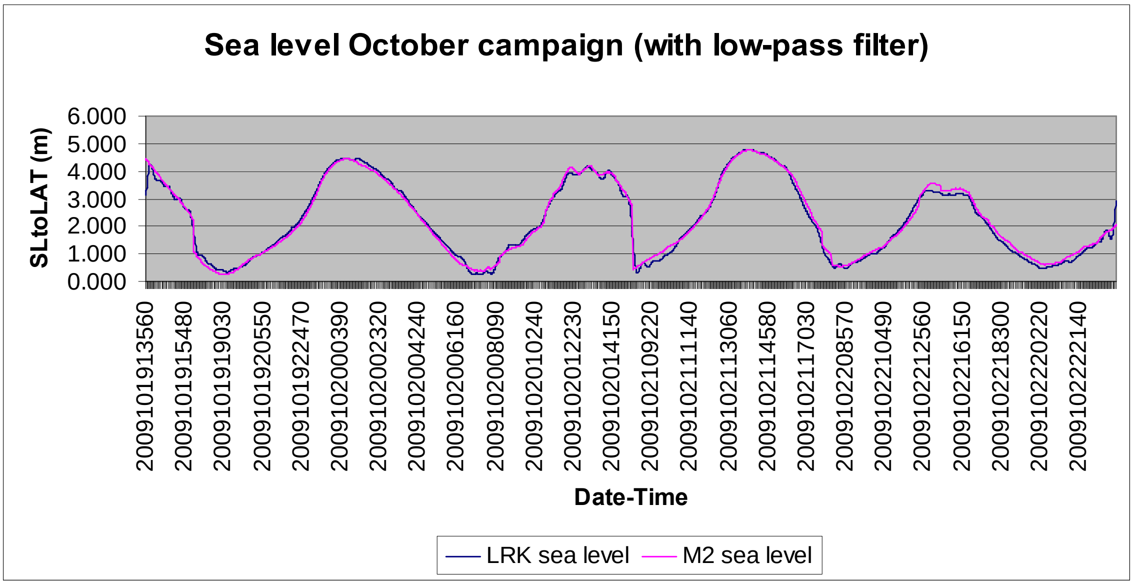


**Figure 30:** M2 sea level values (pink line) and LRK sea level values (blue line) for the October campaign – with low-pass filter on LRK sea level

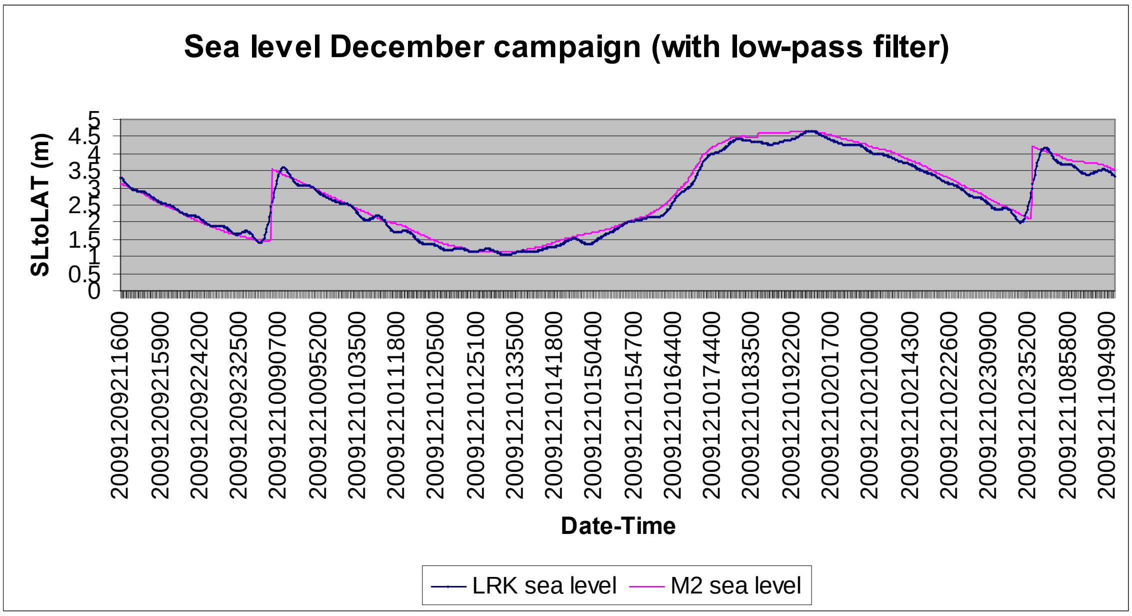


**Figure 31:** M2 sea level values (pink line) and LRK sea level values (blue line) for the December campaign – with low-pass filter on LRK sea level.

# 4. PRACTICAL APPROACH

## 4.1 ASSESSMENT OF THE ACCURACY OF THE EQUIPMENT AVAILABLE ON BOARD THE BELGICA AND THE SURVEY VESSEL TER STREEP – TRIALS ON LAND

### 4.1.1 Description of the tests

An NGI team has performed the tests between 6 and 16 January 2009.

They used the BELGICA's GPS receiver (Aquarius) and hired antennas (of the same type as those on the ship) to carry out observations on a certain number of benchmarks belonging to the national geodetic network. The following criteria were used for the selection of the benchmarks:

- the co-ordinates (x,y and H) are known very accurately, *i.e.* their standard deviation is smaller than or equal to 3 cm.
- the distance to the LRK reference stations has to be variable
- the reception of the radio signals from the reference stations still has to be sufficiently stable.

Figure 32 shows the benchmarks used for the test measures (red dots) and their situation in relation to the various reference stations.

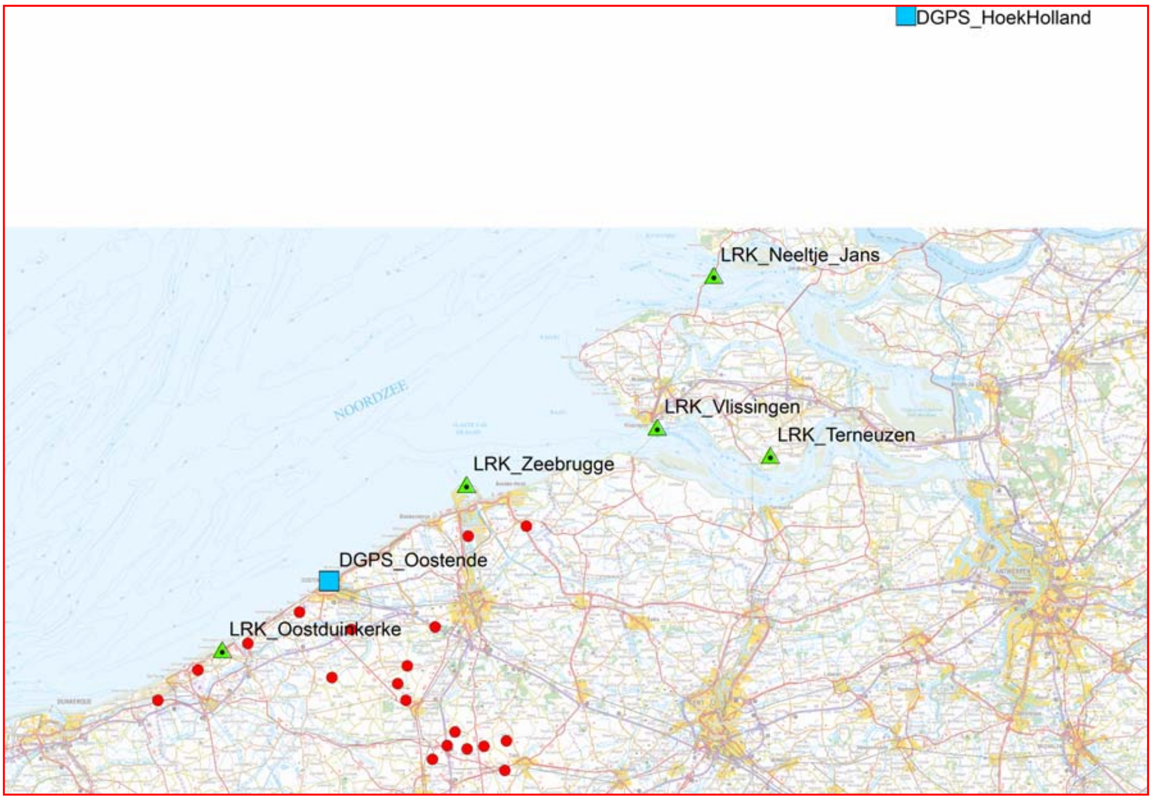


**Figure 32:** Situation of the test points and of the reference stations.

Thanks to the presence of a small hilly area near Roeselare-Tielt, we were able to pick up the radio signals from the Belgian LRK reference stations up to 45 km inland.

In order to carry out the measurements, the GPS antenna was positioned accurately and steadily with a tripod perpendicularly to each geodetic benchmark (Picture 2a). The radio antennas were put up on top of and next to the vehicle (Picture 3b).

**Picture 3a:** Position of the GPS antenna on top of the geodetic benchmark.

**Picture 2b:** Survey position GPS and radio antennas.

The measurements were carried out on all benchmarks as follows:

- One position per second during a 30 seconds period.
- After changing the radio frequency (other reference station), reiteration of the position-finding during 30 seconds, and this for each available reference station
- In order to obtain a second string of results using an other satellite configuration, the whole procedure, as described above, was repeated after an interval of at least 4 hours.

### 4.1.2 Results

The figures below give an overview of the differences between the co-ordinates obtained with LRK or DGPS and the accurately known co-ordinates of the benchmarks.

The results for the height component, determined with the LRK measurements, are given in the Figure 33 to Figure 35. The X-axis shows the distance to the reference station and the Y-axis shows the difference in height, given in meters. The orange inset shows the average of all results and the corresponding standard deviation (σ).

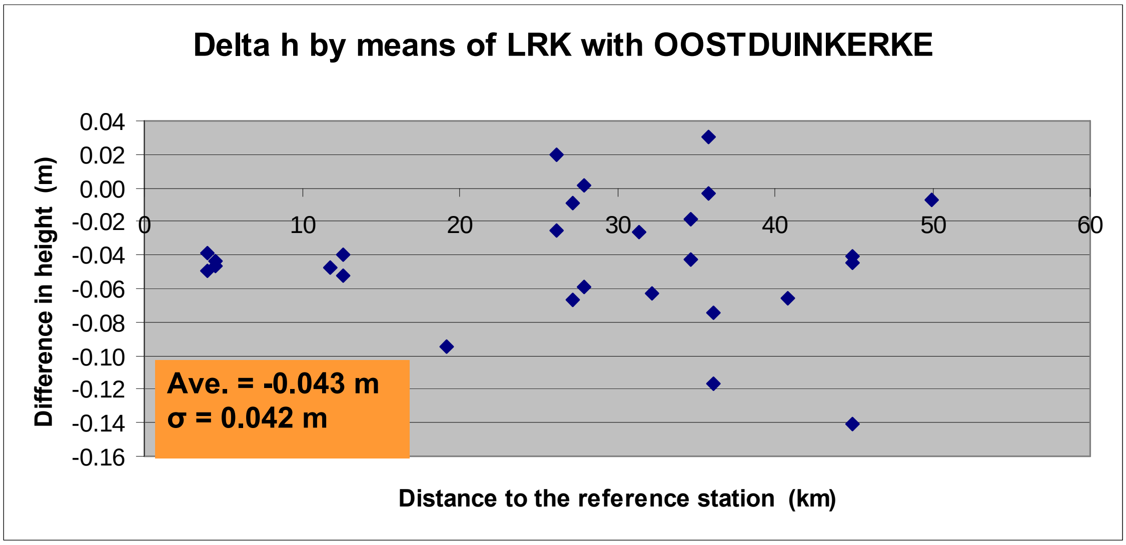


**Figure 33:** LRK results for the height with reference station Oostduinkerke.

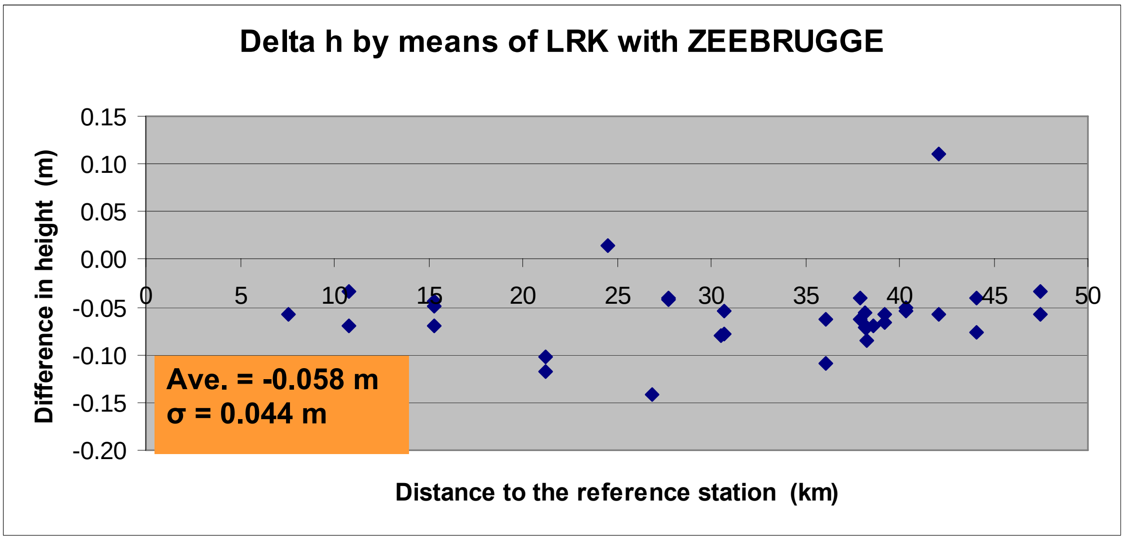


**Figure 34:** LRK results for the height with reference station Zeebrugge.

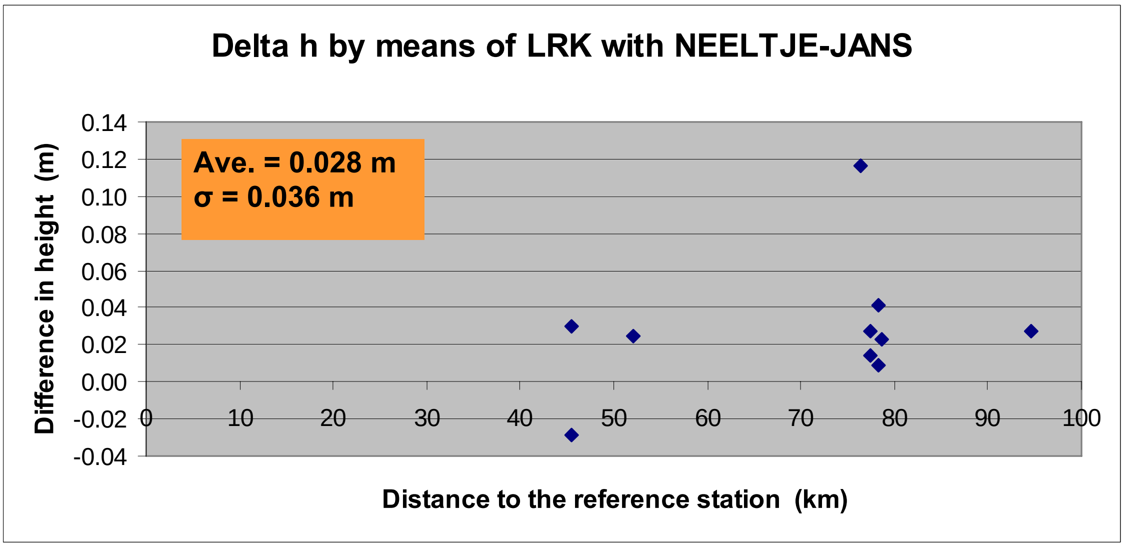


**Figure 35:** LRK results for the height with reference station Neeltje Jans.

We can deduce the following from Figure 33 to Figure 35:

- the deviations of the height component, determined by means of LRK, do not increase with the distance to the reference station, in other words the error caused by the LRK measurement technique is not distance-related.
- The σ-values for the three reference stations oscillate around 4 cm, which is a normal result for GPS LRK.
- The values of the average deviations (in the orange insets) can indicate a systematic deviation from the real value. Especially for Zeebrugge (-5.8 cm), the figure is already rather high. It might be useful to check the accuracy of the height of the antenna in the Zeebrugge station.

Remark: The abovementioned results are the average values of measurements which lasted 2 x 30 seconds. However, since a ship never remains entirely motionless for such a long time, we also checked how big the differences among the 60 measurements can become. In fact, we have 60 results for each test point without the antenna moving.

The spread (difference between the highest and the lowest value) for the three reference stations combined is shown in Figure 36. Again, the X-axis gives the distance to the reference station, the Y-axis shows the spread in terms of meters.

Figure 36 shows that the spread can be as high as 18 cm and once more that no relation to the distance can be found here.

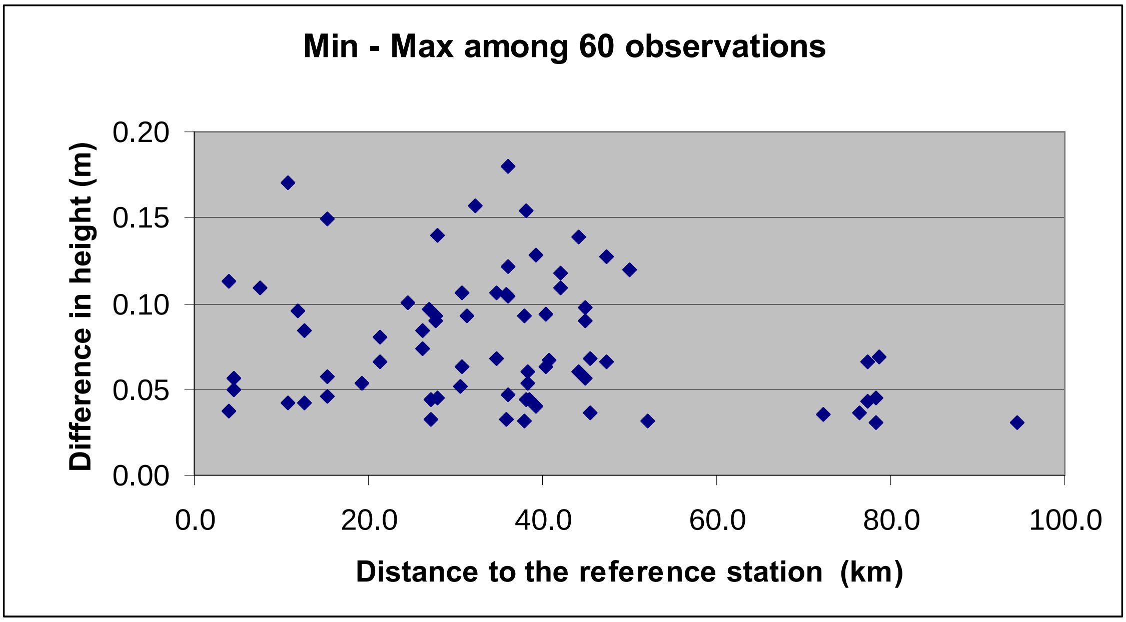


**Figure 36:** Spread of the height values in each test point.

As GPS LRK provides three-dimensional results and as we also know accurately the co-ordinates of the geodetic benchmarks for the three dimensions, we can also check the differences for the x and the y values. Although the height values are the most important for this project, the x,y results offer an additional indication of the accuracy which can be obtained with LRK.

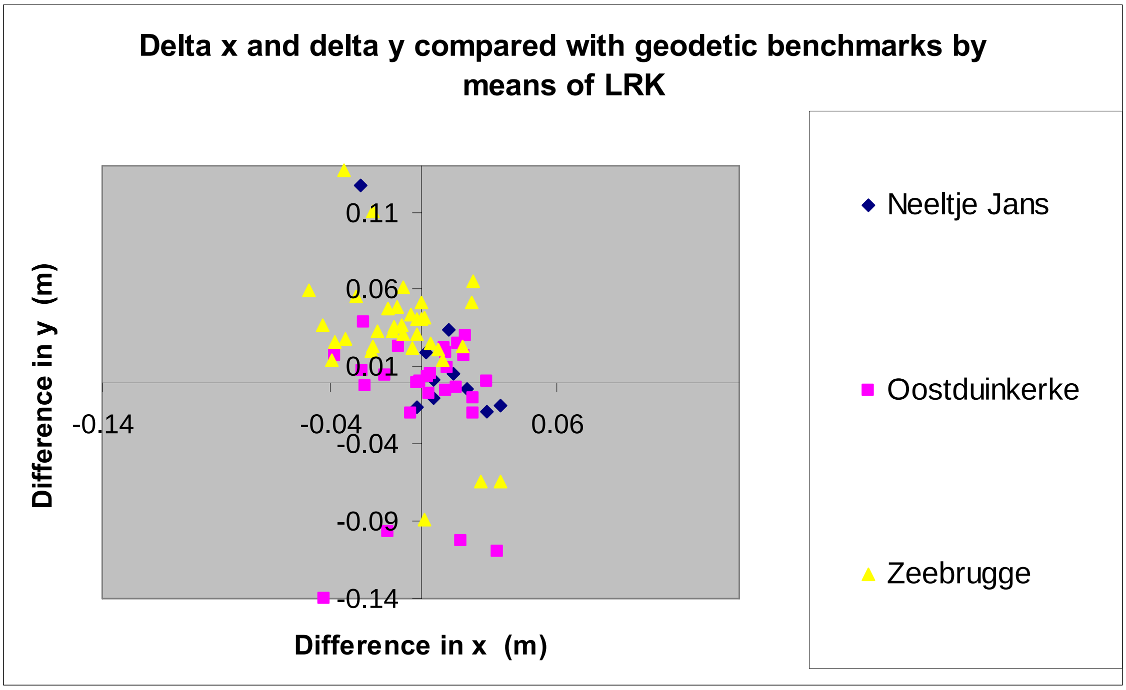


**Figure 37:** Δx and Δy by means of LRK to the three reference stations.

Figure 37 shows the differences for x and y, for the three reference stations together. The values are given in meters and are the averages of observations which lasted 2 x 30 seconds. Once more it is possible to make an average of all the deviations and its standard deviation (σ) for all the measurements, on all the test points and towards each reference station; this can be found in the schedule hereunder:

| *Reference station* | *Ave. Δx (m)* | *Ave. Δy (m)* | *σ x (m)* | *σ y (m)* |
|---|---|---|---|---|
| ***Oostduinkerke*** | 0.00 | -0.01 | 0.02 | 0.05 |
| ***Zeebrugge*** | -0.01 | 0.03 | 0.02 | 0.04 |
| ***Neeltje Jans*** | 0.01 | 0.01 | 0.02 | 0.04 |

The small average differences for x and y indicate that no systematic errors occur. The σ-values are in line with what can be expected when using GPS LRK, as was the case with the height determination.

When LRK radio signals fall away or become too weak during measurements, one has to fall back on DGPS. In order to check the accuracy of this positioning method, we carried out DGPS measurements, in addition to LRK, from each geodetic benchmark towards two reference stations: Ostend and Hoek van Holland.

The results for the height component, determined with DGPS measurements, are shown in Figure 38 and Figure 39. The X-axis shows the distance to the reference station and the Y-axis the difference in height, in terms of meters. The orange inset shows the average of all results and the corresponding average deviation (σ).

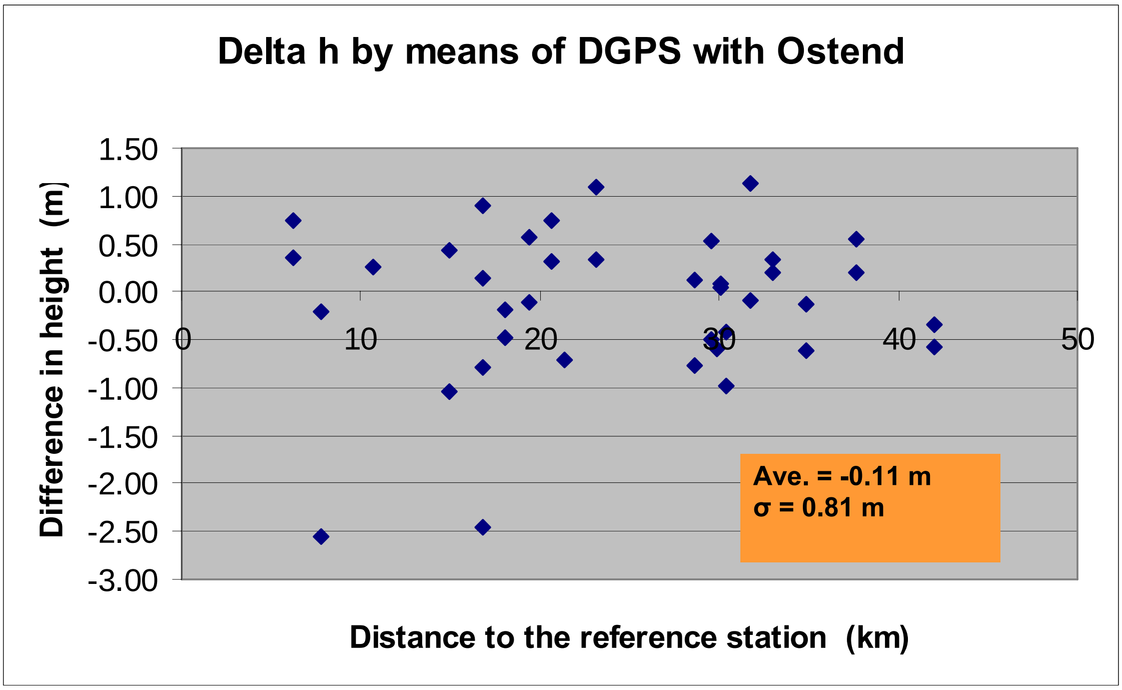


**Figure 38:** DGPS results for the height with reference station Ostend

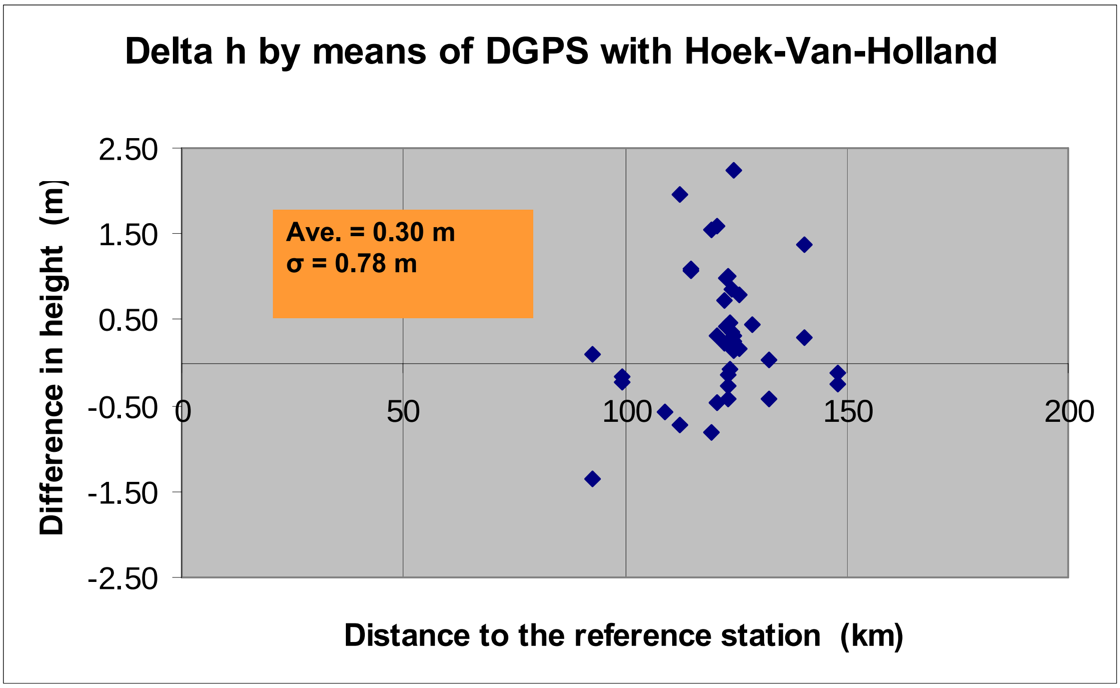


**Figure 39:** DGPS results for the height with reference station Hoek van Holland

An advantage of the DGPS measuring method is that it can be used on the entire continental shelf; a huge disadvantage, however, is the accuracy of the results, as the Figure 38 and Figure 39 clearly show. The σ-value of the deviation amounts to 80 cm, with peaks of 2.5 m.

For the sake of completeness, we also give the differences for the x and the y component for DGPS. A summary can be found in the schedule hereunder and in Figure 40.

| Reference station | Ave. Δx (m) | Ave. Δy (m) | σ x (m) | σ y (m) |
|---|---|---|---|---|
| ***Ostend*** | -0.10 | 0.00 | 0.38 | 0.48 |
| ***Hoek van Holland*** | 0.11 | 0.15 | 0.31 | 0.45 |

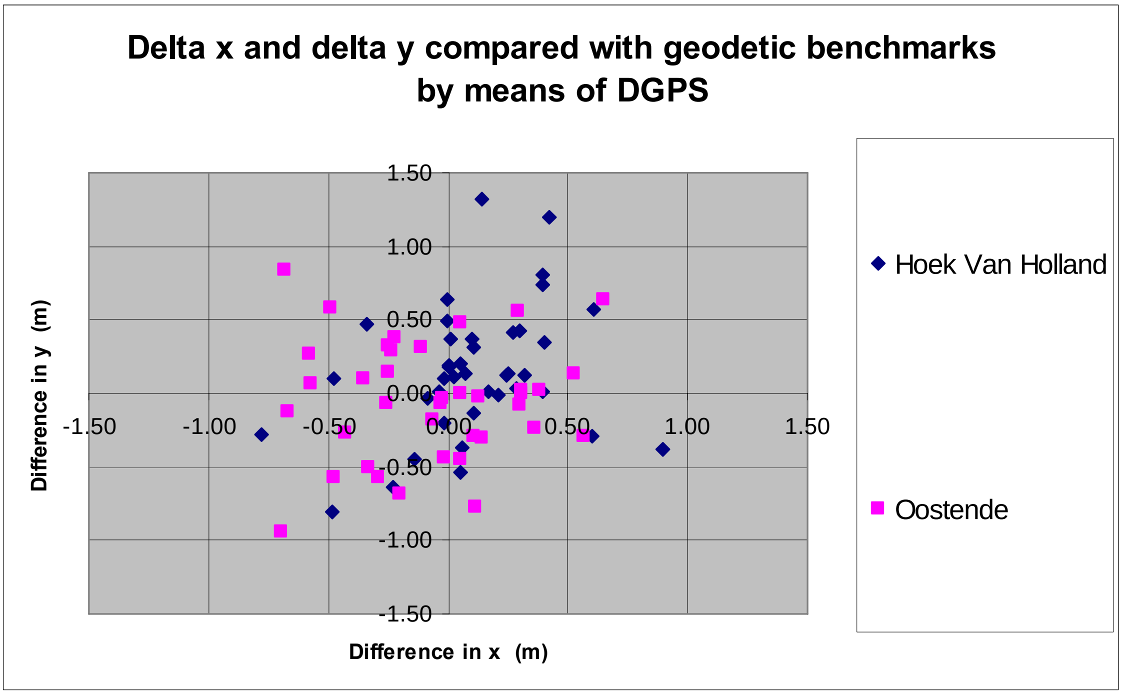


**Figure 40:** Δ x and Δ y by means of DGPS with the two reference stations.

## 4.2 SUMMARY AND CONCLUSIONS

These extensive tests allowed us to form an idea of the accuracy which can be obtained by means of LRK and DGPS. The observations were only carried out under favorable circumstances, i.e. with a good reception of radio and GPS signals.

The schedules hereunder give a realistic idea of the accuracy with which the height can be determined for both measuring methods.

| ***LRK*** | | |
|---|---|---|
| ***Ref.station*** | ***ave. Δh*** | ***σ*** |
| Oostduinkerke | -0.043 | 0.042 |
| Zeebrugge | -0.058 | 0.044 |
| Neeltje Jans | 0.028 | 0.036 |

| ***DGPS*** | | |
|---|---|---|
| ***Ref.station*** | ***ave. Δh*** | ***σ*** |
| Ostend | -0.11 | 0.81 |
| Hoek van Holland | 0.30 | 0.78 |

According to the statistics, chances to obtain a measurement result whose value differs not more than 1 x σ from the real value are 66.27%. If one takes 3 x σ, chances become 99.73%, which is called practical certainty. This allows us to draw the following conclusions:

- The error in the height determination by means of LRK, with the Aquarius and the reference stations which can be used on the Belgian continental shelf, is situated between 0 and 13 cm (plus or minus)

- The error in the height determination by means of DPS with the Aquarius and the reference stations which can be used on the Belgian continental shelf, is situated between 0 and 243 cm (plus or minus)

# 5. RANDOM ERROR OF LRK POSITIONING

## 5.1 INTRODUCTION

Onboard the research vessel R/V BELGICA, a Thales Aquarius® GPS determines the position of the ship. Depending on the kind of research that is performed during a specific campaign, GPS positioning is performed every 0.5, 1 or 10 seconds. The positioning data of the 33 campaigns in 2009 is stored in ODAS (Oceanographic Data Acquisition System), and includes GPS positioning information with an interval of 10 seconds. This data can be used to analyze the quality of the LRK positioning onboard the vessel.

The onboard Aquarius® GPS can register the position of the ship using (Thales Navigation, 2003):

- Long Range Kinematic (LRK), dual-frequency kinematic correction; theoretic accuracy of less than 20 mm;
- Differential GPS (DGPS), metric precision level;
- GPS (absolute navigation position), no corrections, accuracy of ca. 5 meters.

During the R/V BELGICA campaigns in 2009, their relative occurrence was 28% (GPS), 37% (DGPS) and 35% (LRK).

The LRK signal is transmitted by stations in Zeebrugge, Oostduinkerke and Neeltje Jans (Nl). Only the LRK positions are accurate enough for use in bathymetric measurements. Therefore, only the LRK positions were selected for further analysis. Since this research project focuses on the Belgian Continental Plate area, only positions in this area are considered for further analysis.

## 5.2 VISUALIZATION OF THE QUALITY OF THE LRK POSITIONS

We have visualized the Aquarius® LRK positions in ArcMap® 9.3. Each position was assigned a color according to its Root Mean Square (RMS) value. This value is a part of the GPS string and is expressed in m. The RMS is a good indicator of the **random error** of a position.

In order to have enough data to perform a statistical analysis about the random error of LRK positions, all available LRK positioning data of the R/V BELGICA of the year 2009 (33 campaigns) was used. This data was analyzed per LRK station to determine if there is a difference in the positioning accuracy of the BELGICA using these reference stations. Figure 41 to Figure 43 visualize the random error (RMS) of each position achieved using a specific LRK station (Zeebrugge, Oostduinkerke or Neeltje Jans).

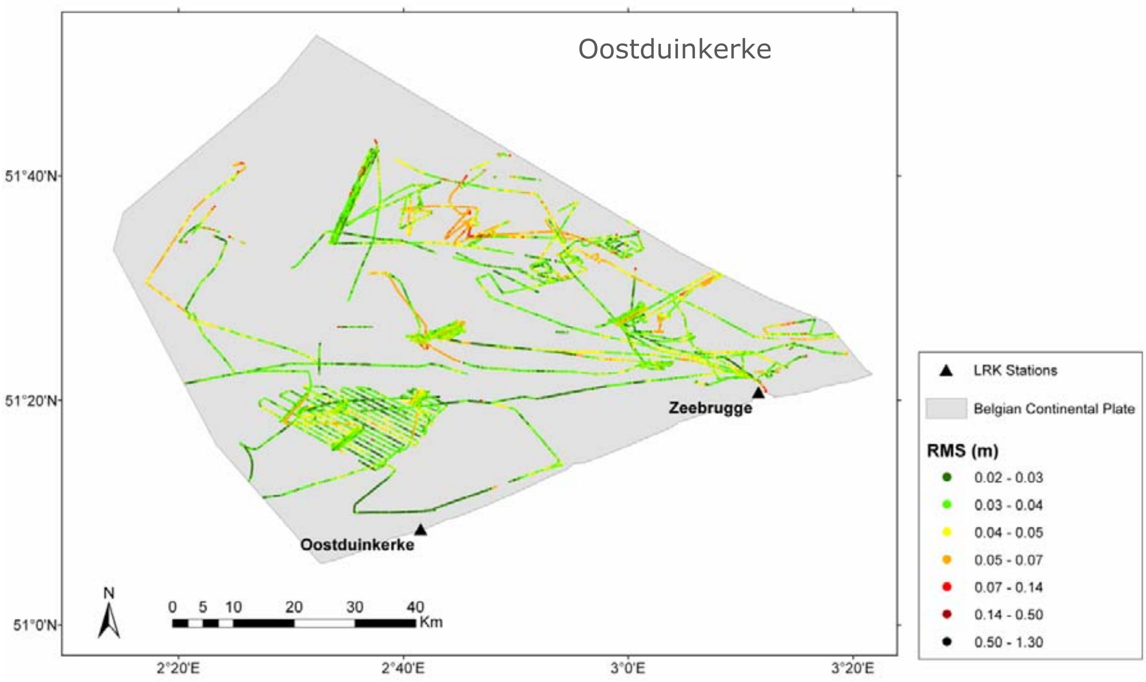


**Figure 41:** RMS of the LRK positions with correction signal from the reference station Oostduinkerke (year 2009) (original data, outliers included).

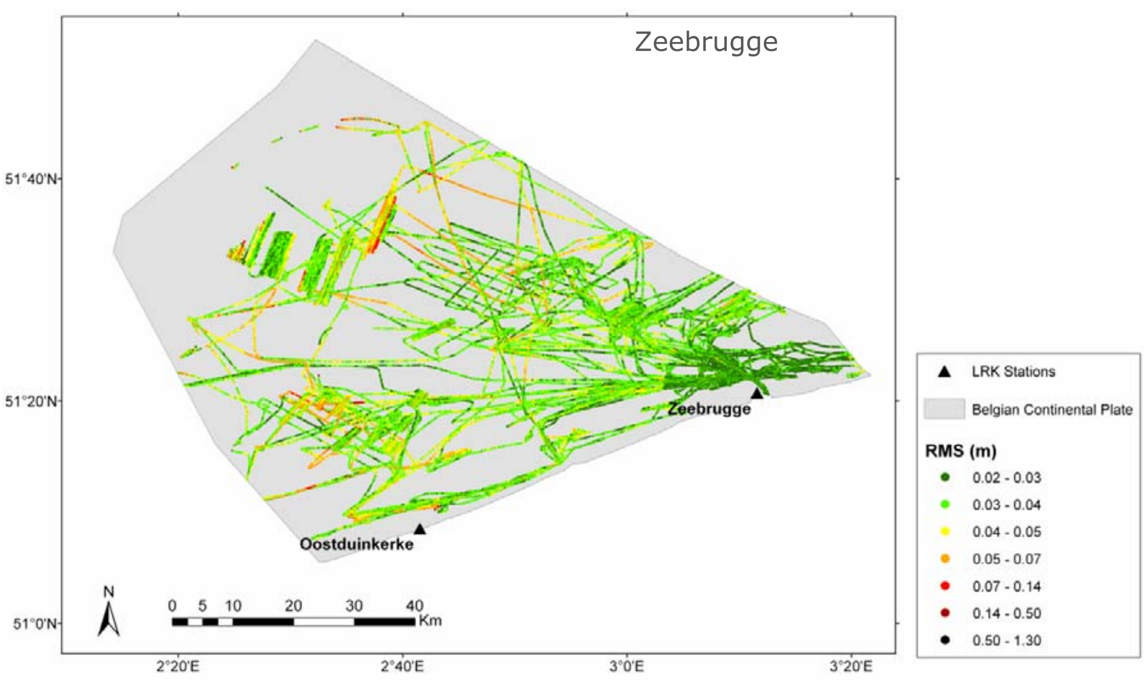


**Figure 42:** RMS of the LRK positions with correction signal from the reference station Zeebrugge (year 2009) (original data, outliers included)

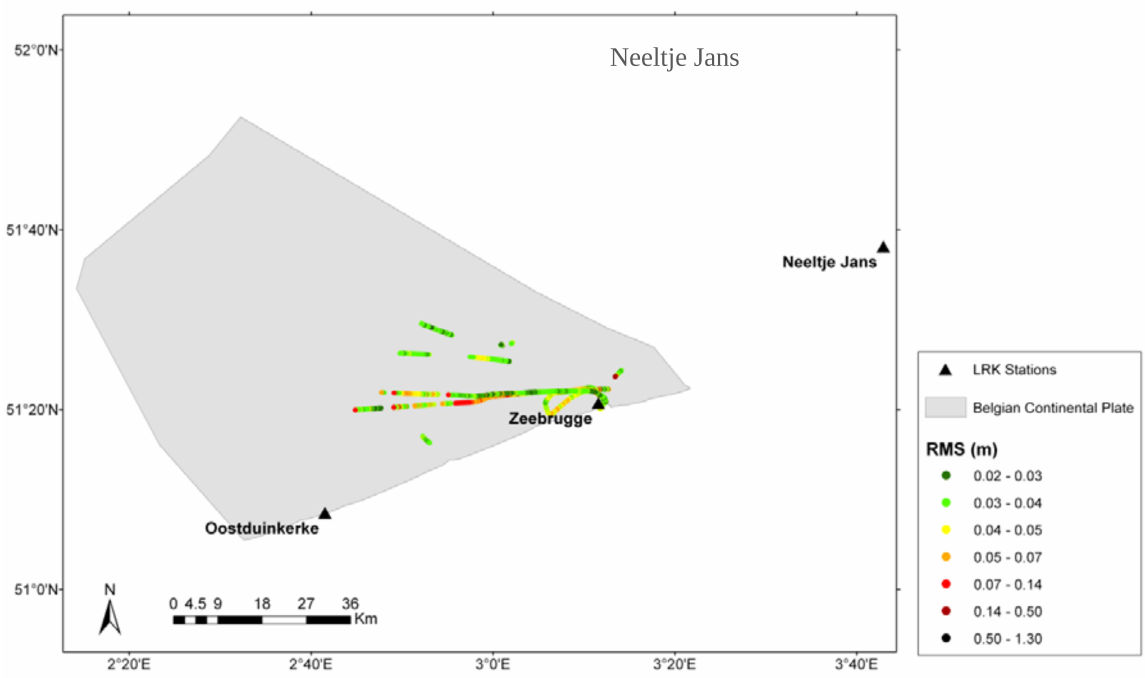


**Figure 43:** RMS of the LRK positions with correction signal from the reference station Neeltje Jans (year 2009) (original data, outliers included)

Figure 41 to Figure 43 show that there is often one (dark) red point at the end of a line. This could be caused by a sudden loss of the LRK signal and the subsequent shift to DGPS use;

In Figure 44 till Figure 51 hereunder, a UTM31 (datum: WGS84) grid model was applied to the original data, with grid cells of 1 by 1 km. In each cell, the average (Figure 44,Figure 46, Figure 48) or the minimum (Figure 45, Figure 47, Figure 49) RMS value was computed, respectively with the use of the reference station of Oostduinkerke, Zeebrugge and Neeltje Jans. The "empty" cells were filled by weighted local interpolation using an inverse squared distance weighting factor and using a maximum range of 10 km.

Figure 50 is computed by taking, in each cell, the minimum RMS value of the three **average** RMS models of Oostduinkerke, Zeebrugge and Neeltje Jans (Figure 44, Figure 46 and Figure 48 respectively).

Figure 51 is computed by taking, in each cell, the minimum RMS value of the three **minimum** RMS models of Oostduinkerke, Zeebrugge and Neeltje Jans (Figure 45, Figure 47 and Figure 49 respectively). It shows the best possible values in optimum circumstances.

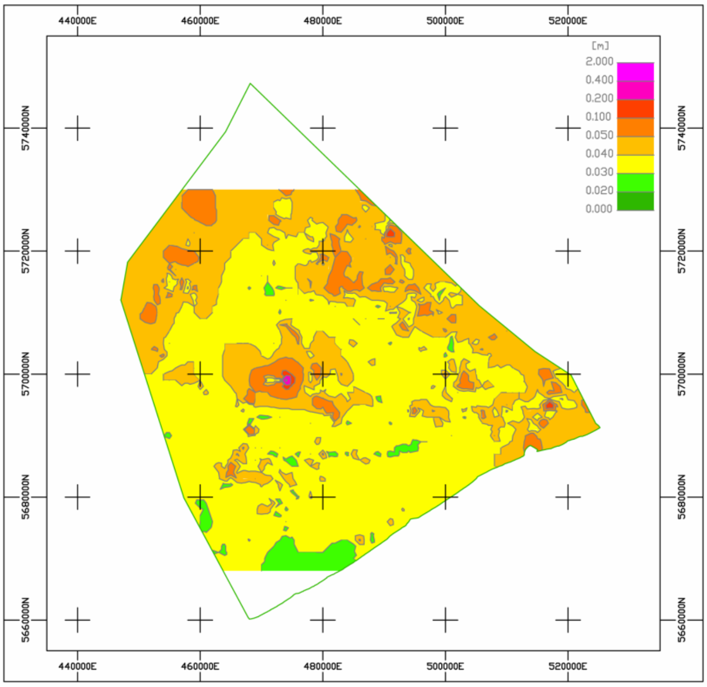


**Figure 44:** Interpolated grid model of the average RMS of the LRK positions with correction signal from the reference station Oostduinkerke (year 2009) (original data, outliers included)

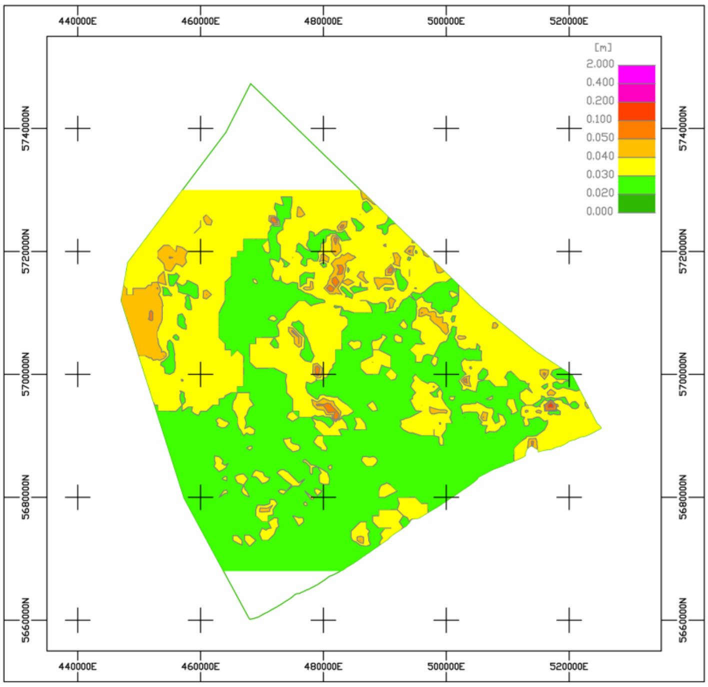


**Figure 45:** Interpolated grid model of the minimum RMS of the LRK positions with correction signal from the reference station Oostduinkerke (year 2009) (original data, outliers included)

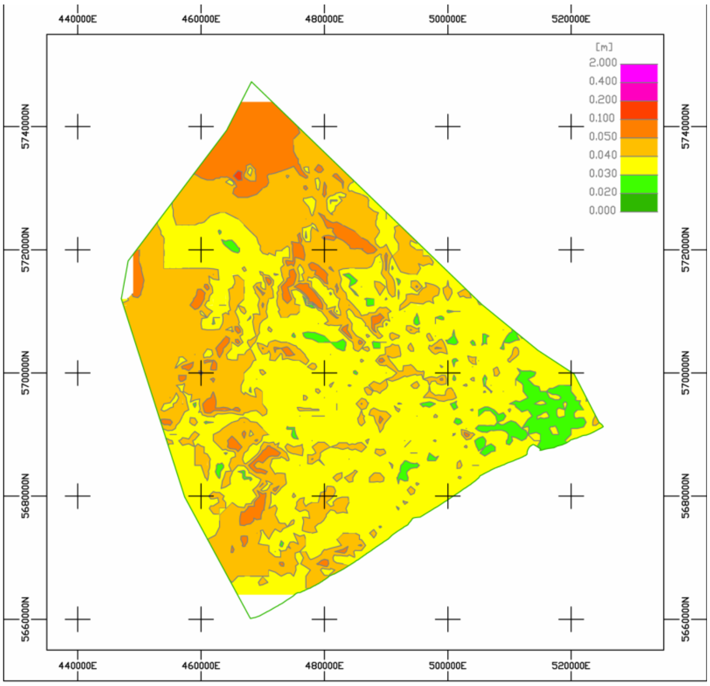


**Figure 46:** Interpolated grid model of the average RMS of the LRK positions with correction signal from the reference station Zeebrugge (year 2009) (original data, outliers included)

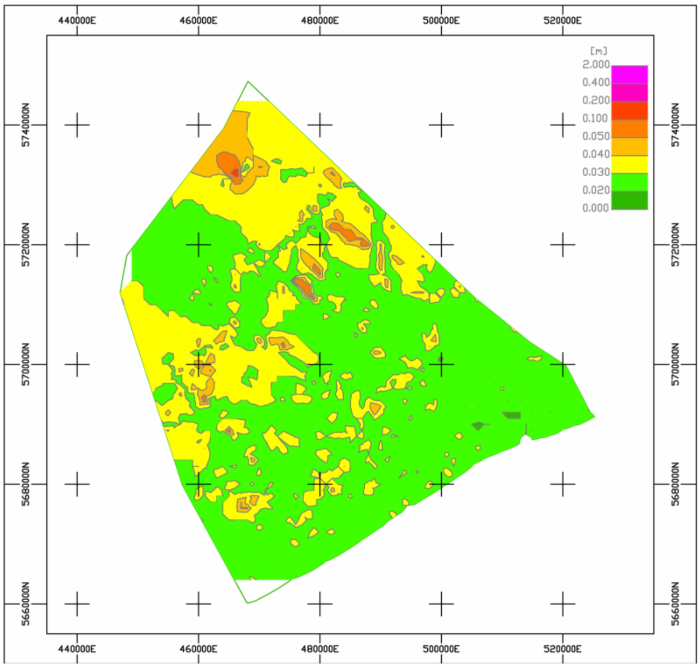


**Figure 47:** Interpolated grid model of the minimum RMS of the LRK positions with correction signal from the reference station Zeebrugge (year 2009) (original data, outliers included)

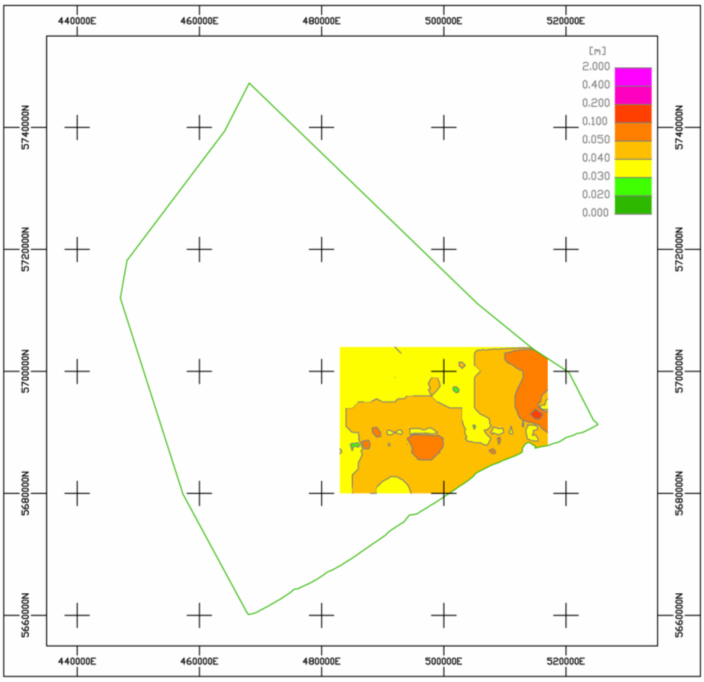


**Figure 48:** Interpolated grid model of the average RMS of the LRK positions with correction signal from the reference station Neeltje Jans (year 2009) (original data, outliers included)

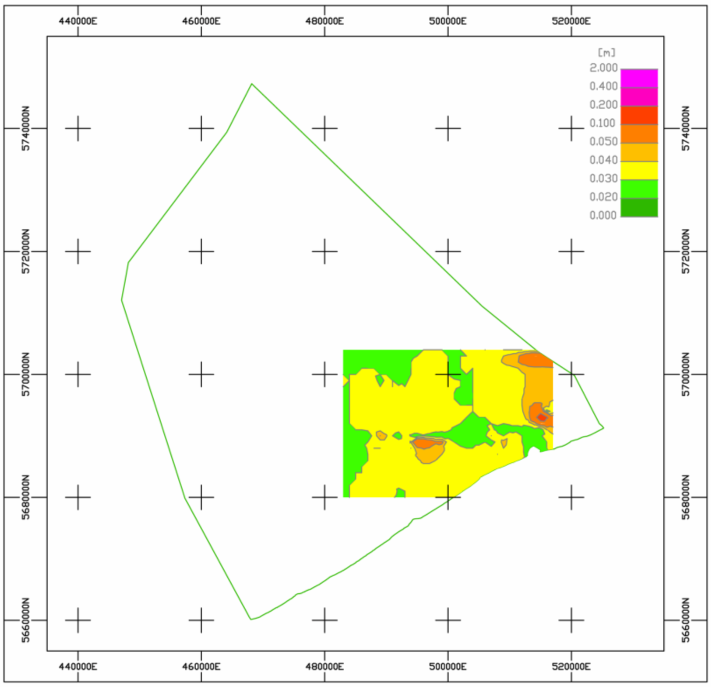


**Figure 49:** Interpolated grid model of the minimum RMS of the LRK positions with correction signal from the reference station Neeltje Jans (year 2009) (original data, outliers included)

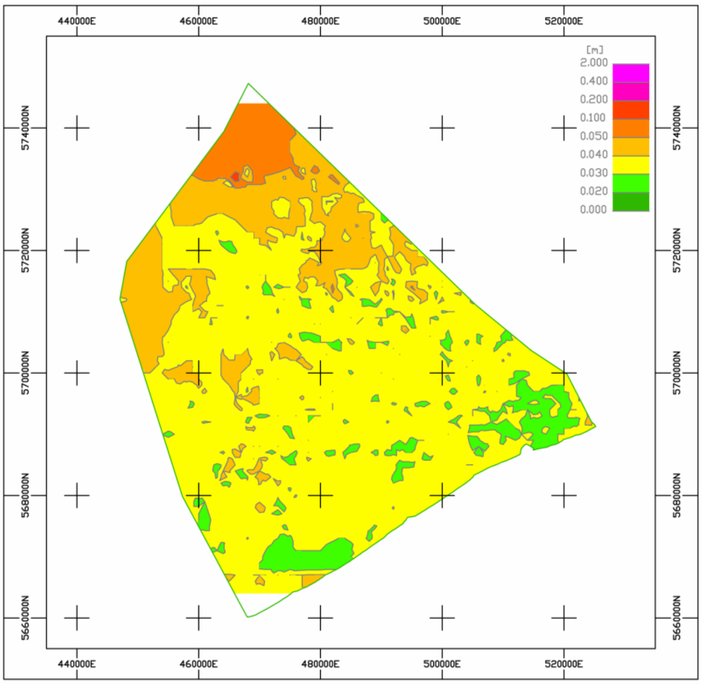


**Figure 50:** Interpolated grid model of the minimum of the three average RMS graphs of the LRK positions with correction signal from reference stations Oostduinkerke, Zeebrugge and Neeltje Jans (year 2009) (original data, outliers included)

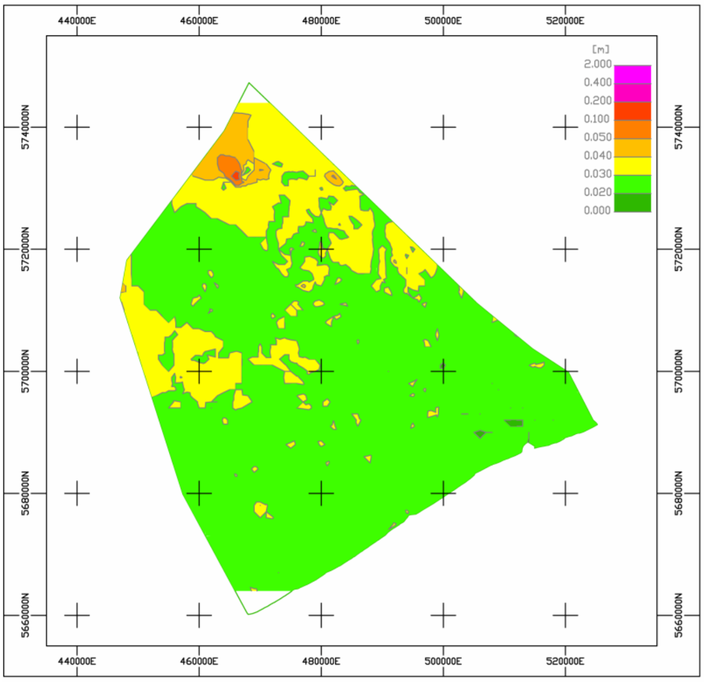


**Figure 51:** Interpolated grid model of the minimum of the three minimum RMS graphs of the LRK positions with correction signal from reference stations Oostduinkerke, Zeebrugge and Neeltje Jans (year 2009) (original data, outliers included)

## 5.3 ANALYSIS OF THE RELATIONSHIP BETWEEN QUALITY AND DISTANCE TO THE LRK STATION

It is generally assumed that the quality of an LRK correction depends on the distance to the LRK station. This hypothesis is tested by performing statistical analysis (using S-Plus® 8.0) on the relation between the RMS (indicates the quality of the LRK position) and the distance to the LRK station.

### 5.3.1 Neeltje Jans LRK station

The RMS value of each LRK position (19 658 in total) that was obtained using a correction signal from the Neeltje Jans reference station is analyzed in function of its distance to this LRK station (Figure 52). In order to analyze the relation between both variables, a linear least-squares regression is performed.

The strength of the linear regression is expressed by the $R^2$ value, i.e. a statistical measure based on the sum of squares that always has a value between 0 (no linear relation between both variables) and 1 (all observations perfectly match the regression line). In this case, $R^2$ is 0.003 which indicates that the variation of RMS is only very little explained by the distance.

The statistical significance of the regression line can be tested by performing a statistical t-test on the slope value. The null hypothesis ($H_0$) of this test states that the slope equals zero, the alternative hypothesis ($H_A$) states that the slope value does not equal zero. In this case, the p-value associated with the slope is 0.0000 and thus smaller than 0.001, which means that ($H_0$) is rejected on the 99.9% significance level. The slope value thus significantly differs from zero.

The conclusions from the $R^2$ and t-test are that there is a significant linear trend between both variables (with a very small slope, i.e. $2\ 10^{-7}$), but in general, the distance does not adequately explain the variation in RMS. Only 0.3% of the total RMS variance is explained by the distance to the reference station.

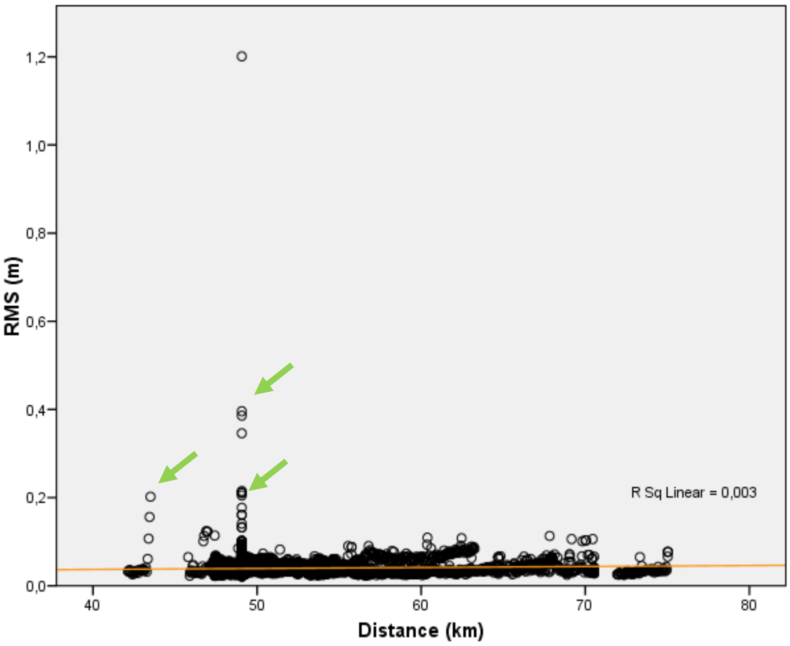


Neeltje Jans

$\bar{x} = 3.92\ cm$
$\sigma = 1.35\ cm$

$n =$ 19 658
$R^2 =$ 0.003

$y = 2 \cdot 10^{-7} \cdot x + 0.0282$ [m]
$p_{slope} =$ 0.0000

**Figure 52:** RMS of the LRK positions in function of their distance to the reference station (Neeltje Jans) and linear regression line (orange) (original data, outliers included)

The scatter plot (Figure 52) indicates that there are some remarkable outliers (green marks). Outliers are defined as all values that deviate more than $3 \cdot \sigma$ from the linear regression line in both directions. After applying this threshold and removing the outliers, a new linear regression is performed (Figure 53). The slope of the regression line has not changed. The associated p-value however indicates that it does significantly differs from zero. The R² value slightly increased, but still indicates a very low association between both variables.

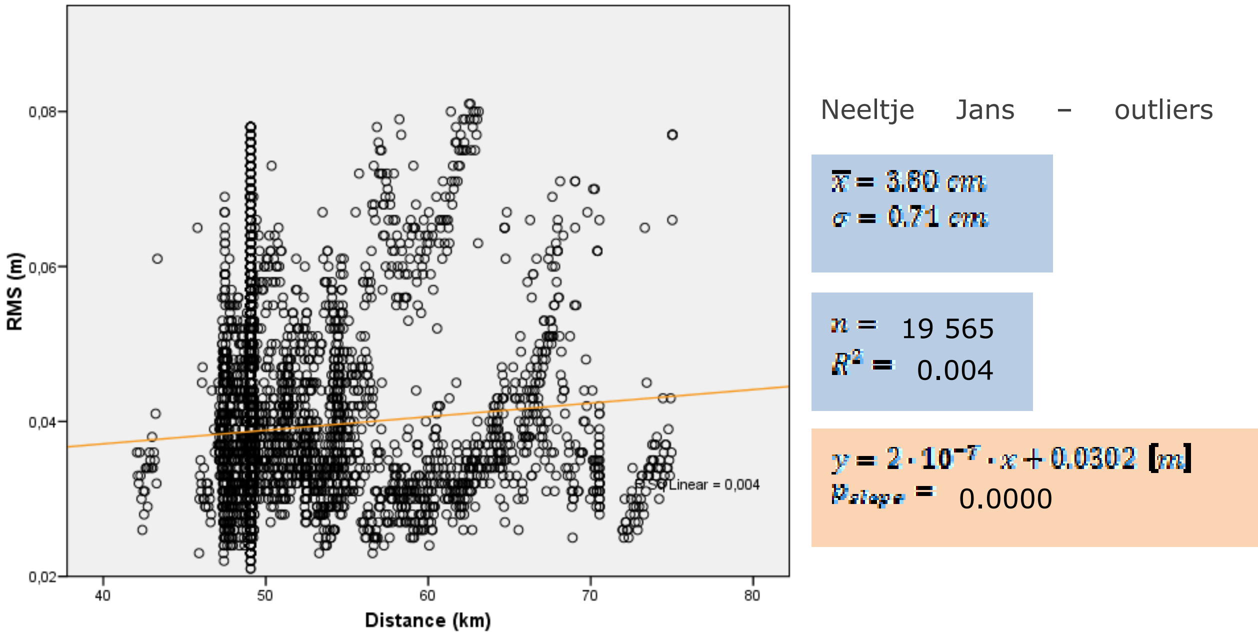


**Figure 53:** RMS of the LRK positions in function of their distance to the reference station (Neeltje Jans) and linear regression line (orange) (outliers excluded from dataset)

### 5.3.2 Oostduinkerke LRK station

Figure 54 visualizes the quality of the LRK positions (66 773 values) relative to their distance from the reference station (Oostduinkerke), and the linear regression line through this data.

After outlier elimination a new linear regression is performed (Figure 55). The slope value significantly differs from zero. The R² value slightly increased, but still indicates that only 3% of the RMS variance is explained by the distance to the reference station.

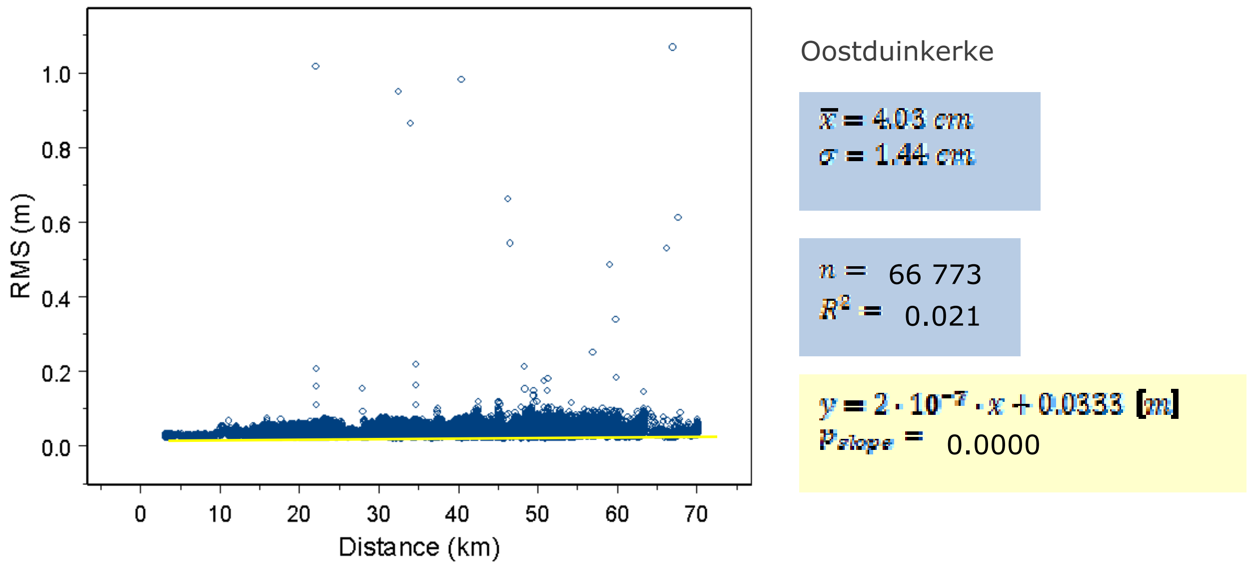


**Figure 54:** RMS of the LRK positions in function of their distance to the reference station (Oostduinkerke) and linear regression line (yellow) (original data, outliers included)

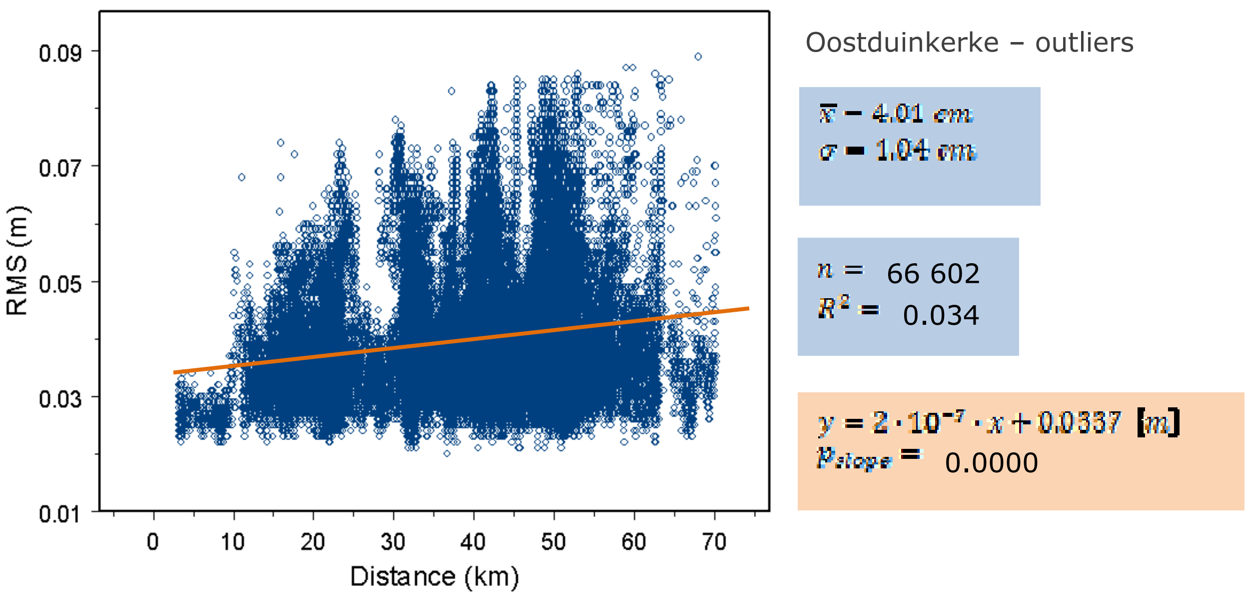


**Figure 55:** RMS of the LRK positions in function of their distance to the reference station (Oostduinkerke) and linear regression line (orange) (outliers excluded from dataset)

### 5.3.3 Zeebrugge LRK station

Figure 56 visualizes the random error of the LRK measurements relative to their distance from the reference station (Zeebrugge) and the linear regression line through this data. All points that are at a distance greater than $3 \cdot \sigma$ from the regression line are considered to be outliers. A total of 1485 values were thus removed from the dataset.

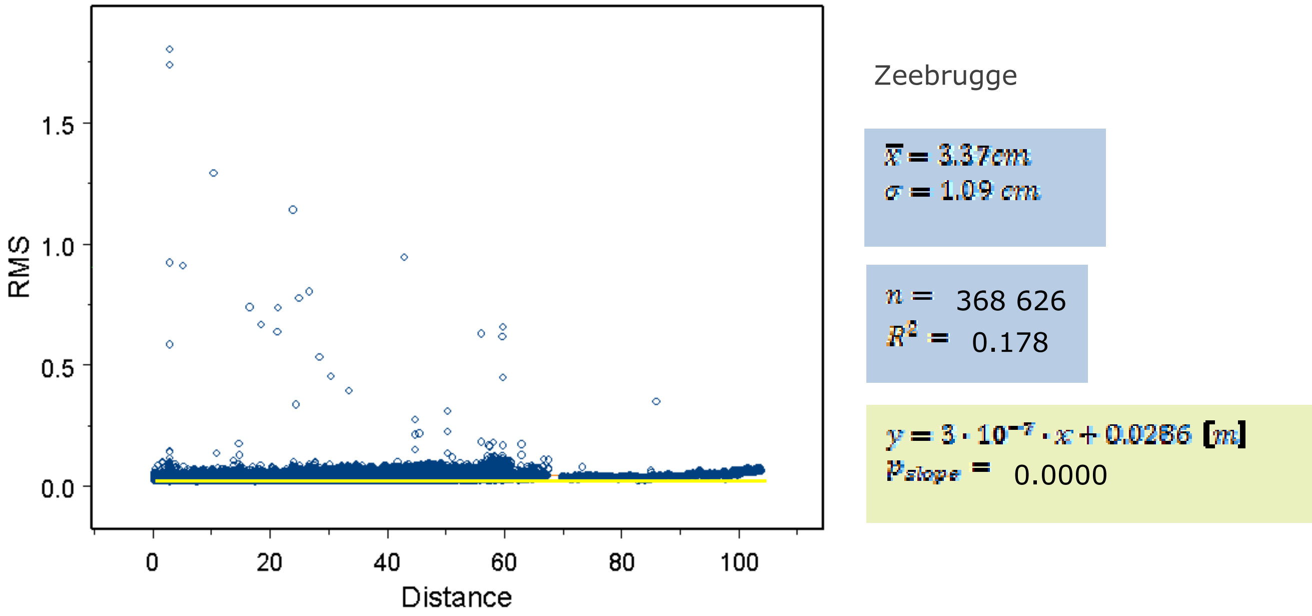


**Figure 56:** RMS of the LRK positions in function of their distance to the reference station (Zeebrugge) and linear regression line (yellow) (original data, outliers included)

On the adjusted dataset (without the outliers), linear regression is performed (Figure 57). Results indicate that the slope value significantly differs from zero ($p < 0.001$) and that 29% of the variance in RMS is explained by the distance. Compared to the previous stations, this is a remarkable higher $R^2$ value. This value however still indicates that there is only a weak linear relation between both variables.

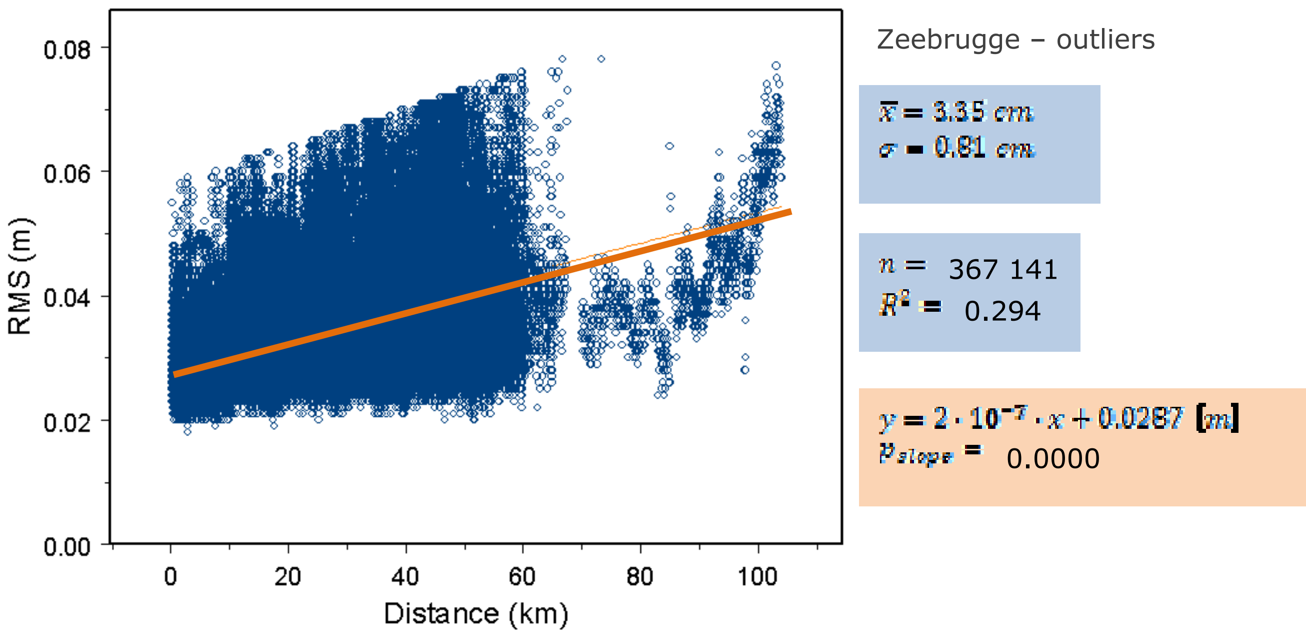


**Figure 57:** RMS of the LRK positions in function of their distance to the reference station (Zeebrugge) and linear regression line (orange) (outliers excluded from dataset).

### 5.3.4 Combined analysis

Finally, all LRK positions of the R/V BELGICA during the year 2009 are combined into one file and statistically analyzed. Figure 58 visualizes the result of the linear regression analysis (yellow line) and the scatter plot of all RMS values.

After removing the outliers, linear regression analysis is performed based on the remaining values (Figure 59).

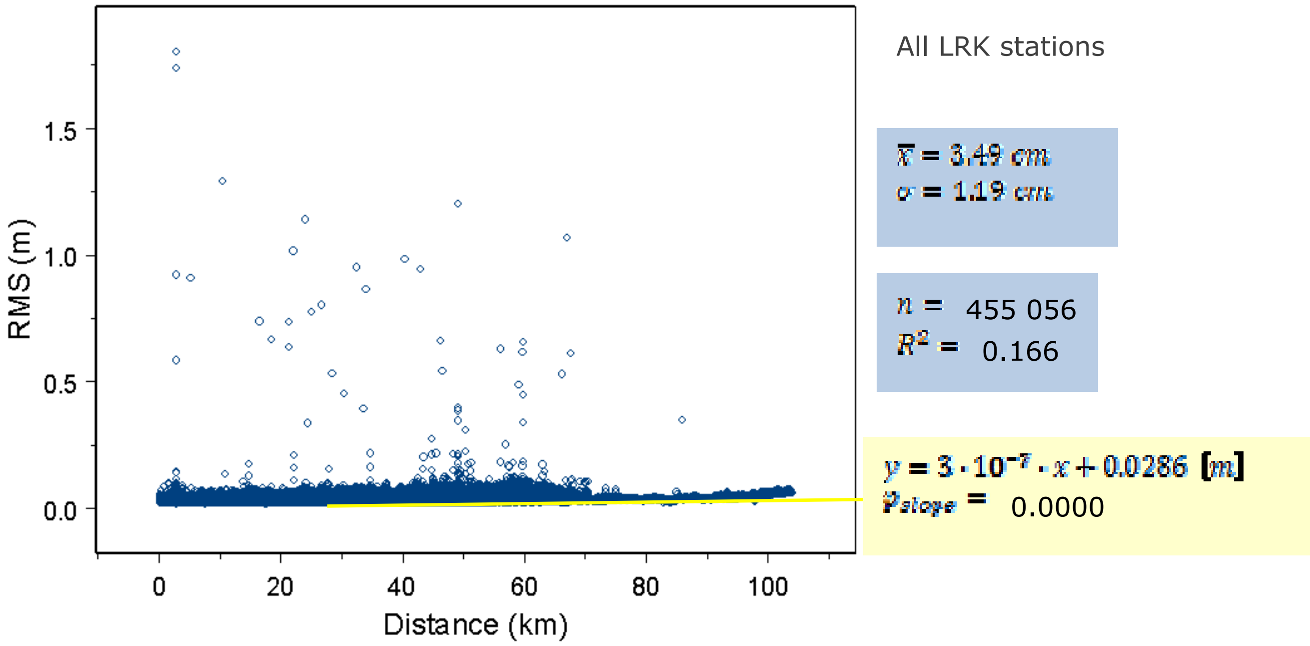


**Figure 58:** RMS of the LRK positions in function of their distance to the reference station (all stations) and linear regression line (yellow) (original data, outliers included)

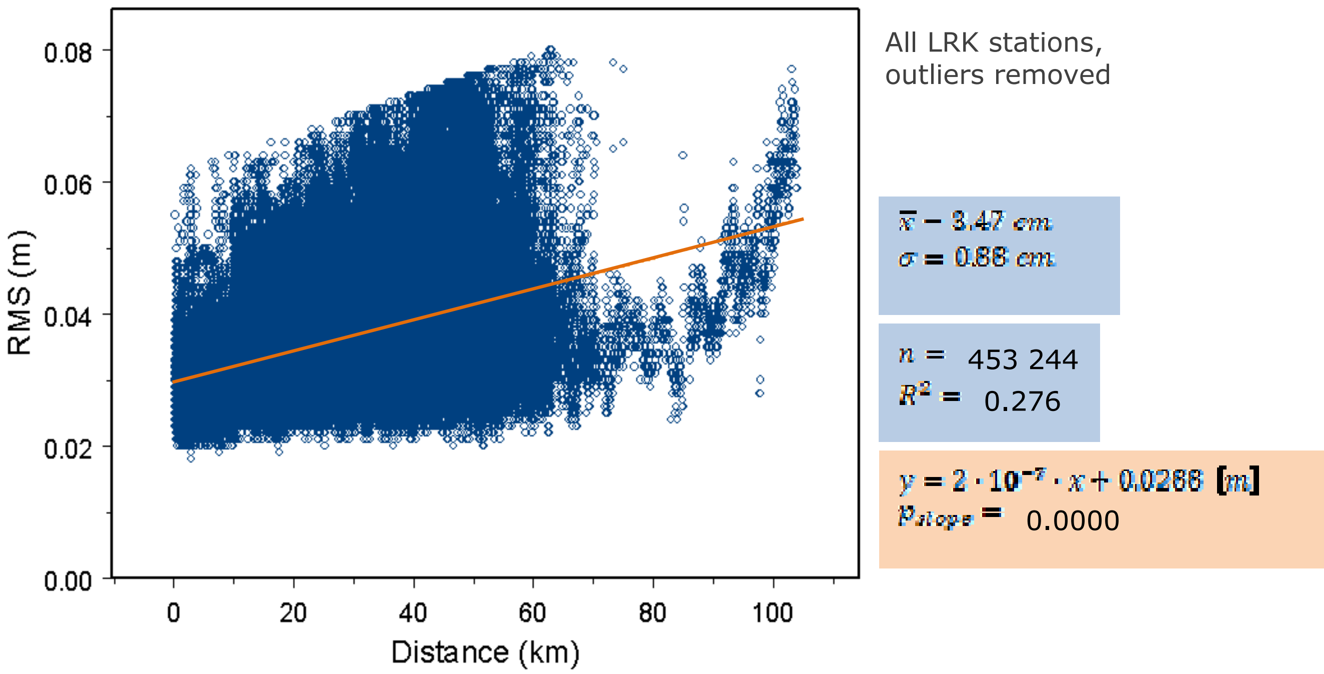


**Figure 59:** RMS of the LRK positions in function of their distance to the reference station (all stations) and linear regression line (orange) (outliers excluded from dataset).

### 5.3.5 Conclusion

Statistical analysis was performed on the random error of dynamic LRK positioning and its relation with the distance from the LRK station. In general, it can be concluded that this relation is weak. Overall, an $R^2$ value of 0.2759 is achieved, which indicates that only 28% of the variance in random error is explained by the distance to the reference station.

## 5.4 Comparison with LRK measurements on land (NGI)

The random error of the dynamic LRK measurements (on sea, see previous chapter) is now compared to the random error of the static LRK measurements (on land) that were performed by the NGI in January 2009. Specifically, the following values are compared:

- The RMS value from the GGA string of the dynamic LRK positioning on the R/V Belgica (data from all campaigns in 2009, all LRK stations)
- The RMS value from the GGA string of the static LRK measurements on land (collected in January 2009)

First, outlier values are removed from both datasets using the $3 \cdot \sigma$ criterion (relative to the regression line through the original data set). Next, a linear regression is performed on both reduced datasets, i.e. the random error of static and dynamic LRK measurements. The result of this regression is visualized in Figure 20.

This analysis shows that

- the random error of static LRK positioning is smaller than the random error of dynamic LRK positioning;
- the random error of dynamic LRK positioning increases more with increasing distance to the LRK station compared to the static LRK positioning;
- the slope of the regression line with regard to static LRK positioning does not significantly differ from 0 ($p > 0.001$);
- the variation in the random error can only partly be explained by the distance from the reference station ($R^2 = 0.14$ for static measurements and 0.28 for dynamic measurements).

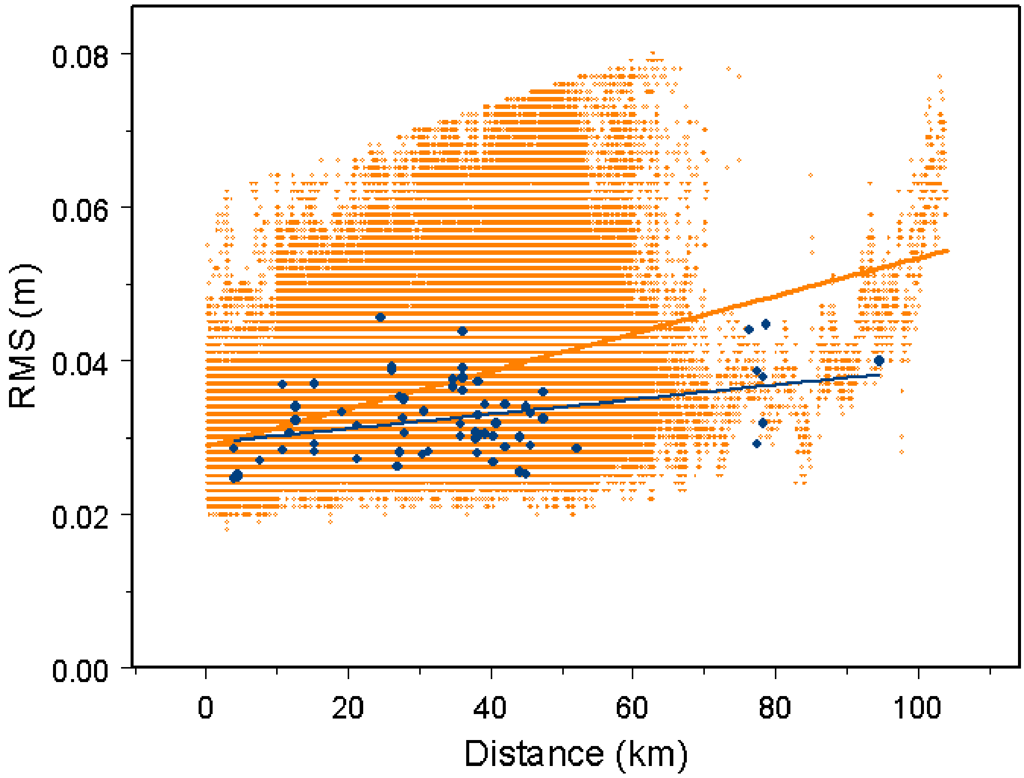


| | | |
|---|---|---|
| $\bar{x}_{static} = 3.26\ cm$<br>$\sigma_{static} = 0.50\ cm$ | $n = 69$<br>$R^2 = 0.14$ | $y = 1 \cdot 10^{-7} \cdot x + 0.0292\ [m]$<br>$p_{slope} =$ 0.0015 |
| $\bar{x}_{dynamic} = 3.47\ cm$<br>$\sigma_{dynamic} = 0.88\ cm$ | $n = 453\ 244$<br>$R^2 = 0.28$ | $y = 2 \cdot 10^{-7} \cdot x + 0.0288\ [m]$<br>$p_{slope} =$ 0.0000 |

**Figure 60:** Random error of static LRK measurements (blue) and dynamic LRK measurements (orange) with regression line.

## 5.5 DETAILS OF THE STATISTICAL ANALYSIS

### 5.5.1 Statistical analysis – Neeltje Jans station

```
Linear regression - original Neeltje Jans data

Call: lm(formula = RMS..m. ~ Distance..km., data = Station16, na.action = na.exclude
          )
Residuals:
      Min         1Q     Median        3Q    Max
 -0.01923 -0.006064 -0.002063 0.003937 1.162

Coefficients:
                Value Std. Error t value Pr(>|t|)
  (Intercept)  0.0282  0.0015    18.8462  0.0000
Distance..km.  0.0002  0.0000     7.3885  0.0000

Residual standard error: 0.01344 on 19656 degrees of freedom
Multiple R-Squared: 0.00277
F-statistic: 54.59 on 1 and 19656 degrees of freedom, the p-value is 1.544e-013
```

```
Linear regression -  Neeltje Jans without outliers

Call: lm(formula = RMS..m. ~ Distance..km., data = SDF13, na.action = na.exclude)
Residuals:
      Min        1Q    Median       3Q     Max
 -0.01774 -0.005703 -0.001703 0.004297 0.03997

Coefficients:
                Value Std. Error t value Pr(>|t|)
  (Intercept)  0.0302  0.0009    31.8289  0.0000
Distance..km.  0.0002  0.0000     9.0985  0.0000

Residual standard error: 0.008421 on 19565 degrees of freedom
Multiple R-Squared: 0.004213
F-statistic: 82.78 on 1 and 19565 degrees of freedom, the p-value is 0
```

### 5.5.2 Statistical analysis – Oostduinkerke station

```
Linear regression -  original Oostduinkerke data

Call: lm(formula = RMS..m. ~ Distance..km., data = Station81, na.action = na.exclude
          )
Residuals:
     Min        1Q    Median       3Q   Max
 -0.0224 -0.007388 -0.002337 0.004579 1.023

Coefficients:
                 Value Std. Error  t value Pr(>|t|)
  (Intercept)   0.0333   0.0002   173.8074   0.0000
Distance..km.   0.0002   0.0000    38.0834   0.0000

Residual standard error: 0.01423 on 66771 degrees of freedom
Multiple R-Squared: 0.02126
F-statistic: 1450 on 1 and 66771 degrees of freedom, the p-value is 0
```

```
Linear regression -  Oostduinkerke without outliers

Call: lm(formula = RMS..m. ~ Distance..km., data = SDF14, na.action = na.exclude)
Residuals:
      Min        1Q    Median       3Q     Max
 -0.02179 -0.007179 -0.002154 0.004665 0.04437

Coefficients:
                 Value Std. Error  t value Pr(>|t|)
  (Intercept)   0.0337   0.0001   244.6570   0.0000
Distance..km.   0.0002   0.0000    48.4184   0.0000

Residual standard error: 0.0102 on 66600 degrees of freedom
Multiple R-Squared: 0.034
F-statistic: 2344 on 1 and 66600 degrees of freedom, the p-value is 0
```

### 5.5.3 Statistical analysis – Zeebrugge station

```
Linear regression -  original Zeebrugge data
```

```
Call: lm(formula = RMS..m. ~ Distance..km., data = Station80, na.action = na.exclude
          )
Residuals:
      Min        1Q    Median       3Q   Max
 -0.02645 -0.004391 -0.001308 0.002607 1.774

Coefficients:
                  Value Std. Error   t value  Pr(>|t|)
  (Intercept)    0.0286    0.0000  1177.5920    0.0000
Distance..km.    0.0003    0.0000   282.5629    0.0000

Residual standard error: 0.009888 on 368623 degrees of freedom
Multiple R-Squared: 0.178
F-statistic: 79840 on 1 and 368623 degrees of freedom, the p-value is 0
1 observations deleted due to missing values

Correlation of Coefficients:
              (Intercept)
Distance..km. -0.7425

Analysis of Variance Table

Response: RMS..m.

Terms added sequentially (first to last)
                  Df Sum of Sq  Mean Sq  F Value Pr(F)
Distance..km.      1   7.80562 7.805625 79841.82     0
    Residuals 368623  36.03792 0.000098
```

---

Linear regression - Zeebrugge without outliers

```
Call: lm(formula = RMS..m. ~ Distance..km., data = SDF12, na.action = na.exclude)
Residuals:
      Min        1Q    Median       3Q     Max
 -0.02547 -0.004206 -0.001161 0.002692 0.03282

Coefficients:
                  Value Std. Error   t value  Pr(>|t|)
  (Intercept)    0.0287    0.0000  1715.4253    0.0000
Distance..km.    0.0002    0.0000   390.9783    0.0000

Residual standard error: 0.006787 on 367062 degrees of freedom
Multiple R-Squared: 0.294
F-statistic: 152900 on 1 and 367062 degrees of freedom, the p-value is 0
1485 observations deleted due to missing values
```

### 5.5.4 Statistical analysis – combination of all reference stations

Linear regression - combination of all reference stations (original data)

```
Call: lm(formula = RMS..m. ~ Distance..km., data = Allstations, na.action =
          na.exclude)
Residuals:
      Min        1Q    Median       3Q   Max
 -0.02637 -0.004564 -0.001432 0.002956 1.773
```

```
Coefficients:
                 Value Std. Error   t value  Pr(>|t|)
  (Intercept)    0.0288    0.0000  1111.7474    0.0000
Distance..km.    0.0003    0.0000   301.1873    0.0000

Residual standard error: 0.01083 on 455054 degrees of freedom
Multiple R-Squared: 0.1662
F-statistic: 90710 on 1 and 455054 degrees of freedom, the p-value is 0
```

**Linear regression - combination of all stations (outliers excluded)**

```
Call: lm(formula = RMS..m. ~ Distance..km., data = SDF15, na.action = na.exclude)
Residuals:
      Min        1Q    Median       3Q     Max
 -0.02545 -0.004569 -0.001285 0.003124 0.03576

Coefficients:
                 Value Std. Error   t value  Pr(>|t|)
  (Intercept)    0.0288    0.0000  1611.8563    0.0000
Distance..km.    0.0002    0.0000   415.6063    0.0000

Residual standard error: 0.007477 on 453242 degrees of freedom
Multiple R-Squared: 0.2759
F-statistic: 172700 on 1 and 453242 degrees of freedom, the p-value is 0
```

### 5.5.5 Statistical analysis – static measurements

**Linear regression - static measurements (original dataset)**

```
Call: lm(formula = RMS..m. ~ Distance..km., data = RMSland, na.action = na.exclude)
Residuals:
       Min        1Q     Median      3Q     Max
 -0.009278 -0.004038 -0.0008312 0.00249 0.02728

Coefficients:
               Value Std. Error t value Pr(>|t|)
  (Intercept)  0.0296  0.0016    18.0152  0.0000
Distance..km.  0.0001  0.0000     2.6394  0.0103

Residual standard error: 0.006564 on 69 degrees of freedom
Multiple R-Squared: 0.0917
F-statistic: 6.966 on 1 and 69 degrees of freedom, the p-value is 0.01026
```

**Linear regression - static measurements (outliers removed from dataset)**

```
Call: lm(formula = RMS..m. ~ Distance..km., data = SDF21, na.action = na.exclude)
Residuals:
       Min        1Q     Median       3Q     Max
 -0.008376 -0.003361 -0.0004521 0.003077 0.01401

Coefficients:
               Value Std. Error t value Pr(>|t|)
  (Intercept)  0.0292  0.0012    25.0714  0.0000
Distance..km.  0.0001  0.0000     3.3011  0.0015
```

```
Residual standard error: 0.004644 on 67 degrees of freedom
Multiple R-Squared: 0.1399
F-statistic: 10.9 on 1 and 67 degrees of freedom, the p-value is 0.001546
```

# 6. Systematic error of dynamic LRK positioning

## 6.1 Introduction

On the R/V Belgica, a Thales Aquarius® GPS registers the ship's position using the LRK, DGPS or GPS method depending on the position of the vessel. The systematic error of this system has however never been tested before. In order to test this positioning system, the NGI has carried out control positioning measurements on board the R/V Belgica during two campaigns in 2009. The accuracy of the GPS onboard the ship will be determined by statistical analysis of these control measurement results, by comparing the Thales LRK system with a more accurate GPS system (Leica SR530).

## 6.2 Methodology and results

During two R/V Belgica campaigns, on 19-23 October and 9-11 December 2009, the position of the R/V Belgica research vessel was determined by two GPS receivers, i.e. (1) the onboard Aquarius® and (2) an external Leica SR530. In order to avoid errors due to the antenna position or time lag, the Thales antenna (type Thales NAP002) signal was split to the Thales Aquarius® on one hand, and the external Leica on the other hand.

Only the LRK positions are, in theory, sufficiently accurate for use in bathymetric measurements. Since one of the objectives of this research project is to determine the accuracy of the Aquarius® GPS on the Belgian Continental Plate, only the LRK positions will be used for further analysis (DGPS and GPS positions are not considered).

During Campaign 28 and 33, two kinds of positions were registered:

1. A 3D position was calculated by the Aquarius® (LRK)
2. The observations of the Leica (interval: one second) that lead to the position determination were registered (i.e. the code and phase observation) and used to post-process the original 3D data in order to achieve more accurate positions. This was done using the code- and phase observations and the equivalent observations of three reference stations on land (i.e. Zeebrugge, Oostende and Veurne) as input data. The original, one-second data was used in combination with the accurately determined position of the land reference stations to calculate accurate base lines to each point measured by the Leica GPS receiver.

The results of both positioning systems can be used to compare the XYZ position of the ship and thus to determine the systematic error of the Aquarius® GPS onboard the R/V Belgica. The number of positions used for this analysis is determined by

- The amount of LRK positions produced by the Aquarius® (Figure 61)
- The amount of fixed ambiguities that are found during the Leica position post-processing. The requirements for these positions are:
    - The Leica GPS post-processing solution has to be the average of two or three base lines, single station solutions were removed;
    - The difference between the individual solution per base line and the average of two or three base lines has to be smaller than 10 cm, otherwise the solution was removed;

During the two campaigns, 99% of the LRK positions were achieved with the Zeebrugge LRK reference station. Therefore, all following analyses are made with regard to this reference station.

A priori, the post-processed Leica positions are more accurate than the Aquarius® positions, because these are network solutions that are achieved through post-processing. These positions are therefore considered to be the reference value.

The comparison between both positions is made on two levels, i.e. (1) in the horizontal plane (XY vector) and (2) in the vertical direction (based on the ellipsoidal height). Practically, the Aquarius® positions are subtracted from the Leica post-processed positions (that are considered to be the reference value).

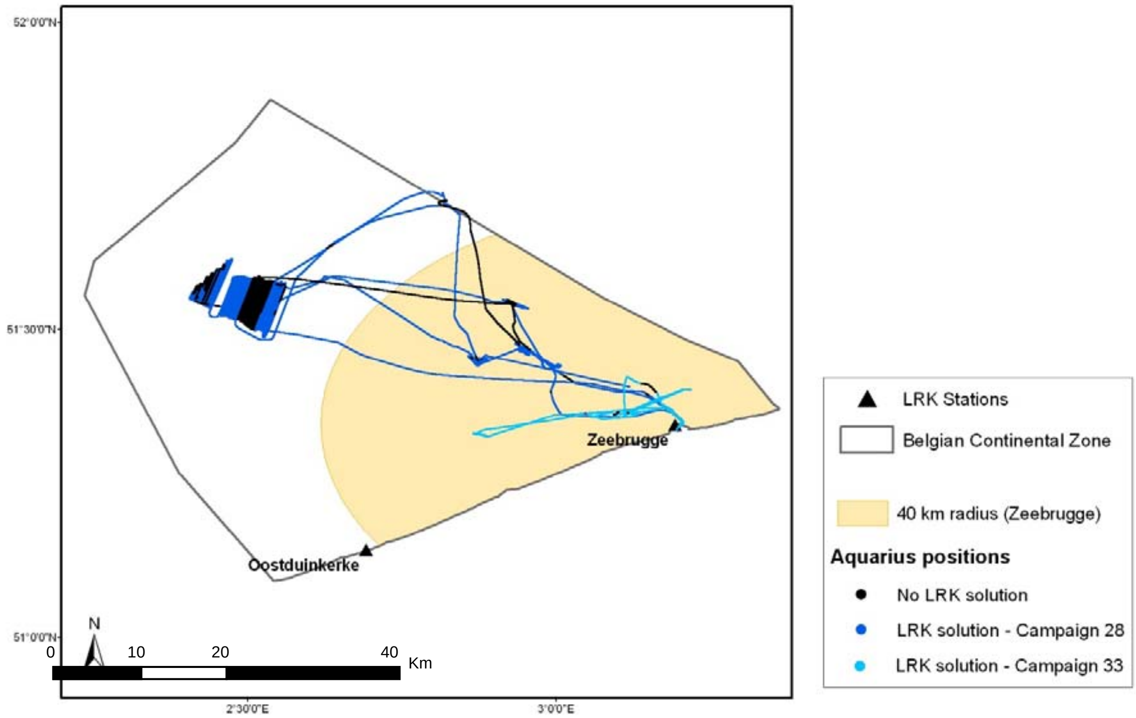


**Figure 61:** Overview of positions registered by Leica during Campaign 28 and 33

### 6.2.1 Systematic planimetric error of dynamic LRK measurements

In order to determine the difference between both coordinates (Leica and Aquarius®), all positions were transformed from ETRS89 into UTM31 (datum: WGS84). Figure 62 visualizes the planimetric (XY) difference between the post-processed Leica and the equivalent Aquarius® positions. Figure 63 visualizes the evolution of this difference with regard to the distance to the LRK station.

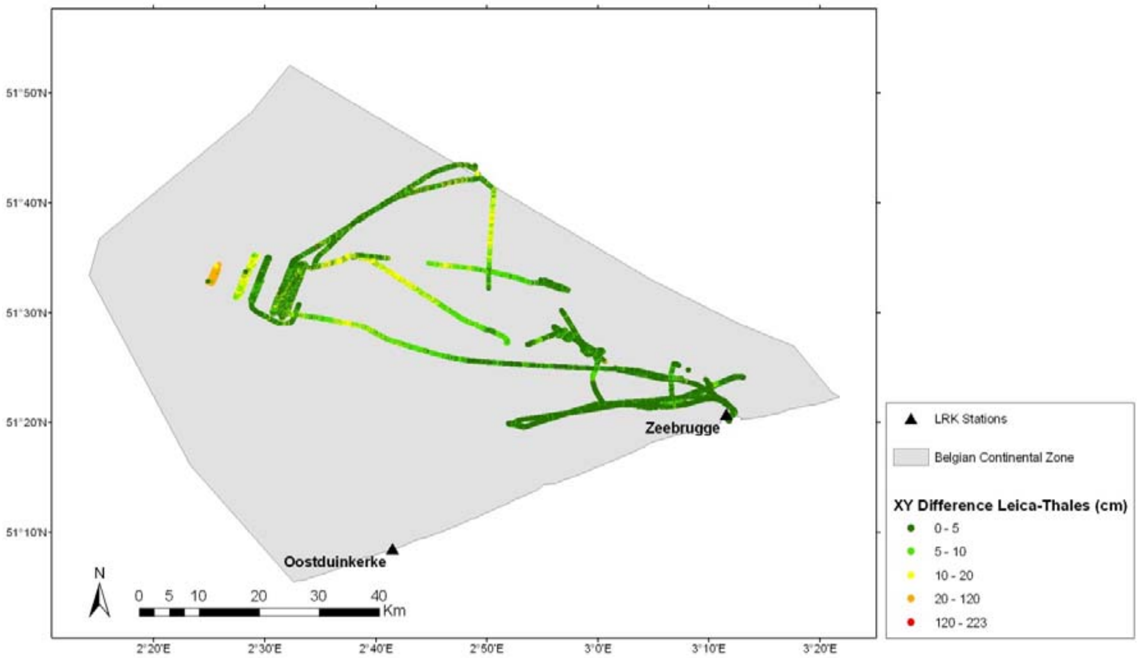


**Figure 62:** Systematic planimetric error

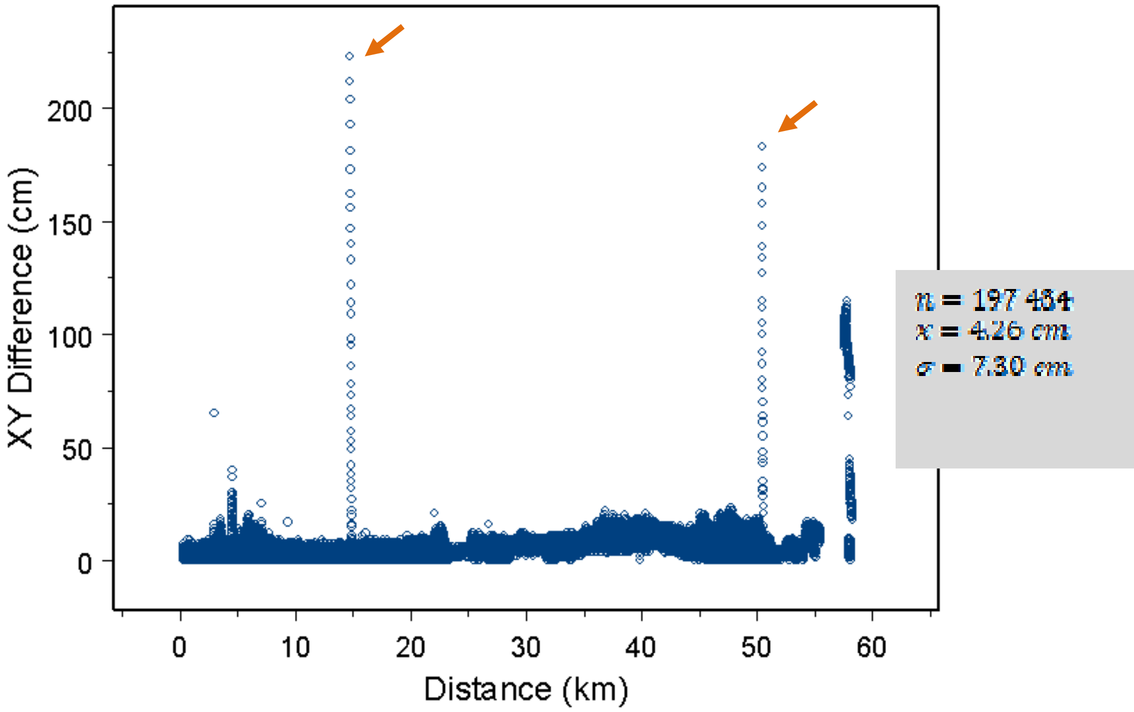


**Figure 63:** Relation between the systematic planimetric error and the distance to the LRK station (Zeebrugge) (original data, outliers included)

There are some remarkable outliers (up to more than 2m), i.e. at a distance of 15 km from the Zeebrugge station and at a distance of 50 to 60 km. The remarkable vertical trends (see orange marks), at a distance of respectively 15 and ca. 51 km are related to the process of gradual losing the LRK signal. Although the planimetric error increases to more than 2m, the Aquarius® receiver however still indicates that these are LRK solutions. The positions and planimetric error of the first outlier trajectory (ca. 15 km from the reference station) is visualized in Figure 64. The movement of the ship was analyzed based on the position metadata and is indicated on the Figure 64. This confirms that the planimetric accuracy progressively worsened. Figure 65 visualizes the RMS that is indicated by the Aquarius® GPS for these LRK (!) positions (based on 10-second data). The RMS value increases from 0.039 m to 0.174 m. Although the RMS increases, the values underestimate the real occurring error.

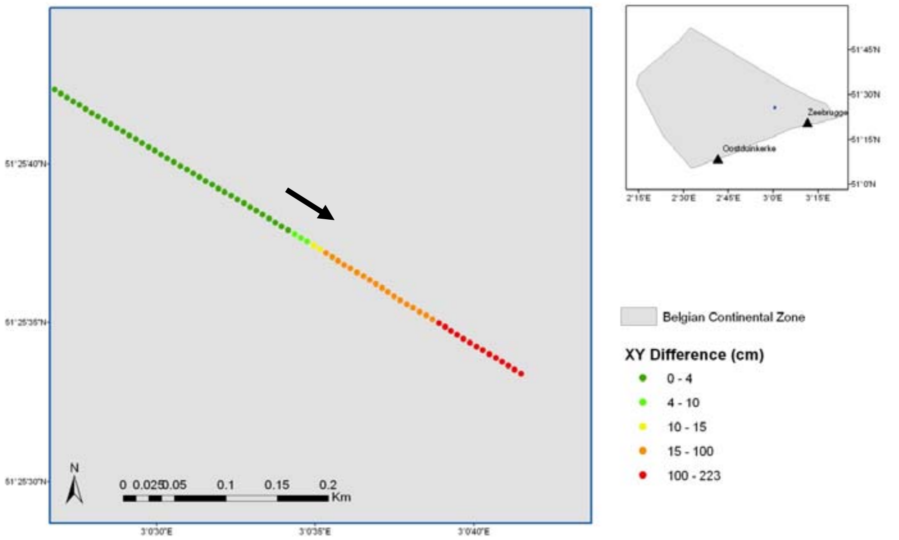


**Figure 64:** Systematic planimetric error of outliers at a distance of ca. 15 km from the Zeebrugge LRK station and ship movement (arrow)

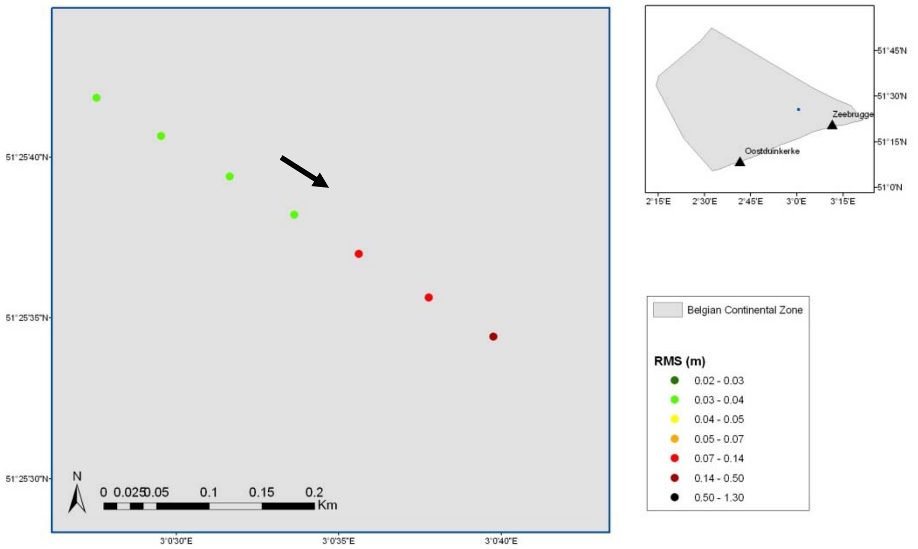


**Figure 65:** RMS of outliers at a distance of ca. 15 km from the Zeebrugge LRK station and ship movement (arrow)

Figure 66 and Figure 67 visualize the position and RMS values of the second vertical trend (at ca. 51 km from the reference station). Again, the systematic planimetric error progressively worsens until finally the LRK signal is lost. The RMS values increase up to a value of 0.309 m.

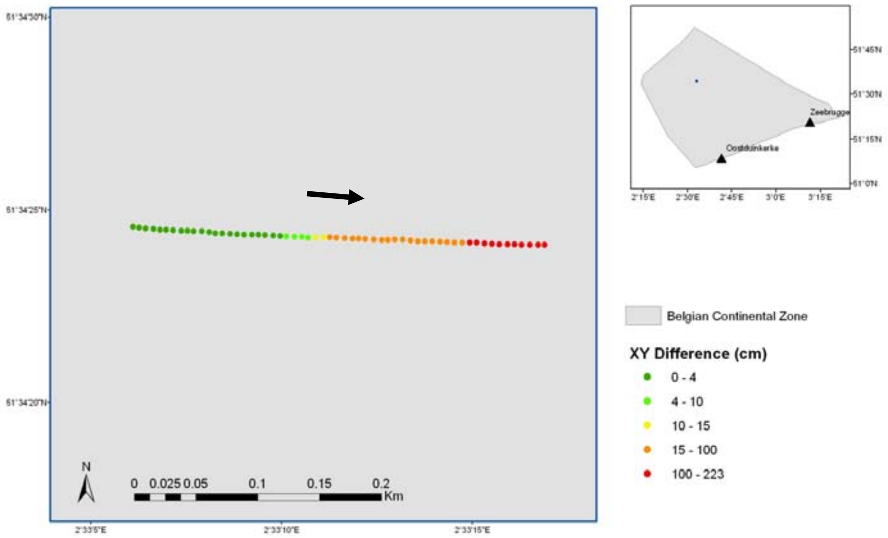


**Figure 66:** XY Difference of outliers at a distance of ca. 50-60 km from the Zeebrugge LRK station and ship movement (arrow)

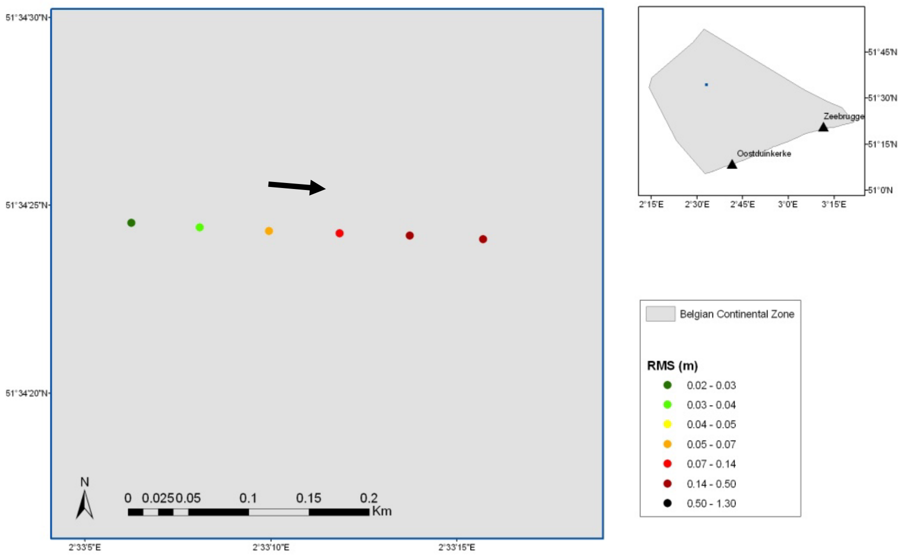


**Figure 67:** RMS values of outliers at a distance of ca. 50-60 km from the Zeebrugge LRK station and ship movement (arrow)

The relation between the distance from the LRK station and the systematic error of the Aquarius® LRK positions is statistically analyzed by performing linear regression and removing the outlier values (every value that is at a distance of more than $3 \cdot \sigma$ from the regression line based on the original data).

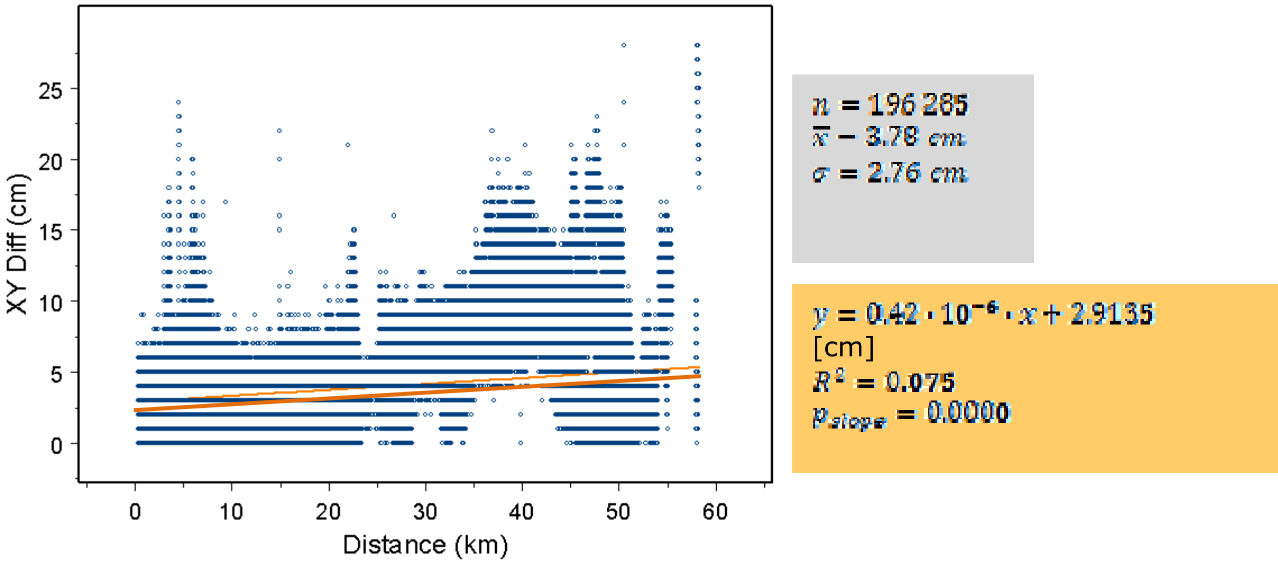


**Figure 68:** Linear regression (orange line) of the relation between the systematic planimetric error and the distance to the LRK station (Zeebrugge)

Although the slope p value (0.0000) indicates that the slope value significantly differs from zero, the $R^2$ value indicates that less than 1% of the variability in the systematic planimetric error is explained by the distance. It can thus be concluded that there is only a small linear trend between both variables.

### 6.2.2 Systematic altimetric error of dynamic LRK measurements

Figure 69 visualizes the systematic altimetric error, i.e. the ellipsoidal height of Leica post-processed positions – the equivalent height of the Aquarius® positions.

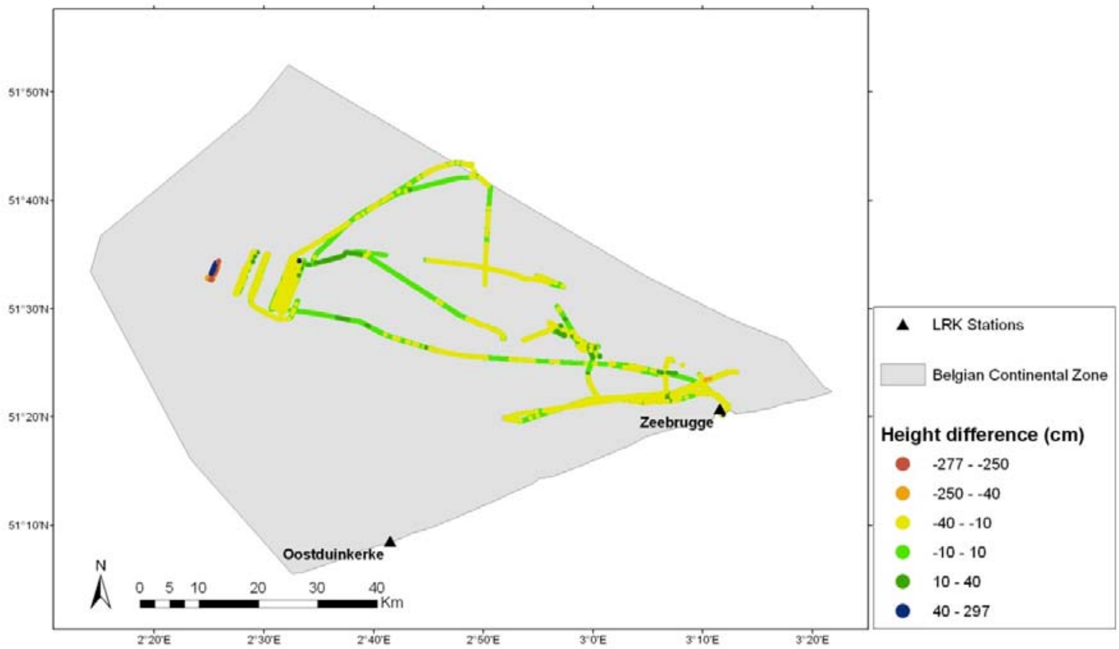


**Figure 69:** Systematic altimetric error

Figure 70 shows the relation between this altimetric error and the distance to the LRK station (Zeebrugge).

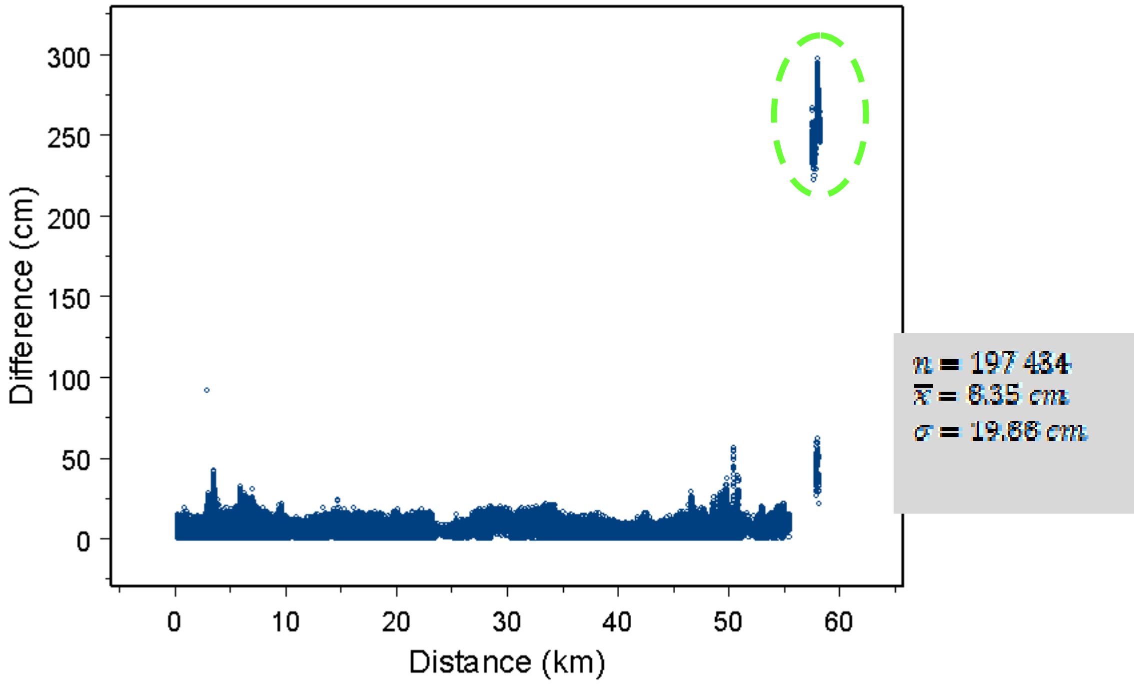


**Figure 70:** Relation between the systematic altimetric error and the distance to the LRK station (Zeebrugge)

There is however one cluster of outliers (green circle) where the systematic altimetric error is 2 to 3m. It has to be noted that these outliers in the altimetric error do not have an equivalent high planimetric error (Figure 63).

The outlier values are clustered in both time and in space, since all points have been registered during the same campaign and even in subsequent transects (Figure 71). The RMS values registered in the GGA String of the Aquarius® however indicate that these positions are LRK positions with a mean accuracy of 0.056 m (σ = 0.021 m) (Figure 72). Based on this data, one can conclude that when bathymetric measurements are carried out at a great distance (> 55km) from the LRK station, caution is necessary concerning the Aquarius® position information. Although the GPS indicates that LRK positions can be calculated (even with high accuracy), this test has pointed out that those positions can be very inaccurate (with height errors up to 3m).

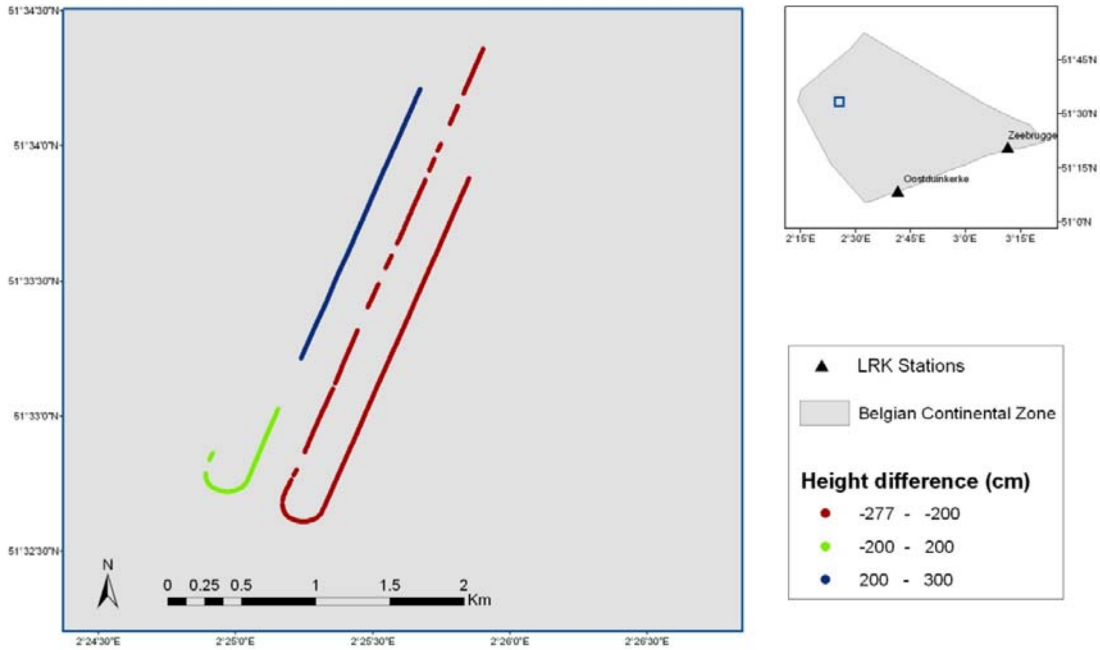


**Figure 71:** Location of the cluster of outlier values (ellipsoidal height difference Leica-Aquarius® >2m)

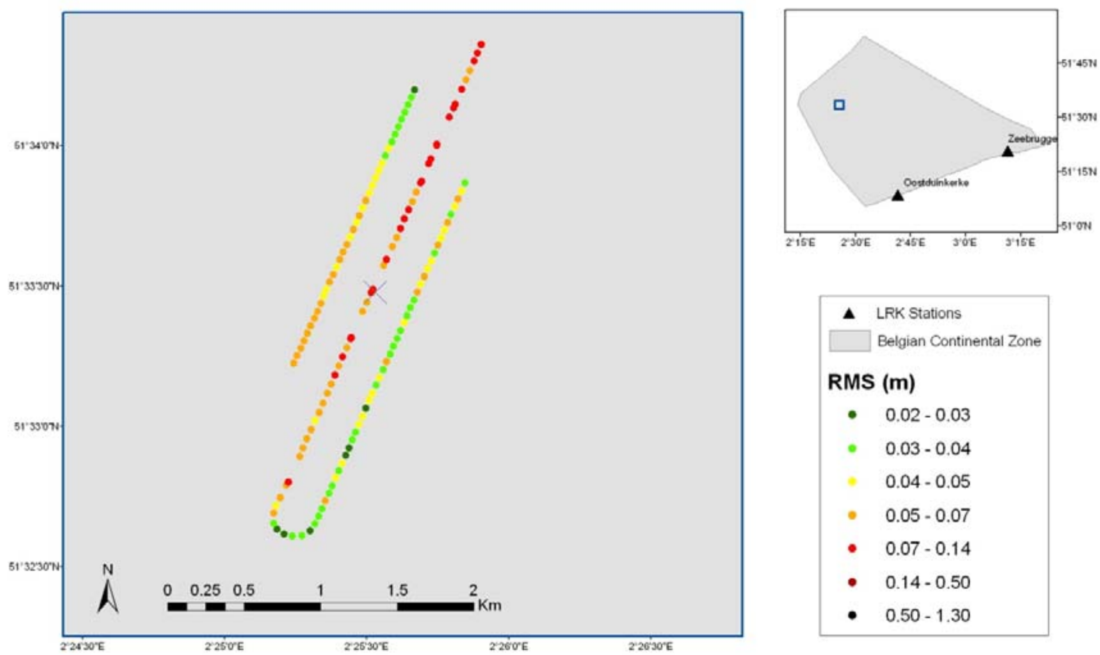


**Figure 72:** GGA String RMS value for the height outlier values

Figure 73 visualizes the results of the linear regression analysis. Again, the slope p-value indicates that the slope value significantly differs from zero, but the $R^2$ value is also very low, indicating that only 0.1% the variation in the altimetric error is explained by the distance to the LRK station.

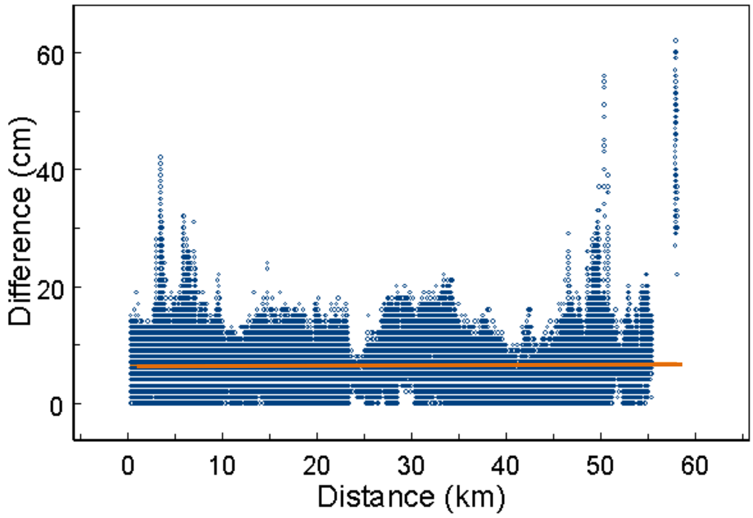


$n = 196\,176$
$\bar{x} = 6.79\ cm$
$\sigma = 3.92\ cm$

$y = 0.08 \cdot 10^{-6} \cdot x + 6.6265$ [cm]
$R^2 = 0.001$
$p = 0.0000$

**Figure 73:** Linear regression (orange line) of the relation between the systematic altimetric error and the distance to the LRK station (Zeebrugge)

## 6.3 Conclusion and discussion

The relation between the systematic error and the distance to the reference station is very similar for the planimetric and altimetric component. In both cases, the slope p-value is zero, indicating that the slope significantly differs from zero. The $R^2$ value is nearly zero in both cases, indicating that the systematic error of the Aquarius® LRK positions (both in the planimetric and height direction) only slightly depends on the distance from the LRK station.

It has to be noted however that the Manual of the Aquarius® system (Thales Navigation, 2003) mentions that the LRK positioning has an operating range of 40 km. This range was visualized on Figure 61. When the distance to the reference station exceeds this limit, systematic errors in LRK positioning can increase to more than 2m (e.g. planimetric and altimetric errors, Figure 63 and Figure 69). However, this analysis has showed that even when the distance to the reference station is smaller than 40 km, the systematic planimetric error can increase to over 2 m (at a distance of ca. 15 km from the reference station).

| **Original data (n=197 434)** | | |
|---|---|---|
| XY Difference (Leica-Aquarius®) | | |
| Regression equation | $y = 0.91 \cdot 10^{-6} \cdot x + 2.3505$ | [cm] |
| Residual standard error | 7.10 | |
| Absolute height difference (Leica-Aquarius®) | | |
| Regression equation | $y = 1.78 \cdot 10^{-6} \cdot x + 4.6184$ | [cm] |
| Residual standard error | 19.61 | |

| **Data without outliers** | | |
|---|---|---|
| XY Difference (Leica-Aquarius®) | | |
| n | 196 285 | |
| Regression equation | $y = 0.42 \cdot 10^{-6} \cdot x + 2.9135$ | [cm] |
| Residual standard error | 2.655 | |
| $R^2$ | 0.07517 | |

| Absolute height difference (Leica-Aquarius®) | |
|---|---|
| n | 196 176 |
| Regression equation | $y = 0.08 \cdot 10^{-6} \cdot x + 6.6265$ [cm] |
| Residual standard error | 3.922 |
| $R^2$ | 0.001306 |

# 7. Comparison with static land measurements

In this chapter, the systematic error of the dynamic LRK measurements on sea is compared to the systematic error of the static LRK measurements on land, performed by the NGI in January 2009.

The following values are compared:

- The systematic error of dynamic LRK measurements, e.g. the difference between Leica and Aquarius® measurements onboard the research vessel (previous chapter)
- The systematic error of static LRK measurements, based on the difference between
  - the known and highly accurate (s < 3cm) coordinates of national geodetic points
  - the coordinates of the same points that were measured using the R/V BELGICA antenna and GPS (Aquarius®, LRK solution)

Figure 74 visualizes the systematic planimetric (XY) error of both the static (land) and dynamic (sea) LRK measurements. Outlier values are removed from the data. The trend lines of both data series are also added in this graph. The static LRK measurements (performed on land) have a smaller systematic planimetric error compared to the dynamic LRK measurements. The regression line of the dynamic error has a slope that significantly differs from zero ($p < 0.001$). The slope of the static error regression line however does not significantly differ from zero ($p = 0.441$). $R^2$ values are near zero in both cases.

It must be noted that the dataset of land measurements consists of 71 points, whereas the dataset of sea measurements consists of 196 285 points. In order to achieve reliable trend lines, more LRK measurements on land are necessary.

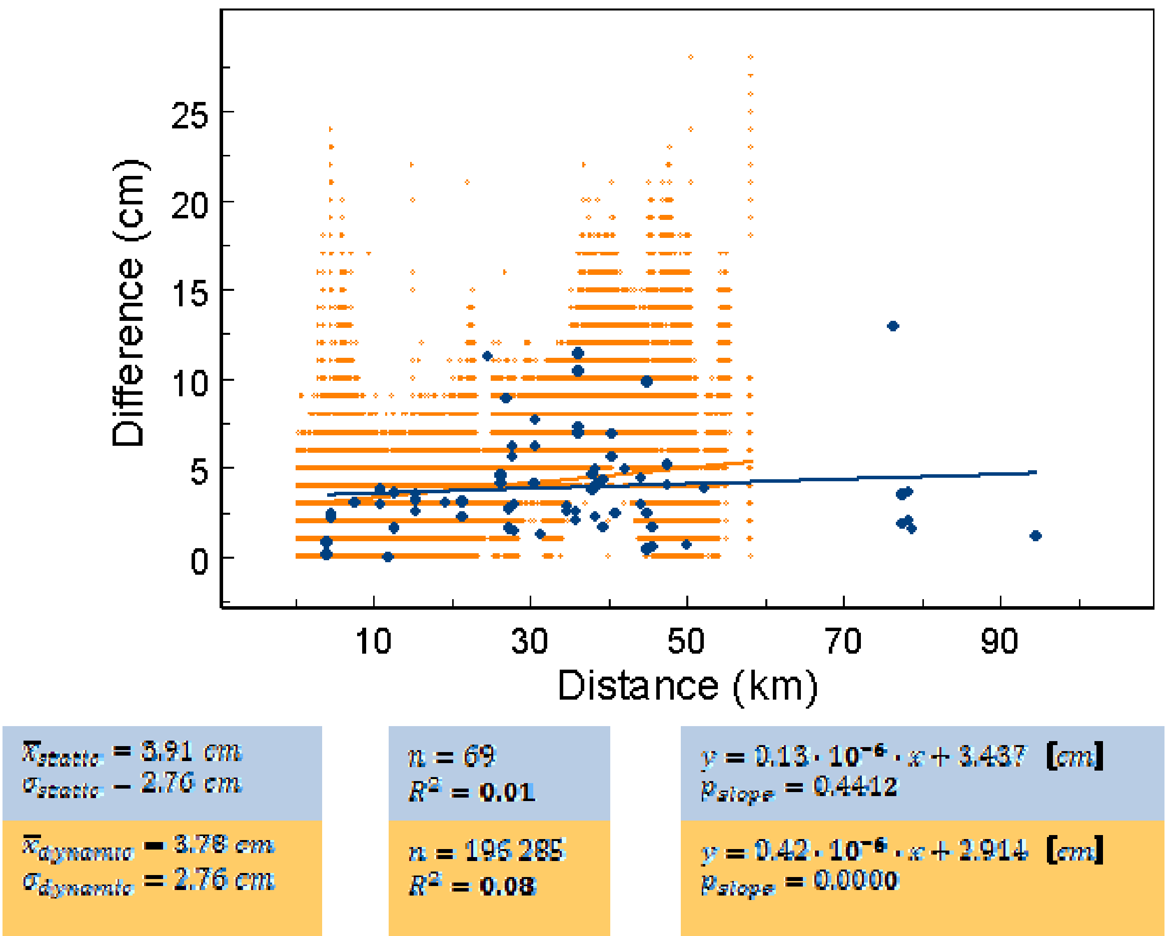


**Figure 74:** Systematic planimetric error of static (blue) and dynamic (green) LRK positioning

Figure 75 visualizes the systematic altimetric error of both the static (land) and dynamic (sea) LRK measurements. The systematic altimetric error of the LRK measurements on land is smaller than the error of LRK measurements on sea. The $R^2$ value is near zero in both cases. The slope p-value is 0.267 for the systematic error of the LRK measurements on land, indicating that the slope value does not significantly differ from zero. Again, this could be related to the limited amount of measurements that were performed on land.

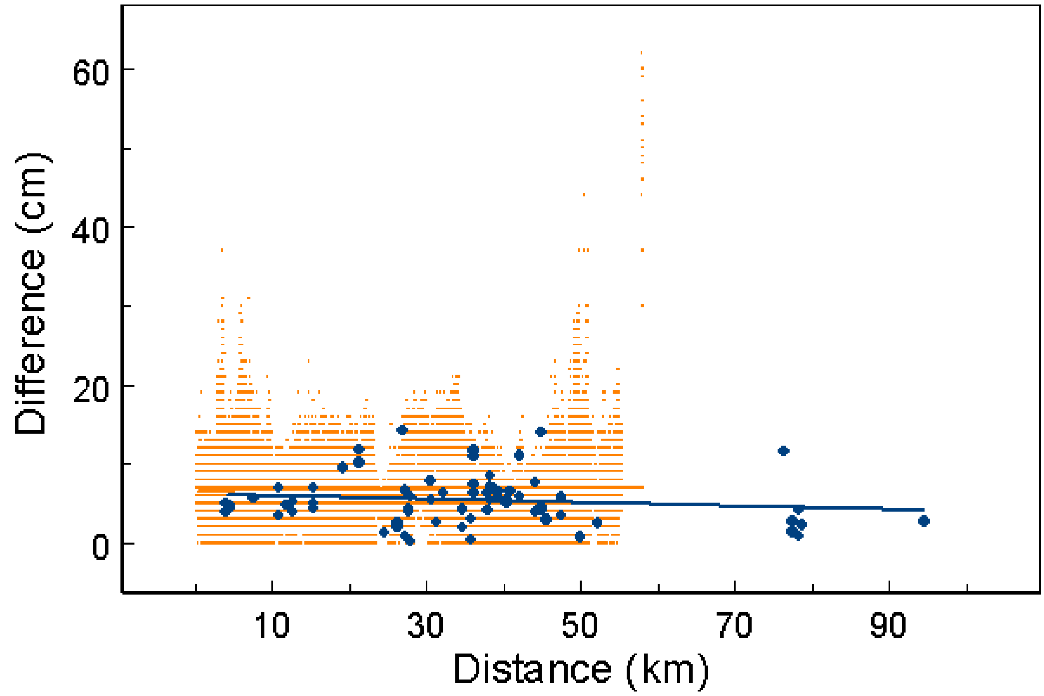


| | | |
|---|---|---|
| $\overline{x}_{static} = 5.41\ cm$<br>$\sigma_{static} = 3.15\ cm$ | $n = 71$<br>$R^2 = 0.02$ | $y = -0.22 \cdot 10^{-6} \cdot x + 6.183\ \ [cm]$<br>$p_{slope} = 0.2666$ |
| $\overline{x}_{dynamic} = 6.79\ cm$<br>$\sigma_{dynamic} = 3.92\ cm$ | $n = 196\ 176$<br>$R^2 = 0.00$ | $y = 0.08 \cdot 10^{-6} \cdot x + 6.627\ \ [cm]$<br>$p_{slope} = 0.0000$ |

**Figure 75:** Systematic altimetric error of static (blue) and dynamic (orange) LRK positioning

It can be concluded that the relation between the systematic error and the distance to the reference station is linear (although the slope is very small) for LRK measurements performed on sea. The systematic error (both planimetric and altimetric) of LRK measurements performed on land does not have a significant linear relationship with the distance to the reference station. For both land and sea LRK measurements, only 1 to 8% of the variability in the systematic error is explained by the distance to the reference station.

## 7.1 DETAILS OF THE STATISTICAL ANALYSIS

### 7.1.1 Analysis of height difference between Leica and Thales values

```
Linear regression -  height difference Leica-Thales (dataset without outliers)

Call: lm(formula = H.Diff..cm. ~ Distance..km., data = H.Zeebrugge.oktdec.zonderout,
na.action = na.exclude)
```

```
Residuals:
    Min      1Q   Median    3Q   Max
 -7.054 -2.681 -0.05282 2.223 54.92

Coefficients:
                 Value Std. Error  t value Pr(>|t|)
  (Intercept)   6.6265   0.0134   493.5973   0.0000
Distance..km.   0.0078   0.0005    16.0178   0.0000

Residual standard error: 3.922 on 196174 degrees of freedom
Multiple R-Squared: 0.001306
F-statistic: 256.6 on 1 and 196174 degrees of freedom, the p-value is 0
```

Linear regression - XY difference (dataset without outliers)

```
Call: lm(formula = XY.Diff..cm. ~ Distance..km., data =
          Vector.Zeebrugge.oktdec.zonderout, na.action = na.exclude)
Residuals:
    Min      1Q  Median     3Q   Max
 -5.326 -1.852 -0.2131 0.9573 22.99

Coefficients:
                 Value Std. Error  t value Pr(>|t|)
  (Intercept)   2.9135   0.0091   320.6838   0.0000
Distance..km.   0.0415   0.0003   126.3093   0.0000

Residual standard error: 2.655 on 196283 degrees of freedom
Multiple R-Squared: 0.07517
F-statistic: 15950 on 1 and 196283 degrees of freedom, the p-value is 0
```

### 7.1.2 Statistical analysis – static measurements

#### 7.1.2.1 Systematic planimetric error – XY (complete dataset, incl. outliers)

Summary statistics - XY error (cm)

```
     Min:         0.02134376
 1st Qu.:         2.21131370
    Mean:         4.20441960
  Median:         3.50478760
 3rd Qu.:         4.94129888
     Max:        14.57925818
 Total N:        71.00000000
   NA's :         0.00000000
Std Dev.:         3.23314989
```

Linear regression - XY error (cm) versus distance (km)

```
Call: lm(formula = XY.Difference..cm. ~ Distance..km., data = XY.land, na.action =
          na.exclude)
Residuals:
    Min      1Q  Median     3Q   Max
 -3.917 -1.941 -0.7268 0.6701 10.42

Coefficients:
               Value Std. Error t value Pr(>|t|)
```

```
  (Intercept) 3.6899 0.8115     4.5472  0.0000
Distance..km.  0.0145 0.0201     0.7204  0.4737

Residual standard error: 3.244 on 69 degrees of freedom
Multiple R-Squared: 0.007465
F-statistic: 0.5189 on 1 and 69 degrees of freedom, the p-value is 0.4737
```

#### 7.1.2.2 Systematic planimetric error – XY (dataset without outliers)

```
Summary Statistics -  XY Error (cm)
     Min:         0.02134376
 1st Qu.:         2.17936279
    Mean:         3.91015415
  Median:         3.18496905
 3rd Qu.:         4.61197868
     Max:        12.97781013
 Total N:        69.00000000
   NA's :         0.00000000
Std Dev.:         2.76405876
```

```
Linear regression -  XY error (cm) versus distance (km)
Call: lm(formula = XY.Difference..cm. ~ Distance..km., data = XYlandzonderout,
          na.action = na.exclude)
Residuals:
    Min     1Q  Median     3Q   Max
 -3.612 -1.702 -0.6035 0.7989 8.524

Coefficients:
               Value Std. Error t value Pr(>|t|)
  (Intercept) 3.4374 0.6955     4.9424  0.0000
Distance..km.  0.0133 0.0172     0.7747  0.4412

Residual standard error: 2.772 on 67 degrees of freedom
Multiple R-Squared: 0.008878
F-statistic: 0.6001 on 1 and 67 degrees of freedom, the p-value is 0.4412
```

#### 7.1.2.3 Systematic altimetric error – ellipsoidal height (complete dataset, including outliers)

```
Summary statistics -  Height error (cm)
     Min:         0.1483333
 1st Qu.:         3.2058333
    Mean:         5.4086854
  Median:         4.9633333
 3rd Qu.:         6.9608333
     Max:        14.2300000
 Total N:        71.0000000
   NA's :         0.0000000
Std Dev.:         3.1464445
```

```
Linear regression -  Height error (cm) versus distance (km)

Call: lm(formula = H.difference..cm. ~ Distance..km., data = Hland, na.action =
          na.exclude)
Residuals:
    Min     1Q  Median    3Q   Max
 -5.427 -2.062 -0.6793 1.268 8.833
```

```
Coefficients:
                Value Std. Error t value Pr(>|t|)
  (Intercept)  6.1832  0.7855     7.8712  0.0000
Distance..km. -0.0218  0.0194    -1.1201  0.2666

Residual standard error: 3.141 on 69 degrees of freedom
Multiple R-Squared: 0.01786
F-statistic: 1.255 on 1 and 69 degrees of freedom, the p-value is 0.2666
```

## 7.2 REFERENCES

Thales Navigation (2003) *Aquarius Receiver. Aquarius Series User Manual*. Carquefou, France, 342 p.

# 8. Error budget

In order to analyze the accuracy of hydrographical data, all uncertainties in each phase of data collection and analysis have to be collected. For normally distributed data, the standard deviation is the plus/minus distance from the mean that encompasses 68% of the area under the curve. The area under the curve between ±2s from the mean is 95% of the area.

## 8.1 International standards

The International Hydrographic Organisation (IHO, http://www.iho.int) has established international standards (IHO, 2008) that determine the minimum requirements for acceptable hydrographic data quality (Table 6).

**Table 6:** Summary of Minimum standards for hydrographical surveys (from IHO, 2008)

| Order | Special | 1a | 1b | 2 |
|---|---|---|---|---|
| Description of areas | Areas where under-keel clearance is critical | Areas shallower than 100m where under-keel clearance is less critical but features of concern to surface shipping may exist | Areas shallower than 100m where under-keel clearance is not considered to be an issue for the type of surface shipping expected to transit the area | Areas generally deeper than 100m where a general description of the sea floor is considered adequate |
| Maximum Total Horizontal Uncertainty (95% Confidence Level) | 2 m | 5 m + 5% of depth | 5 m + 5% of depth | 20 m + 10% of depth |
| Maximum Total Vertical Uncertainty (95% Confidence Level) | a = 0.25 m<br>b = 0.0075 | a = 0.5 m<br>b = 0.013 | a = 0.5 m<br>b = 0.013 | a = 1.0 m<br>b = 0.023 |
| Full sea floor search | Required | Required | Not required | Not required |
| System detection capability | Cubic features > 1m | Cubic features > 2m in depths up to 40m; 10% of depth beyond 40m | Not applicable | Not applicable |
| Maximum Line Spacing | Not defined as full sea floor search is required | Not defined as full sea floor search is required | 3 x average depth or 25m, whichever is greater | 4 x average depth |

a = depth independent error (sum of all constant errors)

b = factor of depth dependent error

The maximum allowable total vertical uncertainty for a specific depth (d), at the 95% confidence level, can be calculated as follows: $\pm\sqrt{a^2 + (b \cdot d)^2}$ (IHO, 2008). The surveying in the Belgian Continental Zone is considered to be Order 1, and with a depth of 20m the total vertical depth error (2 σ) is ± 0.56 m.

## 8.2 Error sources

The errors that are involved when performing bathymetric measurements (IHO, 2008) are listed below.

### 8.2.1 Error sources of the positioning system (GPS)

The accuracy of the ship's position (x, y, z) does not only depend on the positioning system (GPS), but is also influenced by other correction equipment.

The positioning of the R/V Belgica is done using a Thales Aquarius® GPS, that can perform different types of positioning, all based on GPS, i.e. GPS, DGPS and RTK/LRK (see Chapter 4). During multibeam measurements, only LRK positions are used. The random and systematic error of the LRK positioning was determined in Chapters 5, 6 and 7.

The planimetric positional error of a bathymetric sounding depends on

- The accuracy of the positioning system (Aquarius® LRK)
- The physical separation between the echosounder and the Thales GPS antenna. This causes a vertical and horizontal offset that can be a source of systematic and random errors, more specifically when the ship rotates around its axes (roll and pitch movements, see Section 8.2.2).

### 8.2.2 Error sources linked to the movement of the ship

When a ship is at sea, it constantly translates and rotates in three dimensions, due to wave/wind/current interactions. Figure 76 visualizes the ship's X, Y and Z axes and the associated movements (three translations and three rotations).

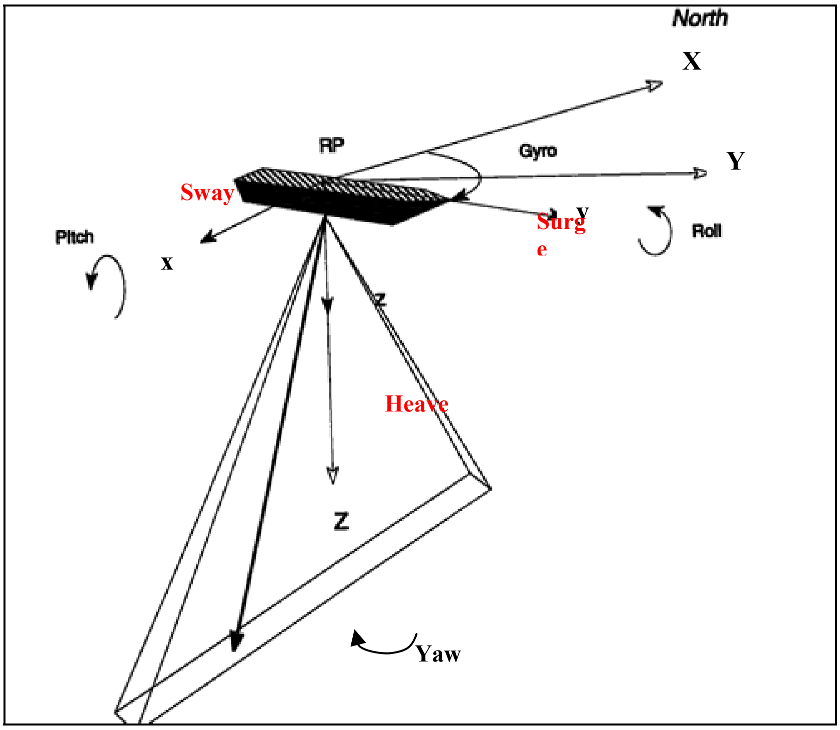


**Figure 76:** Movement of a ship, translations (red) and rotations (black) (after http://www.hydro.gov.hk)

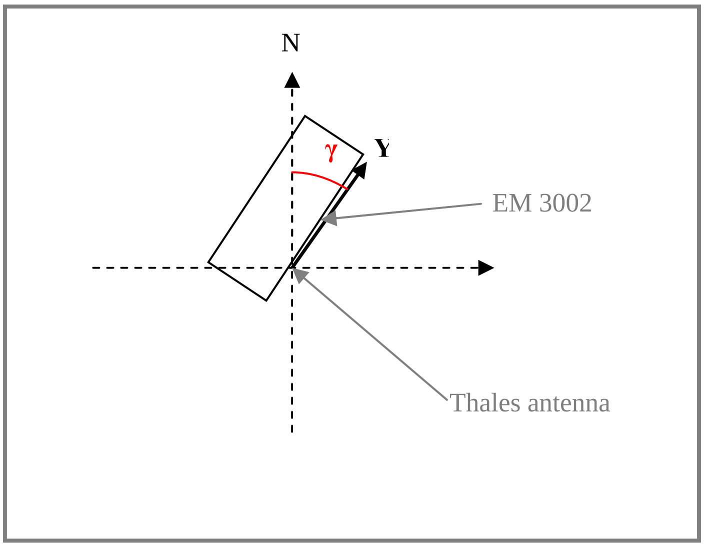


**Figure 77:** Heading error of a ship.

1. **Yaw**
   Rotation around the ship's Z-axis. When the transducers are installed, the recording angle of the multibeam has to be in the vertical plane, perpendicular to the ship's Y-axis (Figure 76). If this requirement is not met, a residual rotation around the vertical axis will occur.

2. **Heading**
   A correction for the heading of a ship is necessary because the GPS antenna and the echosounder are located at two different positions. The heading of a ship (Figure 77) is the angle between (1) the direction of the ship's Y-axis and (2) the geographical north. On board the R/V BELGICA, the heading is determined by a gyrocompass (Anschütz STD20) (MUMM, 2006).

3. **Roll**
   Rotation around the ship's long (Y) axis. The roll movement of a ship can be caused by (1) an unequal ballast distribution on the ship, (2) a problem of the roll-compensator, (3) a rotation of the multibeam around the Y-axis or (4) when plate transducers are used, a differential roll-offset can exist because of faulty assembly angles.

4. **Pitch**
   Rotation around the ship's X-axis. A pitch offset can be caused by (1) an unequal ballast distribution, (2) a faulty calibrated pitch compensator or (3) an excentric location of the pitch compensator with regard to the multibeam echosounder.

5. **Squat**
   Squat is the combination of a vertical translation and a rotation around the X-axis, caused by the subnormal pressure that occurs below the ship due to a hydrodynamical pressure decrease caused by the speed of the ship (Bernoulli's Law). The magnitude of the squat depends on (1) the size and shape of the ship, (2) the water depth, (3) the channel width and (4) the vessel speed. The squat is usually of dm order.

6. **Draught**
   The draught of a ship is the distance between the transducer and the sea level and indicates the depth of the vessel in the water. The draught value depends on the (1) shape of the vessel, (2) weight of the vessel and (3) the ballast distribution on the vessel. This distance varies during a campaign, especially due to a changing amount of load (fuel, ballast, etc.). In order to compensate for the

draught of the R/V BELGICA, measurements are performed in the beginning and at the end of every campaign.

7. **Heave**
The vertical heave movement (translation) is caused by the waves. This translation produces an irregular curve in a vertical plane, which can be dissolved into different sinusoidal curves with different amplitude, phase and period. The periods and their associated amplitudes are less predictable than the tide. The amplitude of the heave depends on the height of the waves (-30 to +30 cm at a calm sea, up to several meters at a rough sea). The period of the heave sinusoid varies from a second (when the vessel is very small) up to more than a minute (when the vessel moves with the waves). A heave sensor can register the heave in real time and can be used to compensate for the heave translation. On the R/V BELGICA, a TSS 320B heave compensator is installed that performs corrections in real time.

### 8.2.3 Error sources linked to the multibeam

1. Range and beam angle error
2. Error sources linked to the ray path model (incl. sound speed profile) and beam pointing angle
3. Transducer misalignment
4. Sensor position offset
5. Penetration
   When a sound wave encounters a medium like sand or rock, a fraction of the energy propagates in the material, while the rest of the energy is scattered or reflected back to the original medium (water). The degree of penetration depends on the frequency of the pulse and the type of sediment. MUMM (2001) states that the penetration error is zero, because the penetration in sand is negligible.

On board the R/V BELGICA, a Kongsberg-Simrad EM3002 multibeam is currently used.

### 8.2.4 Error sources linked to the time synchronization

The position of each multibeam sounding and the sounding depths have to be synchronized. This is done by applying a time lag or latency correction, that translates the time lag, combined with the vessel speed, into a planimetric displacement.

### 8.2.5 Error sources linked to the sound velocity profiler or CTD[12] probe

Due to variable salinity, temperature and depth, the sound speed will never be homogeneous in a water column. This varying sound speed causes ray bending, which strongly influences the accuracy of the outer beams of the multibeam echosounder. Sound speed profiles can be determined using a CTD. This device measures the temperature, depth and salinity (determined based on the conductivity). Using a correction model (e.g. the Wilson formula), the sound speed is calculated. On board the R/V BELGICA multiple CTD and sound velocity profilers are available. Control measurements however show that there is almost no vertical variation in temperature and conductivity in the Belgian Continental Zone (provided that the measurements are performed far enough from the Scheldt mouth) (K. Degrendele, personal communication). Therefore, a permanent built-in sensor, located near the transducer, is used (Valeport mini Sound Velocity Sensor), that continuously measures the sound speed (Valeport, s.d.). This sensor is situated ca.

[12] Conductivity, temperature, depth

4m below sea level, which is below the thermocline. When the deviation exceeds 1 m/s, adjustments are made in the multibeam software.

### 8.2.6 Error sources linked to the vertical reference levels

- Vertical positioning system (only LRK method)

  When the LRK method is used, the vertical position of the ship is determined using GPS (LRK). The random and systematic error of this positioning system has been analyzed in previous chapters of this report. The GPS (LRK) positioning however gives the ellipsoidal height, which then has to be converted to a vertical reference level (i.e. LAT). The ellipsoidal/vertical datum separation model error therefore depends on the accuracy of the GRStoNAP and NAPtoLAT grids. The accuracy of the GRStoNAP grid is 2 cm on land.

- Tidal correction (only M2 method)

  The M2 method is used when no vertical GPS positioning is available or desirable. In order to express the sounding in relation to a known vertical reference level (e.g. LAT), the sea level at the time and place of the sounding has to be determined. The M2 tidal reduction method (Van Cauwenberghe *et al.*, 1993) allows to determine the sea level (tide) at a certain position at sea and a certain moment in time, based on the sea level (tide) at a reference position (coastal tide gauges). The error of this method is therefore determined by the accuracy of the tide gauge measurements and the accuracy of the M2 tidal reduction method itself. Recently, M2 sea levels are expressed as depths relative to the LAT reference level, instead of the former commonly used vertical reference TAW. This conversion is achieved using (1) the known offset between TAW and NAP (i.e. 2.311 m, Figure 78) and (2) the NAPtoLAT grid. Therefore, the accuracy of the NAPtoLAT grid is also relevant when the M2 method is applied.

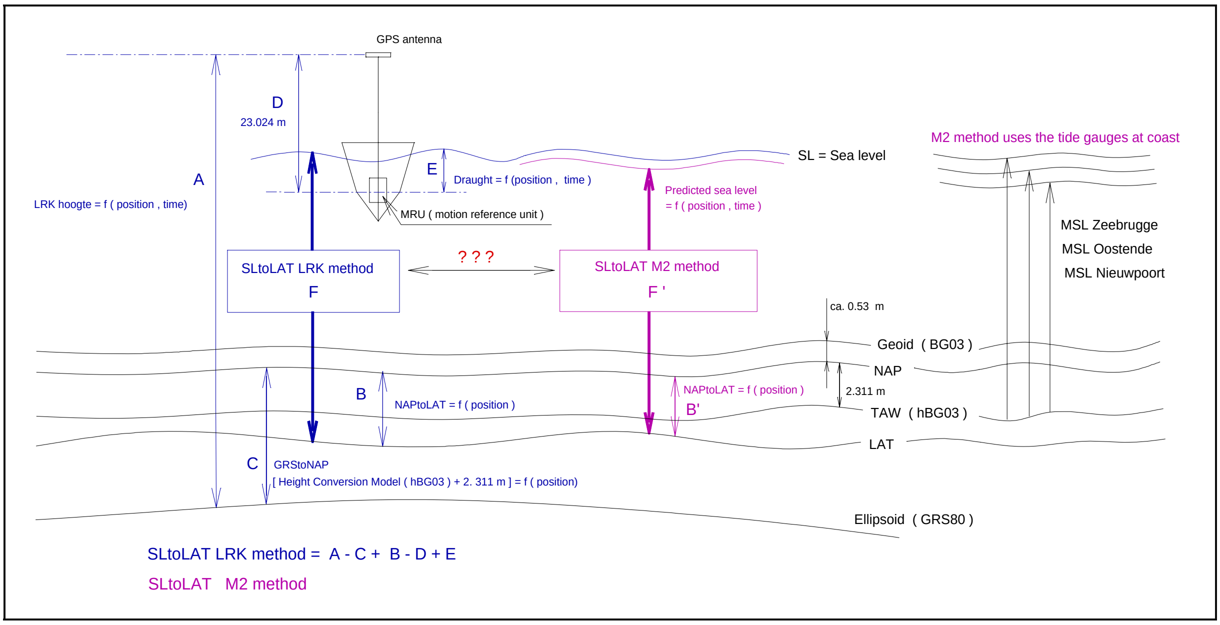


**Figure 78:** Overview of the vertical reference levels

It is difficult to determine or estimate the accuracy of the NAPtoLAT grid (*Agentschap Maritieme Dienstverlening en Kust*, see Figure 79), because this grid is made based on harmonic constants and tidal constituents, that were simulated over a period of 19 years using a mathematic model. The accuracy of this grid was therefore estimated by determining the difference between

- the NAPtoLAT grid from the Agentschap Maritieme Dienstverlening en Kust;

- the NAPtoLAT grid calculated in PCTrans 4.2.5 (Dienst Der Hydrografie, The Netherlands)

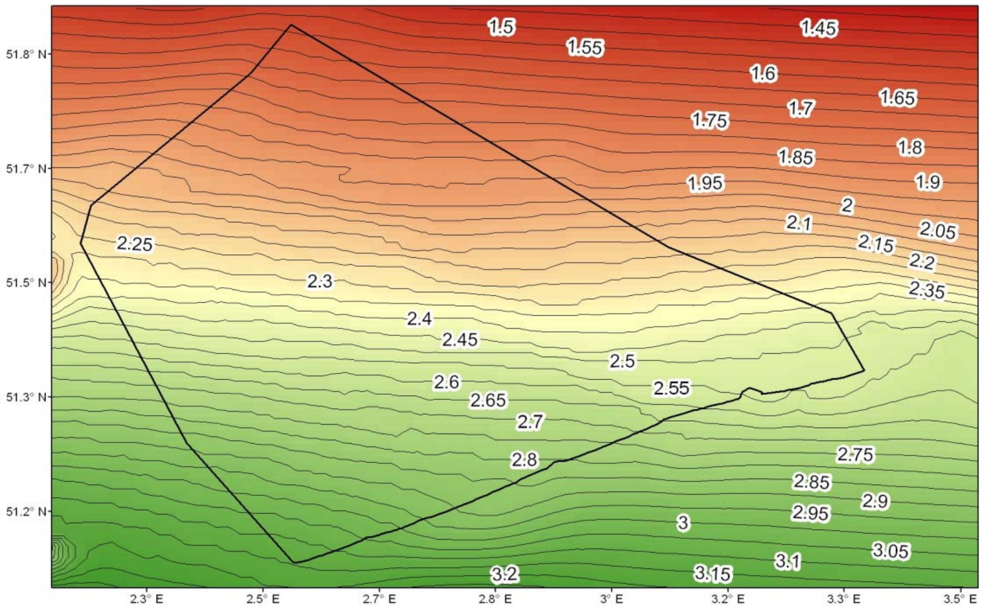


**Figure 79:** NAPtoLAT grid (*Afdeling Maritieme Dienstverlening en Kust*)

Based on Module 5.8 in PCTrans (Tidal reduction for LAT and MLLWS) and the geographical coordinates of the 'Belgian' NAPtoLAT grid, PCTrans calculated a new NAPtoLAT grid (Figure 80). Afterwards, the difference between both NAPtoLAT grids was calculated in ArcMap® 9.3 (Figure 81). Within the Belgian Continental Zone, the difference between both NAPtoLAT grids varies from -0.107 to 0.040 m.

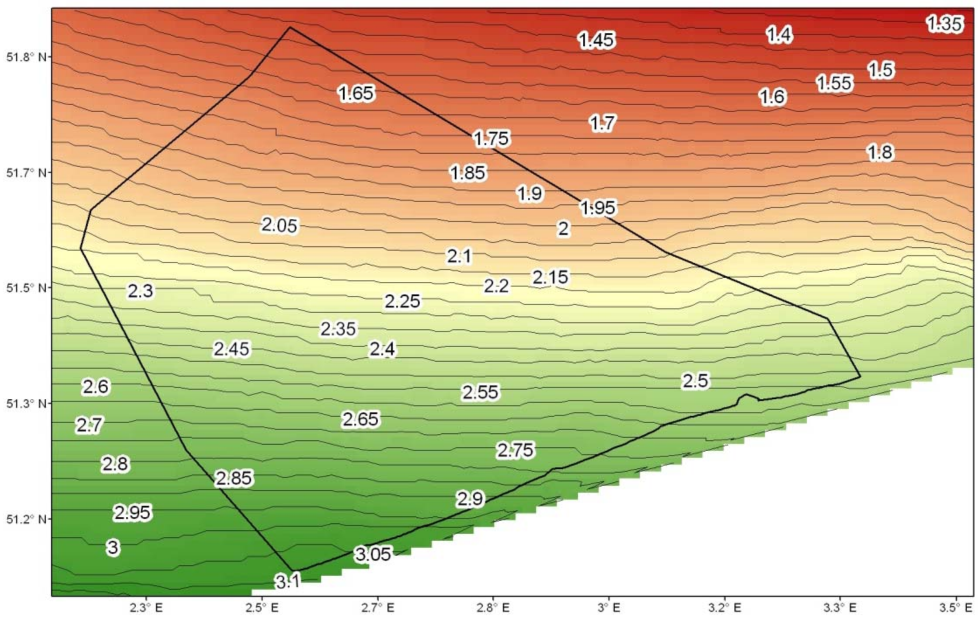


**Figure 80:** NAPtoLAT grid (PCTrans)

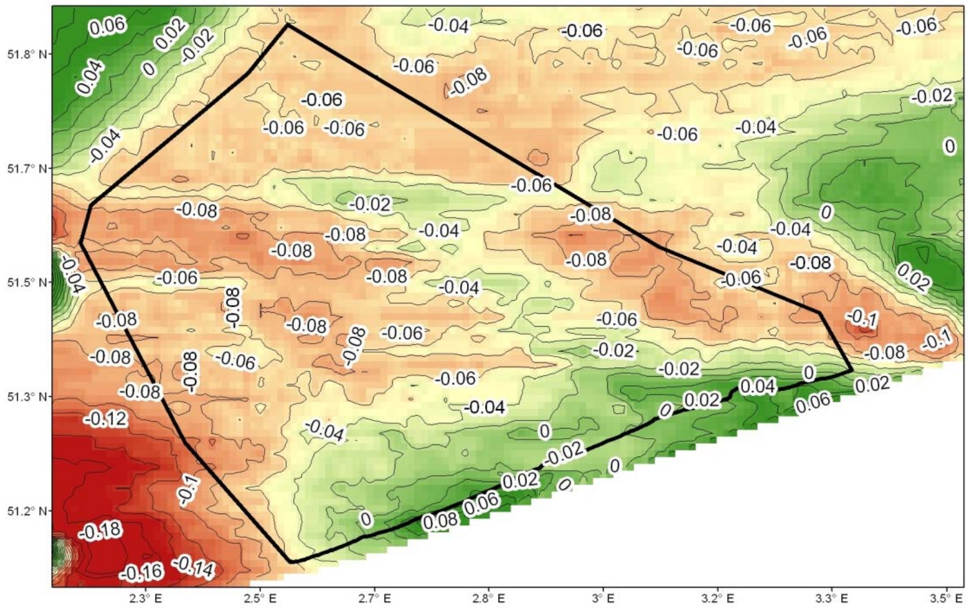


**Figure 81:** NAPtoLAT difference grid (NAPtoLAT(PCTrans) – NAPtoLAT (*Maritieme Dienstverlening en Kust*))

The comparison of NAPtoLAT grid (BE) and NAPtoLAT grid (PCTrans) yields a mean difference of -0.055 m (the NAPtoLAT values are usually bigger in the (BE) model than in the (PCTrans) model). The standard deviation of the difference between both models is 0.026 m

## 8.3 ERROR BUDGET

The errors in an error budget are not the values of the ship's movement etc., but the residual errors that remain after their effect is eliminated using specific equipment.

In order to establish an error budget, random errors (i.e. incoherent errors, that do not have a functional relationship) are separated from systematic errors (i.e. errors that are recursive when the observations are repeated under the same conditions) (Hare *et al.*, 1995).

This report aims to perform a theoretical analysis of the errors involved in multibeam soundings. The values of the parameters in the budget are based on

- Technical specifications of the equipment (operating or service manuals);
- Random and systematic error of the GPS (LRK) system on board (based on control measurements on sea/land);
- Oral communication with MUMM and FOD Economics experts.

The total error can be calculated using the 'Law of Propagation of Variances', that states that if the variance associated with each component is known, the variance of the unknown variable can be calculated (Hare *et al.*, 1995). If the causes of the different error values are independent, the total error is the square root of the sum of the square of all individual components. The total error is compatible with order 1 of the standards defined by IHO (IHO, 2008).

The total error is calculated as follows:

$$Error(x) = \sqrt{\sum_{i=1}^{N} x_i^2}$$

where x = the measured variable amplitude for value i

N = total number of values

Norro *et al.* (2006) analyzed the errors with regard to bathymetric measurements on the RV BELGICA and concluded that the total error is +16/-19 cm (95% confidence level) (Table 7).

**Table 7:** Estimated error of bathymetric measurements on the RV BELGICA (confidence level 95%). These values are valid for an assumed water depth of 20m and slopes of 3°. (Norro *et al.*,2006)

| Source of error | Error to 1993 (cm) | Error from 1993 (cm) |
|---|---|---|
| *Error in recording* | | |
| Echosounder | ±4.0 | ±4.0 |
| Speed of sound | ±2.5 | ±2.5 |
| Heave | ±10.0 | ±2.5 |
| Presence of slopes | −3.0 | −3.0 |
| Subtotal | +10.0/−13.0 | +4.0/−7.0 |
| *Error in reduction procedures* | | |
| Tidal reduction | ±32.0 | ±13 |
| Static draught | ±5.0 | ±5.0 |
| Variation in static draught | ±5.0 | ±5.0 |
| Subtotal | ±33.0 | ±15.0 |
| *Navigational error* | | |
| Navigational error | ±8.5 | ±8.5 |
| Total error | +34.0/−37.0 | +16.4/−19.4 |

On 13 and 14 August 2008, the most recent measurement of the RV BELGICA sensors was organized (Geo Plus, 2008). A total station was used to determine the geometrical classification of the vessel, in a dock as well as on water. The accuracy of all measured values is 1 cm. The position of the multibeam, MRU and GPS antennas was determined, as well as the painted waterline (Plimsol).

**Table 8:** Error budget in cm – random error LRK method (for a depth of 20m, 95% confidence level)

| **Parameter** | **Equipment on R/V BELGICA** | **Accuracy (2s)** | **X(2s)** | **Y(2s)** | **Z(2s)** | **2D(2s)** | **3D(2s)** |
|---|---|---|---|---|---|---|---|
| Error sources linked to the positioning system (GPS) | | | | | | | |
| Random positioning error[13] | Thales Aquarius® LRK | ± 3.8 cm | 1.2 | 1.2 | 3.2 | 2.0 | 3.8 |
| Error sources linked to the movement of the ship | | | | | | | |
| Velocimeter | Consilium SAL 860 T | | | | | | |
| Yaw | Not considered | | | | | | |
| Roll | Kongsberg Seatex Motion Reference Unit 05 [14] | ± 0.04° | 1.6 | | | | |
| Pitch | | | | 1.6 | | | |
| Heave (dynamic accuracy) | | ± 10 cm or 10% of total heave | | | 10 | | |
| Squat or dynamic draught | Not considered | | | | 20 | | |
| Heading[15] | Gyrocompass Anschütz STD20 | Maximum 2° | | | | 17 | |
| Error sources linked to the multibeam | | | | | | | |
| Depth measurement[16] | Kongsberg-Simrad EM3002 multibeam | 4 cm | | | 4 | | |
| Penetration[17] | Sand is assumed => no penetration | | | | 0 | | |
| Error sources linked to the CTD probe | | | | | | | |
| Sound speed[18] | Valeport mini SVS (50mm) | | | | 2.5 | | |

**Table 9:** Error budget – systematic error LRK method (for a depth of 20m, 95% confidence level)

| **Parameter** | **Equipment on R/V BELGICA** | **Accuracy (2s)** | **X(2s)** | **Y(2s)** | **Z(2s)** | **2D(2s)** | **3D(2s)** |
|---|---|---|---|---|---|---|---|

[13] Error determined based on repeated (60 seconds) LRK measurements of fixed points on land
[14] Source: Kongsberg Seatex AS (2006)
[15] Nominal accuracy: $sec_{LAT}$ = 1/(cos Latitude) (source: Raytheon (1999). Estimated accuracy 2° (Source: Vande Wiele, 2000)
[16] Source: Kongsberg Maritime AS (2006)
[17] Source: MUMM (2001)
[18] Source: Valeport (s.d.)

| | | | | | | | |
|---|---|---|---|---|---|---|---|
| Error sources linked to the positioning system (GPS) | | | | | | | |
| Systematic positioning error | Thales Aquarius® LRK | ± 5.52 cm (XY) | 4 | 4 | | | |
| | | ± 7.84 cm (Z) | | | 8 | | |
| Vertical offset between multibeam and GPS antenna (23.024m) | N/A | 1 cm | 0 | 0 | 1 | | |
| Error sources linked to the movement of the ship | | | | | | | |
| Static draught[19] | | ± 5 cm | | | 5 | | |
| Error sources linked to the vertical reference levels | | | | | | | |
| NAP to LAT grid[20] | N/A | 6 | | | 6 | | |
| GRS to NAP grid | N/A | $2 \cdot \sqrt{2^2 + 5^2}$ [21] | | | 11 | | |

**Table 10:** Error budget – error M2 method

| **Parameter** | **Equipment on BELGICA** | **Accuracy** | **X** | **Y** | **Z** | **2D** | **3D** |
|---|---|---|---|---|---|---|---|
| Error sources linked to the vertical reference levels | | | | | | | |
| Sea level measurement at tide gauge[22] | N/A | ± 2 cm | | | 2 | | |
| M2 tidal reduction method (depth relative to TAW)[23] | N/A | ± 13 cm | | | 13 | | |
| NAPtoLAT grid | N/A | 6 | | | 6 | | |

[19] Source: MUMM (2001)
[20] Error based on oral communication (H. Poppe), error of the harmonic analysis (M2 component)
[21] Source: oral communication P. Lambot (combination of error of gravimetric model on land and supplementary uncertainty at sea)
[22] Source of associated error value: MUMM (2001)
[23] MUMM (2001)

## 8.4 REFERENCES

IHO (International Hydrographic Organisation) (2008) *IHO Standards for Hydrographic Surveys. Special publication 44.* Monaco: International Hydrographic Bureau.

Geo Plus (2008) *Inmeting sensoren meetvaartuig "BELGICA"*. Geo-Informatie buro Geo Plus b.v. Nederland, Scheemda.

Hare, R., Godin, A., Mayer, L. (1995) *Accuracy estimation of Canadian swath (multibeam) and sweep (multitransducer) sounding systems*. Canadian Hydrographic Service Internal Report.

Kongsberg Maritime AS (2006) *Multibeam echo sounder. The new generation high performance shallow water multibeam*. Norway, Horten. (http://www.km.kongsberg.com/ks/web/nokbg0397.nsf/AllWeb/7C8510CFA3CD21ABC1256CF00052DD1C/$file/164771ae_EM3002_Product_spec_lr.pdf?OpenElement)

Kongsberg Seatex AS (2006) *MRU5. The ideal Marine Motion Sensor.* Norway, Trondheim.

MUMM (2001) *Accuracy of echosounding recordings carried out in the framework of the 'Westbank' projects.* SUMARE Project Report. Merelbeke, Magelas.

MUMM (2006) *BELGICA technische kenmerken. Status 21/08/2006.* Beheerseenheid Mathematisch Model van de Noordzee. Meetdienst Oostende.

Norro, A., Pichot, G., Pison, V., Ozer, J. (2006) "A bi-dimensional approach to assessing the volumetric evolution of an exploited sandbank". *ICES Journal of Marine Science* 63, 176-186.

Raytheon (1999) *Gyro Compass Standard 20. Service Manual*. Germany, Kiel (http://www.scribd.com/doc/10966741/Gyro-Compass-Service-Manual)

Seatex (2000) *MRU User's Manual. Issued 1999-11-02*. Navia Maritime AS, Division Seatex. Norway, Trondheim.

Valeport (s.d.) *Sound Velocity Sensors. MiniSVS Range*. United Kingdom, Dartmouth, Devon. (http://www.seatronics-group.com/Specification%20Sheets/Valeport%20Mini%20SVS.pdf)

Van Cauwenberghe, C., Dekker, L., Schuurman, A. (1993) M2 Tidal Reduction Method for Coastal zones. *Rapport 33 van de Hydrografische Dienst der Kust, Ministerie van Openbare Werken*, 12 pp.

Vande Wiele, T. (2006) "Aspects of accuracy analysis for soundings". *The Hydrographic Journal* 95, 19-22.

# 9. Conclusions and Recommendations

## 9.1 Conclusions

1. Objectives were achieved: the combination of the GRS2NAP and NAP2LAT grids yields the requested GRS2LAT model.
2. This GRS2LAT model has been implemented on board of the R/V Belgica vessel.
3. This report analyzes the important error sources involved in the GRS2LAT model in comparison with the $M_2$ method.
4. A comparison between the results of the $M_2$ tidal reduction method and those of some operational hydrodynamic models was performed.
5. The systematic and random errors of the LRK postioning system were also studied in detail.
6. The error budget of the Belgica positiong system was established.

## 9.2 Recommandations

1. The manual of the Aquarius® system (Thales Navigation, 2003) mentions that the LRK positioning range is 40 km. The random and systematic error of LRK positioning indeed becomes highly unpredictable when the distance from the reference station is greater than 50 km (see Chapter systematic error of LRK positioning). Although LRK positioning is generally very accurate, position errors of more than 2m have been observed. Therefore, this report recommends to install more LRK reference stations, preferably located in the middle or the northern border of the Belgian Continental Zone.
2. Even when the distance to the reference station is smaller than the theoretical operating range of 40 km, the position error of LRK positioning sometimes augments to more than 2m. It can be concluded that caution is needed when using LRK positioning information and a secondary GPS system is highly advisable.
3. Experiences during the tests have shown that loss of radio contact with the reference stations leads to bad positioning, even within the range of 40 km. The low emitting power, with a legal threshold of 2 Watt, is probably the cause. Therefore we recommend to contact the BIPT and to send them a request for derogation on this rule and increase the emitting power to 10 Watt or to install a higher and more powerfull emitting or directional antenna.
4. The RMS value (s = ca. 0.8 cm) that is indicated in the LRK GGA String of the positioning on sea, is not a realistic random error as the LRK positioning on land (in more optimal conditions, e.g. static measurements) achieves only 3D errors of ca. 1.9 cm (1s).
5. The current method of determining the ship's draught (*i.e.* static measurements at the beginning and end of each campaign, and linear interpolation between those two moments in time) is insufficient. We recommend to perform dynamic draught measurements throughout the campaign and to correct dynamically for the draught.
6. Further research on the following topics is highly advisable:
    1. Comparison of the Belgian bathymetric reference levels (*e.g.* LAT) with the European reference levels.
    2. Further analysis of the differences between "Mean Sea Level" and the different geoid models by setting up and tuning hydrodynamical models.
    3. Study of the error propagation of the multibeam sensor in non-nadir points of the measured cross-section.

4. Further research on and refinement of the NAP2LAT grid and GRS2NAP grids.
5. Additional comparisons between the $M_2$ and LRK methods should be carried out, based on more recorded tracks of the R/V BELGICA.

# 10. DISSEMINATION AND VALORISATION

A meeting was organised at TU Delft on April 7th 2009 with Prof. Roland Klees, expert in hydrodynamic modelling and vertical reference levels. This meeting was attended by partners of the MUMM, NGI and UGENT.

The preliminary results of this study have been presented during a workshop organized by the Hydrographic Society Benelux on the 18th of September 2010 in Lillo (Belgium) that was attended by ca. 50 hydrographers. Lectures were given by different partners of this G2Lat project.

Two technical papers are in preparation.

# 11. ACKNOWLEDGMENTS

The members of the G2LAT consortium want to thank the Belgian Science Policy for having provided the funds to perform this study.

They also want to express their deep gratitude to Koen DEGRENDELE and Marc ROCHE, from the Federal Public Service "Economy", Division of the Continental Plate, for their continuous and constructive support throughout the study. They not only formulated the problem but they also provided many useful hints to solve it. Furthermore, the G2LAT campaigns at sea couldn't have provided as much information as they did if they hadn't been conducted jointly with those of the FPS "Economy".

As usual, but it is always worth underlining it, the crew of the R/V BELGICA, as well as the one of the hydrographic vessel TER STREEP, did its job very professionally, allowing scientists and technicians to concentrate on their tests and measurements.

For many different reasons, the G2LAT projects generated numerous late changes in the planning. We therefore want to also address a special thank to our colleagues in charge of planning the sea campaigns, who had to cope with these changes.

Dr. S. Legrand (MUMM) is thanked for managing MUMM suite of operational models and taking care of properly archiving model results and observations. His comments on the draft version of Chapter 2 were appreciated as well.

# 12. Annexes

## 12.1 Annex 1: Campaigns at sea

## 12.2 Annex 2 : Comparison between the EM3002D multibeam echosounders on the Belgica and Ter Streep

by the FPS Economy.

## 12.3 Annex 3 : Reference paper

« Quasi-geoid BG03 computation in Belgium », R. Barzaghi, A. Borghi, B. Ducarme, M. Everaerts.

## ANNEXE 1 : CAMPAIGNS AT SEA

Members of the G2LAT participated in several research cruises of the BELGICA in order to study the instrumentation and perform measurements.

These campaigns are documented as usual by means of Cruise Summary Reports and Campaign reports. These documents are available on the website of MUMM. See: http://www.mumm.ac.be/EN/Monitoring/BELGICA/campaigns.php?year=2009 .

The tracks of each of these campaigns are shown on Figure 82 to Figure 85.

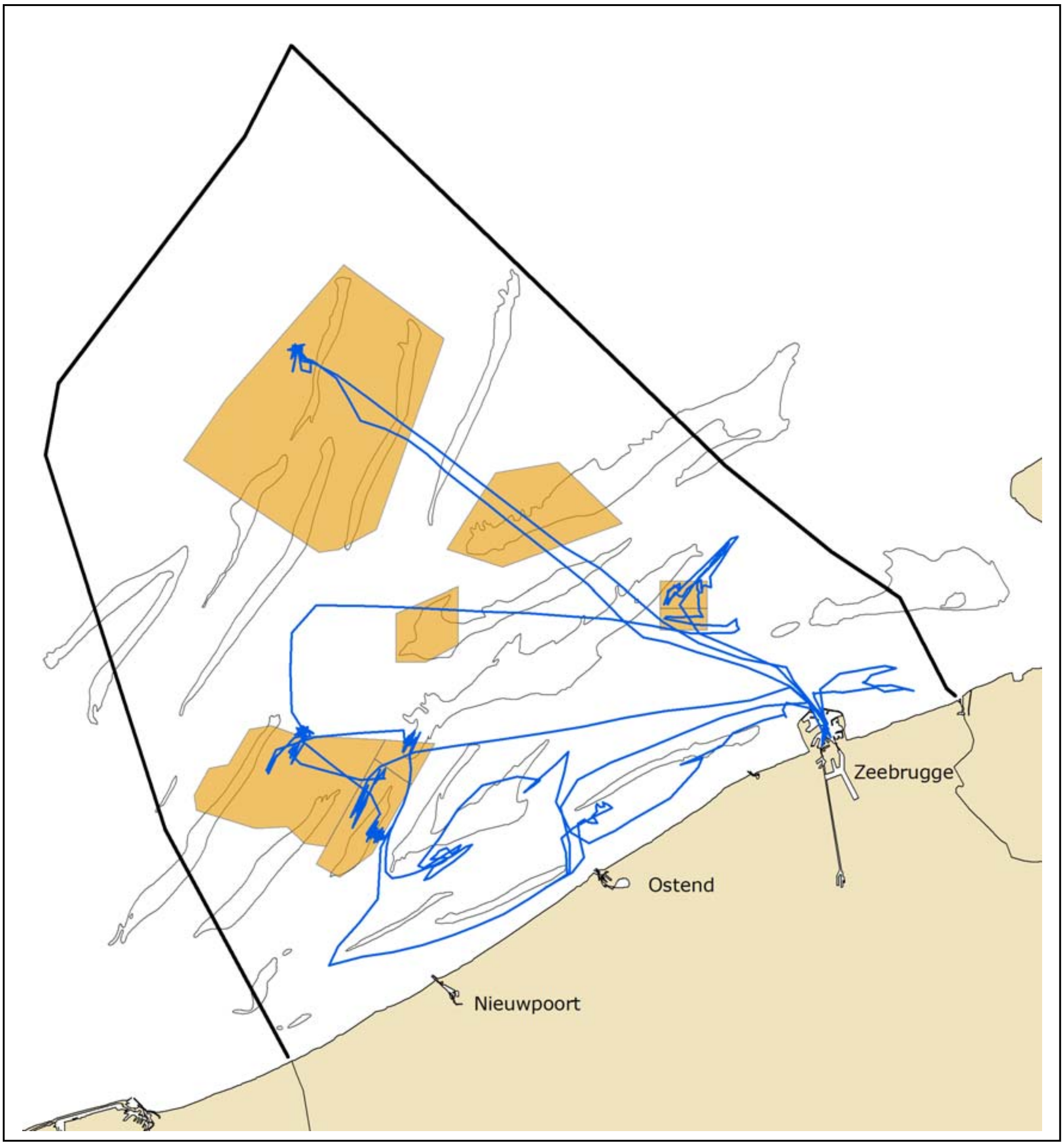


**Figure 82:** Track of the first G2LAT campaign (Campaign 2009/6a). More information at:
http://www.mumm.ac.be/EN/Monitoring/Belgica/table.php?year=2009&view=200906a#200906a


**Figure 83:** Track of the second G2LAT campaign (Campaign 2009/11a). More information at:
http://www.mumm.ac.be/EN/Monitoring/BELGICA/table.php?year=2009&view=200911a#200911a

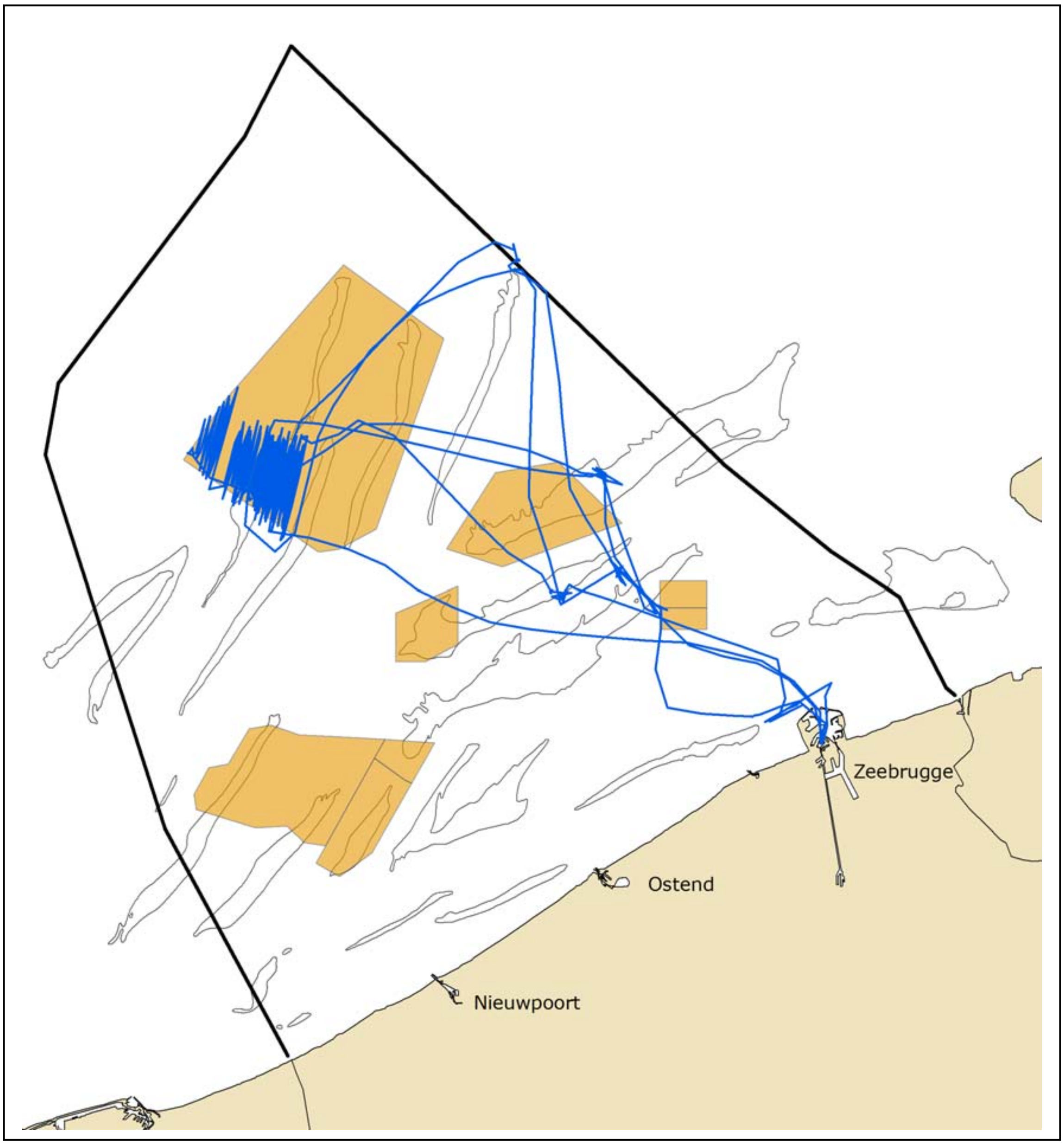


**Figure 84:** Track of the third G2LAT campaign (Campaign 2009/28a). More information at**:**
http://www.mumm.ac.be/EN/Monitoring/Belgica/table.php?year=2009&view=200928a#200928a

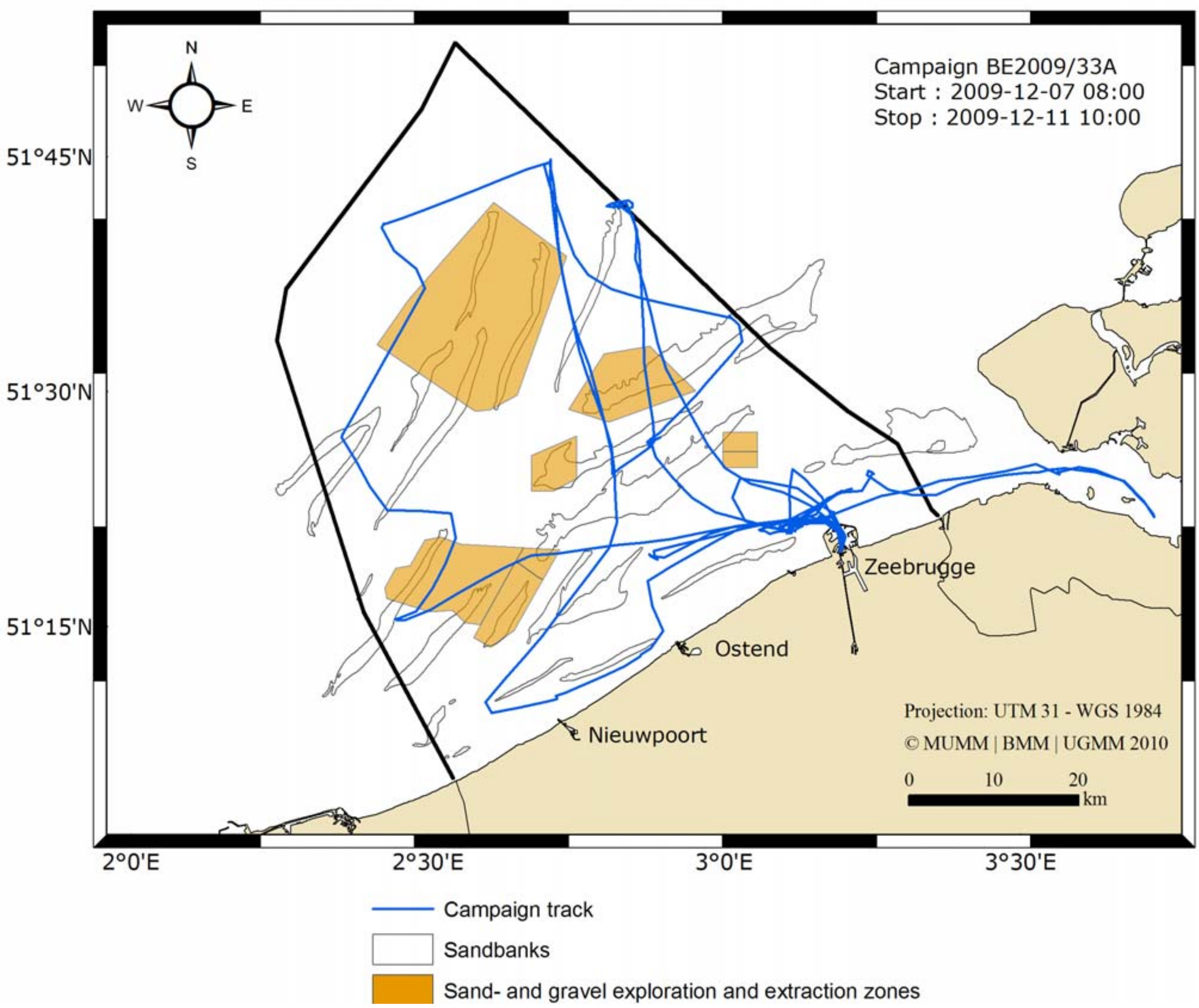


**Figure 85:** Track of the fourth G2LAT campaign (Campaign 2009/33). Between Ostend and Zeebrugge, on the North-East Akkaert bank, the BELGICA and the TER STREEP have sailed jointly during three tracks to gather material for comparison between two similar measurement set-ups. More information in Annex and at: http://www.mumm.ac.be/EN/Monitoring/BELGICA/table.php?year=2009&view=200933#200933